LBL-9057

CROSSED MOLECULAR BEAM STUDIES OF UNIMOLECULAR REACTION DYNAMICS

Richard James Buss
(Ph. D. thesis)

April 1979

Prepared for the U. S. Department of Energy
under Contract W-7405-ENG-48

MASTER

DISTRIBUTION OF THIS DOCUMENT IS UNLIMITED

LBL-9057

CROSSED MOLECULAR BEAM STUDIES OF UNIMOLECULAR REACTION DYNAMICS

Richard James Buss

Materials and Molecular Research Division
Lawrence Berkeley Laboratory

and

Department of Chemistry
University of California
Berkeley, California 94720

April 1979

NOTICE

This report was prepared as an account of work sponsored by the United States Government. Neither the United States nor the United States Department of Energy, nor any of their employees, nor any of their contractors, subcontractors, or their employees, makes any warranty, express or implied, or assumes any legal liability or responsibility for the accuracy, completeness or usefulness of any information, apparatus, product or process disclosed, or represents that its use would not infringe privately owned rights.

ABSTRACT

The study of seven radical-molecule reactions using the crossed molecular beam technique with supersonic nozzle beams is reported. Product angular and velocity distributions were obtained and compared with statistical calculations in order to identify dynamical features of the reactions. In the reaction of chlorine and fluorine atoms with vinyl bromide, the product energy distributions are found to deviate from predictions of the statistical model. A similar effect is observed in the reaction of chlorine atoms with 1, 2 and 3-bromopropene. The reaction of oxygen atoms with ICl and CF_3I has been used to obtain an improved value of the IO bond energy, 55.0 ± 2.0 kcal mol^{-1}. In all reactions studied, the product energy and

angular distributions are found to be coupled, and this is attributed to a kinematic effect of the conservation of angular momentum.

ACKNOWLEDGEMENTS

My sincerest gratitude goes to Professor Yuan T. Lee whose guidance in my pursuit of this research was invaluable. The assistance both intellectual and technical of the other members of our research group are greatly appreciated. In particular, I wish to thank Dr. Michael Coggiola who introduced me to the techniques of reactive scattering and assisted in all aspects of the Cl + C_2H_3Br study. The study of the oxygen reactions would have been impossible without the excellent RF source developed by Steven Sibener, and my thanks to him for his help on the reactions of oxygen with ICl and CF_3I. I am also most grateful to Dr. Peter W. Tiedemann for his assistance in the development of the CMLB program.

Special appreciation goes to Ann Weightman for her patience in typing this manuscript.

I would also like to thank the Office of Naval Research and the Division of Chemical Sciences, Office of Basic Energy Sciences, U. S. Department of Energy under contract No. W-7405-Eng-48 for providing funds with which to complete this work.

My deepest gratitude is reserved for my parents whose unfailing support of my endeavors has always been a source of great comfort.

CROSSED MOLECULAR BEAM STUDIES OF UNIMOLECULAR REACTION DYNAMICS

Contents

I. INTRODUCTION 1

References 13

II. MOLECULAR BEAM STUDIES OF UNIMOLECULAR REACTIONS: Cl, F + C_2H_3Br 15

Introduction 15

Experiment 23

Results and Discussion 24

Summary and Conclusion 31

References 34

Tables 36

Figure Captions 38

Figures 40

III. THE REACTIONS OF Cl WITH 1, 2 AND 3-BROMOPROPENE 48

Introduction 48

Experimental 51

Results and Analysis 53

Discussion 58

Conclusion 69

References 71

Tables 74

Figure Captions 78

Figures 80

IV. THE CROSSED BEAM REACTION OF ATOMIC OXYGEN WITH IC1 AND CF_3I 88

Introduction 88

Experimental 93

Results 95

Discussion 100

Conclusion 106

References 108

Tables 111

Figure Captions 114

Figures 115

V. APPENDIX 122

References 129

Program CMLB 130

Sample Calculation 151

I. INTRODUCTION

The existence of a long-lived intermediate in a reaction occuring under the single collision environment of crossed molecular beams was first demonstrated some 12 years ago.[1] This observation during the so-called alkali age when the technology of molecular beams was in its infancy began the study of unimolecular decomposition under carefully controlled conditions. In subsequent years as molecular beam techniques developed to permit tight control of the reactant state distributions and universal product detection, a large number of reactions were identified which proceed through the formation of a complex. Analysis of product energy and angular distributions have been compared with model calculations in order to understand the dynamics of the decomposition of a species excited above the dissociation limit.

In this chapter, the history of the molecular beam study of unimolecular decay will be reviewed in order to define terminology and place in context the reactions reported in later chapters. The reactions of fluorine and chlorine atoms with vinyl bromide are the subject of Chapter II, in which is introduced a mechanism by

which a long lived complex might exhibit coupling of the energy and angular distributions. A discussion of the use of multiphoton excitation in molecular beams to study unimolecular decay is also included here. Chapter III describes the bromine substitution reaction of chlorine atoms with 1, 2 and 3-bromopropene for which the product energy distributions are quite similar and decidely non-statistical. Finally a study of the iodine abstraction reactions of oxygen atoms with ICl and CF_3I which have yielded an improved value for the IO bond strength will be discussed in Chapter IV. Of the seven reactions reported here, only O + CF_3I exhibits statistical behavior. The comparison of data obtained from a crossed beam experiment with statistical calculations is most reliable if one can smooth the calculated energy and angular distribution over the reactant beam conditions to produce laboratory frame of reference distributions. A flexible computer program to permit such a direct comparison of calculations with unmanipulated data is presented in the appendix.

The earliest use of molecular beams to study reaction dynamics identified a host of direct reactions in which the time for the reactive encounter was approximately the duration of a single collision event. For

these single atom transfer reactions, two principle categories were established, pictorially named stripping and rebound, and distinguished by the angular distribution of product. Characteristic of these reactions, for example $K + CH_3I \rightarrow KI + CH_3$, rebound[2] and $K + Br_2$, stripping[3] is a large exoergicity and the absence of any deep wells on the potential energy surface. The resulting strong forces of attraction between reactants, or repulsion of products dominate the reaction dynamics.

During this period when surface ionization detection limited molecular beam experiments to alkali atom reactions, the first evidence for a long-lived intermediate was found in the study of $K + RbCl \rightarrow KCl + Rb$ by Herschbach and coworkers.[1] The distribution of product was found to exhibit symmetry about the center of mass suggesting that a complex had been formed which rotated several times before decomposition. Here, then, was a way to investigate the unimolecular decay of a molecule uncomplicated by secondary collision events. With the development of the universal quadrupole mass spectrometric detector by Lee et al.,[4] a vast realm of reaction chemistry became accessible. Among the most exciting application of this new flexibility was the study of some forty reactions of fluorine atoms with unsaturated

carbon compounds by Lee and coworkers. These early studies identified dynamical effects occuring in the long-lived complexes, and raised questions concerning energy redistribution in the complex and exit channel effects on the product energy distributions.

Before discussing these and other results, I will digress to clarify the nature of the reactions under consideration. There is no distinct division separating the direct reactions from the long-lived complex reactions. The duration of the collision may range from the very short 0.1 ps necessary for one molecule to travel past the other, to many milliseconds in the case of some complexes in which electronic curve crossing occurs.[5] The so-called sticky collision in which the reactants remain in close proximity long enough to vibrate many times, is only possible when a sizeable well occurs in the potential energy surface. The lifetime of the complex will be determined by the specific shape of the surface and, in general, its exact quantum mechanical calculation is infeasible because the complexity of even most triatomic systems exceeds current machine capabilities. However, several methods have been developed to treat the decomposition of an excited molecule statistically, that is, with the assumption that all

states of the molecule, consistent with energy and angular momentum conservation, are equally probable. The RRKM theory,[6] in particular, has proven quite successful in calculating the rate constants for unimolecular reactions which have been studied in bulk phase systems. These comparisons can rarely distinguish whether the success of the theory stems from the random nature of the excitation process, or a true redistribution of internal energy in the excited molecule. The chemical activation in the single collision occuring in crossed molecular beams releases energy in some localized region of the complex. Observation of the product energy distributions and their deviations from statistical predictions should make feasible the investigation of the processes occuring between the moment of activation and the final separation of products.

During the early years of molecular beam development, a more phenomenological system of identification for reactions came into use. In the reaction of two molecules in the crossed beam environment, the experimenter has a clock with which to obtain some lifetime information, namely the rotational period, τ_r, of the complex. The symmetry of the product about 90° in the center of mass reference frame is a measure of the lifetime of the

intermediate relative to τ_r, because a complex which rotates many times before decomposition loses memory of the incident direction and has equal probability of scattering in the forward or backward hemisphere. Three classifications for the molecular beam reactions have come into use. The direct reactions have product restricted to the forward or to the backward hemisphere. The so-called long-lived complexes exhibit forward backward symmetry while the intermediate case is referred to as an oscullating complex and represents a reaction in which the intermediates lifetime is comparable to the rotational period. Unfortunately, the notation has created some confusion in which the existence of symmetry in the angular distribution is taken, by some authors, as a necessary criterion for recognizing that a reaction proceeds via a statistical complex. It is quite possible, though, for the statistical lifetime to be comparable or less than the rotational period in which event the angular distribution would show asymmetry. With the above classification scheme, all of the reactions discussed in this paper are probably of the oscullating type.

The investigation of long lived complexes, formed from alkali atom and molecule reaction $M + M'X \rightarrow M' + MX$ and $MX + M'X' \rightarrow M'X + MX'$ have continued since the original

paper, but the dynamical information derived from these studies has been disappointingly little. This stems mainly from the difficulty in distinguishing the reactants from products with the surface ionization detector and from poor velocity resolution resulting from the use of thermal beams. Ham and Kinsey,[7] in studying the decay of a long lived complex formed in the reaction of potassium atoms with SO_2 by detecting inelastic scattering have obtained an angular distribution considerably broader than statistical but uncertainties in the theoretical treatment limit the significance of this difference. For the reaction $K + RbCl \rightarrow Rb + KCl$ Aniansson et al.,[8] have observed a ratio of reactive to nonreactive scattering significantly less than statistical predictions and they attribute this to potential energy surface effects preventing free migration of the potassium atom. Similar disagreement is observed in this ratio for the four center reactions of CsCl with KCl and KI.[9] Other studies of alkali atom and molecule reactions[10] have been in fair agreement with statistical calculations and thus provide little dynamical information.

The reactions of fluorine atoms with unsaturated hydrocarbons has proven to be a valuable source of dynamical information. The fluorine carbon bond formation

releases some 50 kcal mol^{-1} into the complex which lives many rotational periods before decomposition. Careful choice of the substituted hydrocarbons has enabled the study of relative cross sections for competing decomposition channels and product energy distributions, from which have been derived several interesting conclusions. Almost invariably, when several competing channels are accessible to the complex, the energetically most favorable one predominates as is expected from statistical considerations. In molecules which are symmetrical with respect to fluorine attack, such as 1,2 dichloroethylene[11] and cis-2 butene,[12] the relative cross sections for the competing H elimination and Cl or CH_3 elimination agree well with statistical calculations. In this respect, only the reaction of F with tetramethylethylene[13] has deviated from statistical, giving much less CH_3 elimination than expected. Shobatake et al. found for the reaction of F with 1,1 dichloroethylene[11] that the cross section for chlorine elimination was reduced relative to that for hydrogen production, from which they deduced that atom migration occuring in the complex was slow. A similar observation was made in the reaction of F + chlorobenzene.[14]

The product energy distributions P(E') which are obtained by analysis of the product angular and velocity

distributions provide another probe of the reaction dynamics. The comparison with statistical theory is not always straightforward because additional assumptions must be added to the models which are used to calculate rate constants. For reactions in which the entrance and exit channels are both dominated by long range forces, the theoretical developement is quite good. The RRKM-AM theory,[15] phase space theory,[16] and the statistical adiabatic theory[17] all become essentially identical for this so-called loose complex. Examples of reactions which are thought to proceed in this way are $X + RX' \rightarrow X' + RX$ where X and X' are halogens and R is an unsaturated hydrocarbon, for example the reactions discussed in Chapter II and III. These systems lack potential barriers in the entrance and exit channels and are thought to have little orientation dependence. The chlorine elimination reactions $F + C_2H_2Cl_2$[11] and C_6H_5Cl[14] have yielded P(E') which agree well with statistical calculations for a loose complex. It is the reactions which are known to have a barrier in the exit channel that are most difficult to treat theoretically because so little is known concerning the dynamical effect of a force between the two fragments as they depart. For this reason, the observation of nonstatistical P(E') in the H and CH_3 elimination reactions for a series of

fluorine reactions with hydrocarbons has generated much debate. These reaction channels are known to have barriers, 1-3 kcal mol^{-1} for hydrogen and 6-8 kcal mol^{-1} for methyl elimination. The P(E') obtained for these channels in the reaction of F with C_2H_4,[18] C_4H_8,[12] C_6H_6[19] and toluene,[14] have all deviated from the statistical calculations in having more product translational energy and broader distributions. The original suggestion that the emission of a light particle might not occur with the participation of all modes of the complex was ill-received and was countered with an alternative explanation which attributed the effect to coupling of other modes to the reaction coordinate in the exit channel. An exhaustive study of the F + C_2H_4[20] reaction has adequately demonstrated that the nonstatistical P(E') cannot be the result of exit channel interactions beyond the critical configuration. When the collision energy was increased by a factor of two, the energy in product translation doubled as well, while a statistical model would predict a small fraction of this increase. Because the collision energy was increased sufficiently high to make exit channel effects negligible, the nonstatistical effects must be occuring prior to the critical configuration. These results are suggestive, but do not prove

that the nonstatistical P(E') in other H and CH_3 elimination reactions are the result of dynamical constraints in the complex.

There are three stages of the reaction in which one might expect nonstatistical effects to arise. In the initial bond formation, the energy may not become statistically distributed among the internal modes of the complex before bond breakage occurs. If instead, the energy is randomized, dynamical constraints may cause only a fraction of the modes to contribute energy to the reaction coordinate. Finally, even when the molecule reaches the critical configuration with a statistical energy distribution, dynamical effects occuring during separation of the fragments may introduce nonstatistical features to the P(E'). Crossed molecular beams may be the tool with which to distinguish which long-lived complexes cannot be treated statistically and at which time during the reaction the nonstatistical effects arise.

The reactions which are reported in this paper were chosen for study primarily to help elucidate the questions of energy randomization in systems which proceed through quasi-stable intermediates. The energetics are such that the statistical lifetimes of all these complexes is relatively short, 0.1 - 5 ps, comparable to a rotational

period. In addition to observing nonstatistical translational energy distributions for all but the O + CF_3I reaction, an interesting coupling effect of the energy and angular distributions was observed, and can probably be attributed to angular momentum conservation.

The nonstatistical effects observed in the decomposition of chemically activated complexes in molecular beams are contributing to the study of unimolecular decay processes. Similar effects have been identified with such different techniques as the imaginative bulk phase experiments of Rabinovitch[21] and the infrared chemiluminescence measurements of McDonald.[22] Ultimately, through this combined effort, we will arrive at a thorough understanding of the unimolecular decay process.

REFERENCES

1. W. B. Miller, S. A. Safron, and D. R. Herschbach, Disc. Faraday Soc., 1967, 44, 108.

2. P. R. Brooks and E. M. Jones, J. Chem. Phys., 1966, 45, 3449.

3. R. E. Minturn, S. Datz and R. L. Becker, J. Chem. Phys., 1966, 44, 1149.

4. Y. T. Lee, J. D. McDonald, P. R. LeBreton, and D. R. Herschbach, Rev. Sci. Instrum., 1969, 40, 1402.

5. T. M. Sloane, J. Chem. Phys., 1977, 67, 2267.

6. W. Forst, Theory of Unimolecular Reactions, Academic Press, New York, 1973.

7. D. O. Ham and J. L. Kinsey, J. Chem. Phys., 1970, 53, 285.

8. G. Aniansson, R. P. Creaser, W. D. Held, L. Holmlid, and J. P. Toennies, J. Chem. Phys., 1974, 61, 5381.

9. W. B. Miller, S. A. Safron, and D. R. Herschbach, J. Chem. Phys., 1972, 56, 3581.

10. S. J. Riley and D. R. Herschbach, J. Chem. Phys., 1973, 58, 27; M. K. Bullitt, C. H. Fisher, and J. L. Kinsey, J. Chem. Phys., 1974, 60, 478.

11. K. Shobatake, Y. T. Lee, and S. A. Rice, J. Chem. Phys., 1973, 59, 6104.

12. J. M. Parson, K. Shobatake, Y. T. Lee, and S. A. Rice, J. Chem. Phys., 1973, 59, 1402.

13. K. Shobatake, J. M. Parson, Y. T. Lee, and S. A. Rice, J. Chem. Phys., 1973, 59, 1416.

14. K. Shobatake, Y. T. Lee, and S. A. Rice, J. Chem. Phys., 1973, 59, 1435.

15. S. A. Safron, N. D. Weinstein, D. R. Herschbach, and J. C. Tully, Chem. Phys. Lett., 1972, 12, 564.

16. J. C. Light, Disc. Faraday Soc., 1967, 44, 14; P. Pechukas, J. C. Light, and C. Rankin, J. Chem. Phys., 1966, 44, 794.

17. M. Quack and J. Troc, Ber. Bunsenges Phys. Chem., 1975, 79, 469.

18. J. M. Parson and Y. T. Lee, J. Chem. Phys., 1972, 56, 4658.

19. K. Shobatake, J. M. Parson, Y. T. Lee, and S. A. Rice, J. Chem. Phys., 1973, 59, 1427.

20. J. M. Farrar and Y. T. Lee, J. Chem. Phys., 1976, 65, 1414.

21. J. D. Rynbrandt and B. S. Rabinovitch, J. Phys. Chem., 1971, 75, 2164.

22. J. F. Durana and J. D. McDonald, J. Chem. Phys., 1976, 64, 2518.

II. MOLECULAR BEAM STUDIES OF UNIMOLECULAR REACTIONS: Cl, F + C_2H_3Br

INTRODUCTION

Slightly over a decade ago, evidence for the existence of long-lived intermediates from reactive encounters of molecules in beams was presented at a Faraday Discussion meeting. This suggested the attractive possibility of studying the dynamics of unimolecular decomposition by the measurement of angular and velocity distributions of products in a collision free environment after preparing long-lived complexes by chemical activation. In the years since, a great number of reactions which appear to proceed via persistent complex have been studied in molecular beams. Although the early experiments frequently employed thermal beams and, hence, provided poor characterization of the collision energy, later refinement in beam techniques, especially the use of supersonic nozzle sources, has greatly increased the effectiveness of the method in providing insight into reaction dynamics.

More recently, a new technique, infrared multiphoton excitation in beams, in which molecules are excited under collision free conditions by absorbing tens of photons during an intense single laser pulse, has proven to be an excellent way to prepare excited molecules and to gain dynamical information about unimolecular decomposition.

The study of some forty reactions ranging from simple bond rupture to three and four center eliminations has revealed trends which can likely be generalized to large classes of unimolecular decay.

These two methods, chemical activation and multiphoton excitation, differ substantially in several important respects. As a consequence the information obtained is complementary rather than overlapping.

The nature of the excitation process places limitations on the certainty with which we know the total energy of the dissociating molecules. With chemical activation in crossed beams, the total energy is simply the sum of internal energy of the reactants, energy released in formation of the new chemical bond, and the collision energy. The principal uncertainty, arising from the spread in collision energies, can be reduced to a small fraction of the total energy. With the use of two supersonic nozzle beams, the collision energy may typically be defined to FWHM = 5-10 kJ mol^{-1} which is often only 2-3% of the total excitation energy of the complex. This excellent energy characterization, combined with the variability of collision energy obtainable by seeding of the reactants with rare gases, make this technique a sensitive probe of the dynamics of unimolecular decomposition.

In sharp contrast, infrared multiphoton absorption produces excited molecules with a spread in excitation energies which can be an exceedingly large fraction of the average total energy. This problem is fundamental to the process, being governed by the mechanism of absorption of many photons. In the sequential absorption of photons, after an initial excitation through a region of discrete transitions, the molecule is excited to a region referred to as the quasi-continuum. The density of states, here, is sufficiently high that all transitions are near-resonant, essentially independent of laser frequency. A fairly adequate description of the population distribution of each level is given by a set of rate equations with transition rates depending on laser intensity, energy level dependent infrared absorption cross sections and density of states.[1] The result is somewhat similar to thermal excitation with a simple dependence of average excitation level on the energy fluence of the laser pulse. When the laser fluence is sufficient to drive the molecules above the dissociation threshold, an extra term must be added to the rate equations, to account for depletion by dissociative processes. At some high excitation level, the dissociation rate becomes much faster than the rate of excitation and

population of higher states will not be significant. For a large molecule with high density of states around the dissociation levels, the unimolecular rate constant will increase gradually with excitation. Substantial dissociation will occur over a large range of levels. SF_6, for example, is calculated[1] to undergo detectable multiphoton dissociation (MPD) at levels from 4 to 13 photons above threshold, the total energy in the system then being defined to FWHM = 60 kJ mol^{-1} or about 15%. For smaller molecules, in which the rate constant increases more rapidly with excitation energy, the uncertainty in energy of the reacting molecules will be much narrower since most of the molecules dissociate from a level only a few photons above threshold.

The degree to which angular momentum affects the outcome of the unimolecular decay is also considerably different for the two processes. In both cases, cooling of the rotational degrees of freedom during supersonic expansion of the beam results in a low and relatively well-defined rotational temperature. In the bimolecular collision which produces the chemically activated species, orbital angular momentum can be very large, even at thermal energies, and sometimes dominating in its effects on the product translational energy distribution. Although the

theoretical treatment of the effect of angular momentum on product energy distributions is fairly well developed, it remains a fundamental limitation in the analysis of this type of experiment that the probability of formation of the complex as a function of impact parameter which governs the distributions of angular momentum of the complexes is indeterminant. In consequence, it is incumbent on the theory to account correctly for angular momentum conservation, though this may require knowledge of dynamical features of the reaction, such as preferred orientation of reactants.

In MPD, angular momentum is found to play a much less significant role in the unimolecular decay. The depletion of low translational energy product expected for reaction with an exit channel centrifugal barrier associated with rotational motion is not observed in halogen atom detachment reactions using this technique. This indicates that the absorption of some forty photons does not appreciably increase the originally low average rotational energy. This greatly facilitates the comparison of product translational energy with statistical calculations.

The two methods lend themselves, most conveniently, to the study of different chemical systems. MPD in beams has been used extensively to study unimolecular decay of

closed-shell molecules.[2] In particular, molecules with huge barriers to dissociation, for example, the three-center elimination of HCl from CHF_2Cl with approximately 225 kJ mol^{-1} barrier, are accessible with the energy fluence attainable in a high power CO_2 laser pulse. Indeed, MPD has been applied to systems ranging from such highly endoergic reactions to the nearly thermoneutral dissociation of ammonia dimers.[3]

Chemical activation has been applied principally to the investigation of open-shell systems. The addition of a radical species, eg. halogen atom, oxygen atom or methyl radical, to an unsaturated hydrocarbon to produce an excited radical intermediate constitutes the majority of long-lived complex reactions studied in crossed beams. The study of closed-shell systems by radical-radical combination collisions should become more frequent as these beam sources are developed.

A final aspect which distinguishes MPD from chemical activation is the time domain of the reactions. The multi-photon excitation always raises the molecules to a level at which the dissociation rate approximately equals the up-pumping rate. For the typical energy fluences attainable in a 50 nsec CO_2 laser, this fixes the upper limit of the average lifetime of the system at close to a nanosecond,

fairly independent of the chemical nature of the molecule or type of dissociation process occurring. Using chemical activation, with its rapid deposition of bond-formation energy into the molecule, systems with average lifetimes shorter than a picosecond can be studied using the rotational period of the complex as an indicator. The method offers the possibility of finding a range of applicability of the statistical model for unimolecular decay. By studying reactions with a wide range of lifetimes, one can hope to place a bound on the time necessary for memory of the excitation event to be lost, though this time would undoubtedly be dependent on the exothermicity of the reaction, the stability and complexity of the intermediate.

The MPD of a large number of systems in which a single halogen atom is detached from a halocarbon has convincingly demonstrated the statistical nature of the process.[4] The primary pathway for decomposition is always found to be the statistically most favorable. The product translational energy distribution peaks at zero energy and has the correct statistical fall-off. Because the molecules undergoing dissociation have an average lifetime around one nanosecond after absorbing the final photon, we can conclude that the time for energy to be effectively randomized over all internal degrees of freedom should be much less than one

nanosecond. Unfortunately, due to the limitation in the multiphoton excitation, it is not likely that these experiments will reveal exactly how fast the energy randomizes in the highly excited molecules.

In order to investigate the extent of intramolecular relaxation before chemical decomposition in a shorter time span than that of multiphoton decomposition, reactions of Cl and F with C_2H_3Br have been carried out in molecular beam experiments. In these chemical activation studies, as mentioned before, the product translational energy distributions, henceforth denoted P(E'), may be strongly influenced by angular momentum conservation, as well as by any potential barrier in the exit channel. The substitution reactions of fluorine and chlorine atoms with vinyl bromide are known to proceed with negligible potential barrier to bromine elimination. Angular momentum effects are large, though, and careful consideration of this is necessary in order to draw conclusions concerning the statistical nature of the process. Some important consequences of angular momentum, especially the coupling of angular and energy distributions of products will be discussed below.

EXPERIMENT

The crossed beam scattering apparatus and data acquisition methods used for these experiments has been described in detail.[5] The supersonic fluorine beam was produced by thermal dissociation of a 1% F_2 in argon mixture in a resistively heated nickle oven at about 1080°K. The chlorine source was similar, except the oven was high density graphite, and the mixture, 10% Cl_2 in argon, was heated to 1400°K. Vinyl bromide, undiluted, at a pressure of 250 torr was expanded from a 0.2 mm glass nozzle at room temperature. Time of flight characterization of the beams gave the information listed in Table I. The spread in collision energies is determined from these parameters to be FWHM = 7.1 kJ mol^{-1} or 5.6% of the total energy for the chlorine reaction and FWHM = 4.2 kJ mol^{-1} or 2.2% of the total energy for the fluorine reaction. The laboratory angular distributions of product, shown in Fig. 1, were obtained by repeated scans with 100 second counts at each angle. In the fluorine experiment, elastic scattering of impurity from the secondary beam contributed to the signal at angles greater than 30°. The intensities at these angles were corrected by subtracting from them, the signal measured with a pure hot argon beam replacing the F/Ar mixture. The product flux distributions shown in Fig. 2

and 3 were obtained by the cross correlation time of flight method. The best fit lines in Fig. 1, 2 and 3 were obtained using the ratio method iterative deconvolution procedure. The angular and velocity data have been combined to produce center of mass flux contour plots shown with the canonical Newton diagram in Fig. 4 and 5.

RESULTS AND DISCUSSION

The product angular distribution provides some information about the average lifetime of the reaction intermediate. The existence of symmetry of the product angular distribution about 90° in the center of mass reference frame, reflects a complex lifetime which is longer than the average rotational period of the molecule. An approximation to the mean rotational period is obtained by assuming a geometry for the complex to generate moments of inertia, and estimating the average angular momentum of the complex. For the chlorine reaction, the mean rotational period is estimated to be 3 ps. The RRKM theory predicts a mean lifetime of 0.1 ps, though this number is rather sensitive to the frequencies used in the calculation. We would expect, then, that the reaction should not exhibit forward backward symmetry if its lifetime is entirely

determined by a statistical distribution of internal energy. In the laboratory reference frame, for this reaction, the back-scattered product is de-emphasized in the center of mass to laboratory transformation, and most back-scattered product is also beyond the range of the detector. The single datum at 99° was compared with a detailed calculation in which the RRKM-AM P(E') calculated for a range of collision energies and weighted by calculated total cross sections, with assumed forward backward symmetry, was transformed to the laboratory reference frame. The calculated intensity at 99° was a factor of 1.7 times the observed intensity, or six standard deviations away, thus strongly suggesting that the lifetime is indeed less than a rotational period. Were the product to exhibit a longer lifetime than statistical, one might conclude that there was decoupling of the reaction coordinate from the major excitation modes causing a bottleneck in the energy transfer or possibly a slow atomic migration limiting the rate of decomposition.[11] The statistical calculations for the fluorine reaction also predict asymmetry in the angular distribution, but the impurity in the vinyl bromide beam prevented detection of any back-scattered vinyl fluoride product. Although use of the rotational period for measuring the lifetime in these experiments provides only the crudest estimate of the statistical behavior of

the system, the product translational energy distribution gives a far more sensitive test, if careful attention is paid to the treatment of angular momentum conservation.

One of the most interesting observations in the reaction of chlorine and vinyl bromide is the presence of coupling of the product angular and energy distributions. In Fig. 4 the dashed line through the peak in product flux at 0° is contrasted with the dotted line through the observed peak at each center of mass angle as the average translational energy of the products become smaller at wide angle. Considerable attention has been paid to this type of coupling arising in direct reactions with a large impulsive force in the exit channel.[7] The effect has been observed in a number of alkali atom reactions with halomethanes,[8] but in the analysis of long-lived complexes, it has usually been assumed that the energy distribution is independent of scattering angle. In fact, angular momentum conservation is also expected to create such coupling in reactions proceeding through long-lived complexes. When the impact parameter is large, the orbital angular momentum will often dominate the molecular angular momentum in the reaction, the angular momentum of the activated complexes will be highly polarized, perpendicular to the relative velocity, and a large fraction of the

initial relative kinetic energy will become rotational energy of the complex as a consequence of the conservation of angular momentum. If most of the angular momentum of the complex is carried away as orbital angular momentum of the products, the product angular distribution will be strongly peaked in the forward and backward direction and most of the rotational energy of the complex will be converted to translational energy, such that the product energy distribution will be shifted to higher average energy than that released along the reaction coordinate from the sharing of excess vibrational energy. On the other hand, if the impact parameter is small, the orbital angular momentum will no longer dominate the molecular angular momentum. Consequently, the angular momentum of the complex will be distributed more isotropically due to random orientation of the molecular angular momentum of the reactants and the angular distribution of products will tend to be more isotropic. In addition, with a small impact parameter, most of the initial translational energy will become vibrational energy of the complex, the rotational to translational energy release in the formation of product molecules is less important and the energy distribution will be closer to what one would expect from simple statistical considerations with a translational energy distribution peaking closer to

zero energy. This coupling of angular and energy distributions due to the constraint of the conservation of angular momentum should be observable in the experiment if the contribution from large impact parameter collisions does not overwhelm the small impact parameter collisions.

A simple calculation to demonstrate this effect is shown in Fig. 6. The contour map of product flux distributions compare a calculation of RRKM-AM product energy distribution decoupled from the angular distribution with one including coupling. The latter calculation is the sum of fifty distributions in which P(E') and P(θ) are varied together considering the magnitude and polarization of angular momentum, simulating the range of impact parameters expected in the chlorine reaction with vinyl bromide as shown in Fig. 7. Despite the lack of sophistication of the model, the major features of this coupling are evident. At 0° the flux peaks at higher velocities with coupling while the reverse is true at 90°. The effect would be less noticeable in reaction with larger cross sections in which large impact parameter collisions dominated. Of course, this demonstration of the existence of coupling in the angular and energy distribution of product molecules in the long-lived complex does not imply the existence of a long-lived complex between chlorine and vinyl bromide.

Comparison of the product energy distributions with RRKM-AM calculations for the two reactions is shown in Fig. 8. The experimental curve for the chlorine reaction is the average P(E') for the product scattered between 0 and 90 degrees in the center of mass frame. Parameters used in the calculations are shown in Table II. The vinyl chloride product from the chlorine reaction is seen to be in poor agreement with the statistical calculation, the product energy being substantially higher than calculated. Extensive testing with the model demonstrated that the failure is not the result of the chosen vibrational frequencies, the energetics, or the choice of maximum centrifugal barrier B_m' in the angular momentum treatment. The calculated P(E') is very insensitive to the first and second within reasonable range of the parameters. The dotted curve is produced with the parameter B_m' having been set at an unreasonably high value, 60 kJ mol^{-1}, beyond which its effect is negligible.

There are two principle explanations for the discrepancy observed. The first is the much-discussed possible failure of the energy randomization hypothesis. The lifetime for this reaction is calculated by the statistical theory to be approximately 0.1 ps. It would not be improbable that this reaction is beyond the scope of a unimole-

cular decay theory since, if statistical theory is applicable here, intramolecular energy transfer must be faster than 0.1 psec. The second explanation is that the treatment of angular momentum is inadequate. The theory assumes a distribution of angular momentum which is linear in impact parameter with a cutoff determined by the long range forces.[9] In practice, the relative cutoff for entrance and exit channel has been treated as a variable to obtain best fit. The linearity with impact parameter may be questioned. For this reaction, dynamical constraints may require that the atom attack at the double bond which is removed from the center of mass of the vinyl bromide. Approach at small impact parameter could be less favorable for reaction. A simple calculation based on this idea suggests that the angular momentum distribution might be more nearly quadratic in impact parameter. Assuming this distribution, the statistical calculation is found to fit the observed P(E') quite well, though this is likely fortuitous. In the fluorine reaction, again, the agreement with theory is poor. While the experimental energy distribution below 5 kJ mol^{-1} has large uncertainty resulting from the elastic impurity in the C_2H_3Br beam, it is clear that the observed intensity of both low and high energy product is reduced. This is not easy to explain with a

simple model and will probably require more information about dynamical effects of the potential energy surface for a thorough understanding, but it is quite clear for this system that the reaction lifetime is shorter than the intermolecular relaxation time.

SUMMARY AND CONCLUSION

McDonald and coworkers[10] have measured the infrared chemiluminescence from these reactions. They find that the product vibrational energy distribution is statistical for the fluorine reaction and non-statistical for the chlorine. While an earlier crossed beam study of the chlorine reaction using a beam of chlorine atoms with a thermal velocity distribution[11] seemed to indicate that product translation was statistical, our higher resolution results suggests that product translational is not statistical in either reaction. One explanation for the discrepancy for the fluorine reaction lies in the different energetics of the two systems. The greater exothermicity of the fluorine reaction leaves about 170 kJ mol^{-1} in internal excitation of the product compared to about 60 kJ mol^{-1} for the chlorine reaction. The chemiluminescence experiment measures the product emission milliseconds

after reaction. If the vibrational energy is large enough that the molecule is above the ergodic limit, even if the initial distribution is not statistical, energy will be redistributed before the emission of the infrared photon is observed. Perhaps the higher internal excitation of the vinyl fluoride product allows randomization before the emission is detected while the vinyl chloride product retains its non-statistical distribution. The lifetime of the activated complex in the fluorine with vinyl bromide reaction is only 0.05 psec, according to statistical theory. If such a treatment is applicable, as implied in the chemiluminescence experiment, the intramolecular energy transfer has to be faster than 0.05 psec which is highly unlikely.

The two techniques of MPD and chemical activation in beams are seen to produce complementary results. MPD has demonstrated that, without exception, energy appears to be randomized in the nanosecond time period of the reaction. Chemical activation in beams has revealed non-statistical effects appearing for reactions with sub-picosecond lifetimes. These observations are not in contradiction to the general conclusion obtained by Rabinovitch and coworkers[12] that the intramolecular relaxation time of highly excited molecules is on the order of several

simple model and will probably require more information about dynamical effects of the potential energy surface for a thorough understanding, but it is quite clear for this system that the reaction lifetime is shorter than the intermolecular relaxation time.

SUMMARY AND CONCLUSION

McDonald and coworkers[10] have measured the infrared chemiluminescence from these reactions. They find that the product vibrational energy distribution is statistical for the fluorine reaction and non-statistical for the chlorine. While an earlier crossed beam study of the chlorine reaction using a beam of chlorine atoms with a thermal velocity distribution[11] seemed to indicate that product translation was statistical, our higher resolution results suggests that product translational is not statistical in either reaction. One explanation for the discrepancy for the fluorine reaction lies in the different energetics of the two systems. The greater exothermicity of the fluorine reaction leaves about 170 kJ mol^{-1} in internal excitation of the product compared to about 60 kJ mol^{-1} for the chlorine reaction. The chemiluminescence experiment measures the product emission milliseconds

after reaction. If the vibrational energy is large enough that the molecule is above the ergodic limit, even if the initial distribution is not statistical, energy will be redistributed before the emission of the infrared photon is observed. Perhaps the higher internal excitation of the vinyl fluoride product allows randomization before the emission is detected while the vinyl chloride product retains its non-statistical distribution. The lifetime of the activated complex in the fluorine with vinyl bromide reaction is only 0.05 psec, according to statistical theory. If such a treatment is applicable, as implied in the chemiluminescence experiment, the intramolecular energy transfer has to be faster than 0.05 psec which is highly unlikely.

The two techniques of MPD and chemical activation in beams are seen to produce complementary results. MPD has demonstrated that, without exception, energy appears to be randomized in the nanosecond time period of the reaction. Chemical activation in beams has revealed non-statistical effects appearing for reactions with sub-picosecond lifetimes. These observations are not in contradiction to the general conclusion obtained by Rabinovitch and coworkers[12] that the intramolecular relaxation time of highly excited molecules is on the order of several

picoseconds. The lifetime range available with chemical activation, together with its good energy specification should make it the method of choice for investigation of the efficiency of intramolecular energy transfer and detailed dynamics of unimolecular decay. Nevertheless, the MPD method should prove valuable for the study of exit channel dynamical effects in the highly endoergic three and four-center elimination reactions.

REFERENCES

1. E. R. Grant, P. A. Schulz, Aa. S. Sudbø, Y. R. Shen and Y. T. Lee, Phys. Rev. Letters, 1978, 40, 115.

2. Aa. S. Sudbø, P. A. Schulz, Y. R. Shen and Y. T. Lee, J. Chem. Phys., 1978, 69, 2312.

3. Aa. S. Sudbø, D. J. Krajnovich, P. A. Schulz, Y. R. Shen and Y. T. Lee, in preparation.

4. Aa. S. Sudbø, P. A. Schulz, E. R. Grant, Y. R. Shen and Y. T. Lee, J. Chem. Phys., 1979 (in press).

5. Y. T. Lee, J. D. McDonald, P. R. LeBreton and D. R. Herschbach, Rev. Sci. Instrum., 1969, 40, 1402. See also reference 6.

6. J. J. Valentini, Ph.D. dissertation, University of California, Berkeley, California, 1976.

7. N. D. Weinstein, Ph.D. dissertation, Harvard University, Cambridge, Massachusetts, 1972.

8. S. J. Riley, Ph.D. disseration, Harvard University, Cambridge, Massachusetts, 1970.

9. S. A. Safron, N. D. Weinstein, D. R. Herschbach and J. C. Tully, Chem. Phys. Letters, 1972, 12, 564.

10. J. G. Moehlman and J. D. McDonald, J. Chem. Phys., 1975, 62, 3052; J. F. Durana and J. D. McDonald, J. Chem. Phys., 1976, 64, 2518.

11. J. T. Cheung, J. D. McDonald and D. R. Herschbach, J. Am. Chem. Soc., 1973, 95, 7889.

12. J. D. Rynbrandt and B. S. Rabinovitch, J. Chem. Phys., 1970, 74, 4175; J. Chem. Phys., 1971, 54, 2275.

Table I.

	Peak Velocity x 10^4 cm/sec	Mach Number	Mean Collision Energy kJ mol^{-1}	Energy Spread FWHM kJ mol^{-1}
Cl	11.5	9.1	20.54	7.1
F	10.9	8.3	11.55	4.2
C_2H_3Br	4.9	7.7	---	---

Table II.

	Cl + Vinyl Bromide		F + Vinyl Bromide	
	Complex	Critical Configuration	Complex	Critical Configuration
Total internal energy/kJ mol^{-1}	144.5	78.8	191.5	128.7
Moments of inertia/AMU $Å^2$	76.8	71.0	41.7	40.2
	207.5	385.5	254.4	563.5
	271.2	571.3	296.1	603.5
Frequencies/ wavenumbers	3125	3125	3150	3150
	3086	3086	3115	3115
	3030	3030	3080	3080
	1437	1586	1479	1612
	1374	1374	1380	1380
	1281	1281	1306	1306
	1036	1036	1097	1156
	897	897	929	929
	648	706	863	863
	621	621	711	711
	274	122	458	483
	103	46	450	500
	450	500	285	63
	250	102	177	30
	426	---	389	---
Ratio of maximum entrance to maximum exit channel impact parameter	dashed curve in Fig. 8	.77		.67
	dotted curve in Fig. 8	4.0		2.0

FIGURE CAPTIONS

Fig. 1. Laboratory angular distribution of vinyl fluoride product from the reaction $F + C_2H_3Br \rightarrow Br + C_2H_3F$, above, and vinyl chloride product from the reaction $Cl + C_2H_3Br \rightarrow Br + C_2H_3Cl$, below. The solid lines are best fits obtained by the ratio deconvolution method of Siska.

Fig. 2. The vinyl chloride product flux distribution measured at 15 laboratory angles. Solid lines are best fits obtained by the ratio deconvolution method. Dashed lines connect data points for clarity.

Fig. 3. The vinyl fluoride product flux distribution at 4 laboratory angles. Lines are best fit calculated curves.

Fig. 4. Center of mass C_2H_3Cl product flux, deconvoluted for beam velocity spread, shown with the most probable Newton diagram. The dotted line is through the peak flux at each center of mass angle. The dashed line is at constant center of mass velocity 580 m s^{-1} for comparison.

Fig. 5. Contour map of center of mass C_2H_3F product flux, shown with the most probable Newton diagram.

Fig. 6. Model calculation of product flux distributions. Dashed curves are generated from a single RRKM-AM P(E') with a single angular distribution. Solid curves are the sum of fifty P(E') with coupled T(θ) distribution.

Fig. 7. P(E') and T(θ) used to compare effect of angular momentum coupling. Shown are the RRKM-AM distributions for the uncoupled calculation. Also shown are three P(E') and T(θ) for orbital angular momentum $L = \ell h$.

Fig. 8. Product translational energy distribution. Solid curves are experimental. Dashed curves are RRKM-AM with B_m' determined by C_6 constants. Dotted curves show calculations with B_m' increased to unphysically large values.

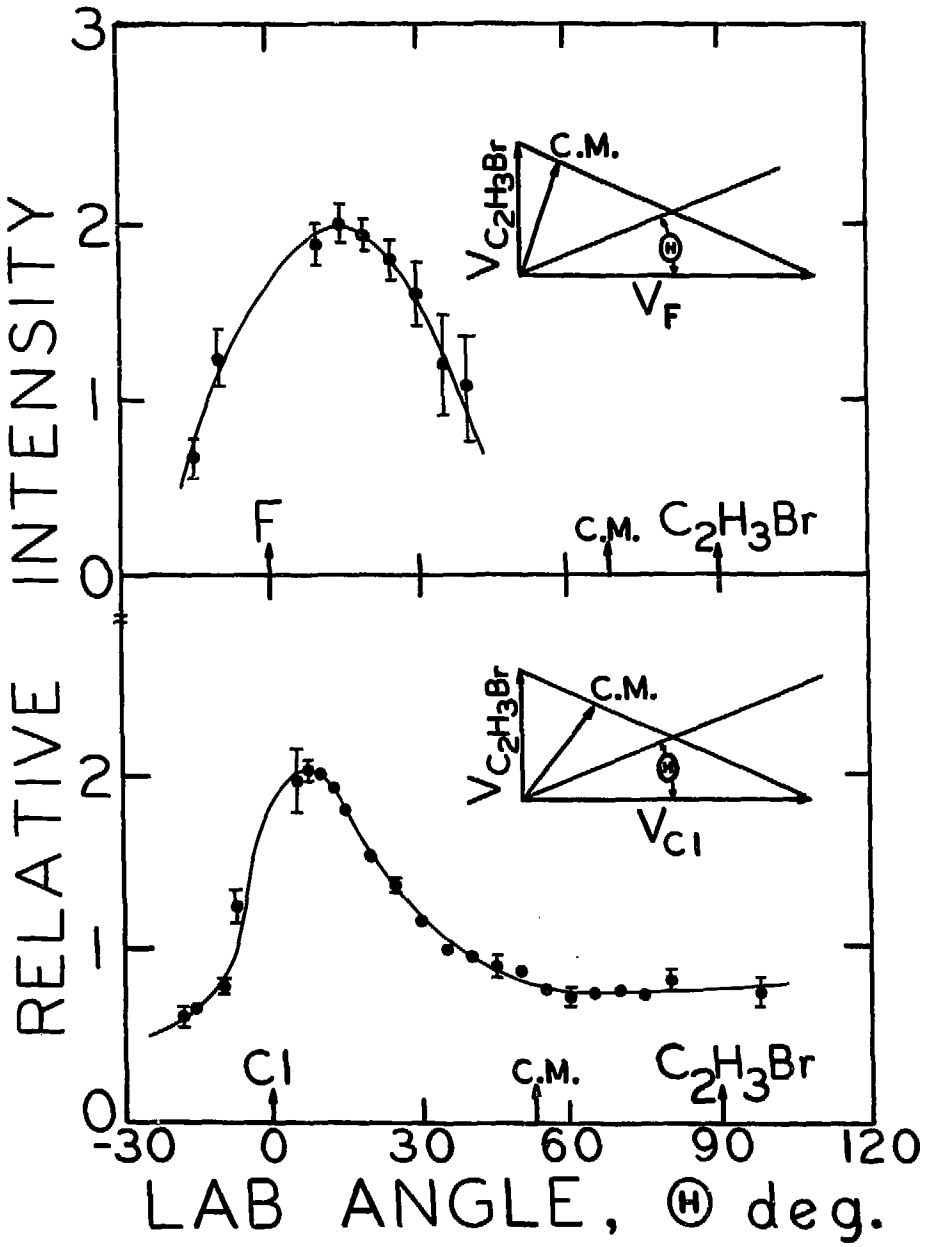

Fig. 1

XBL 7811-13180

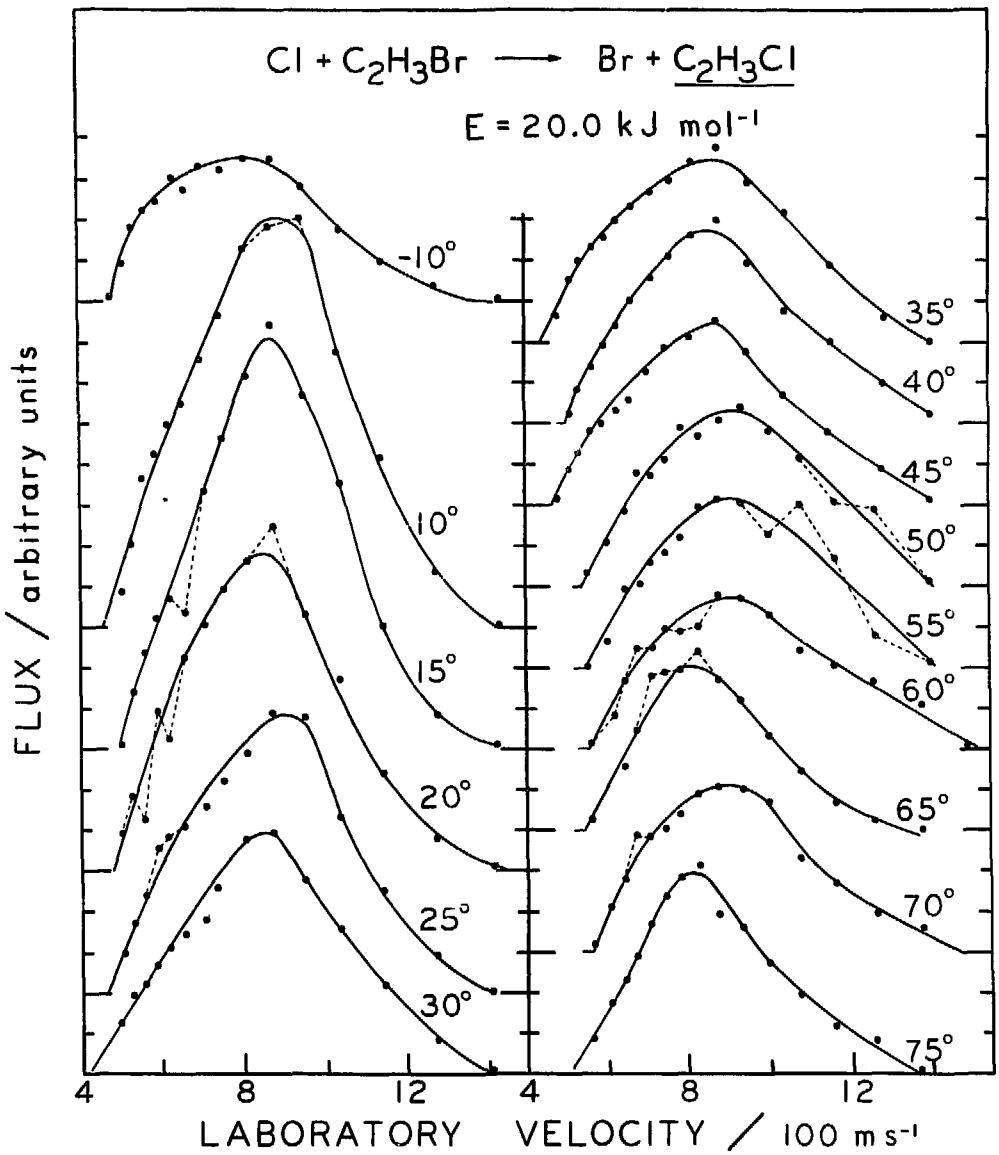

XBL 7811-13183

Fig. 2

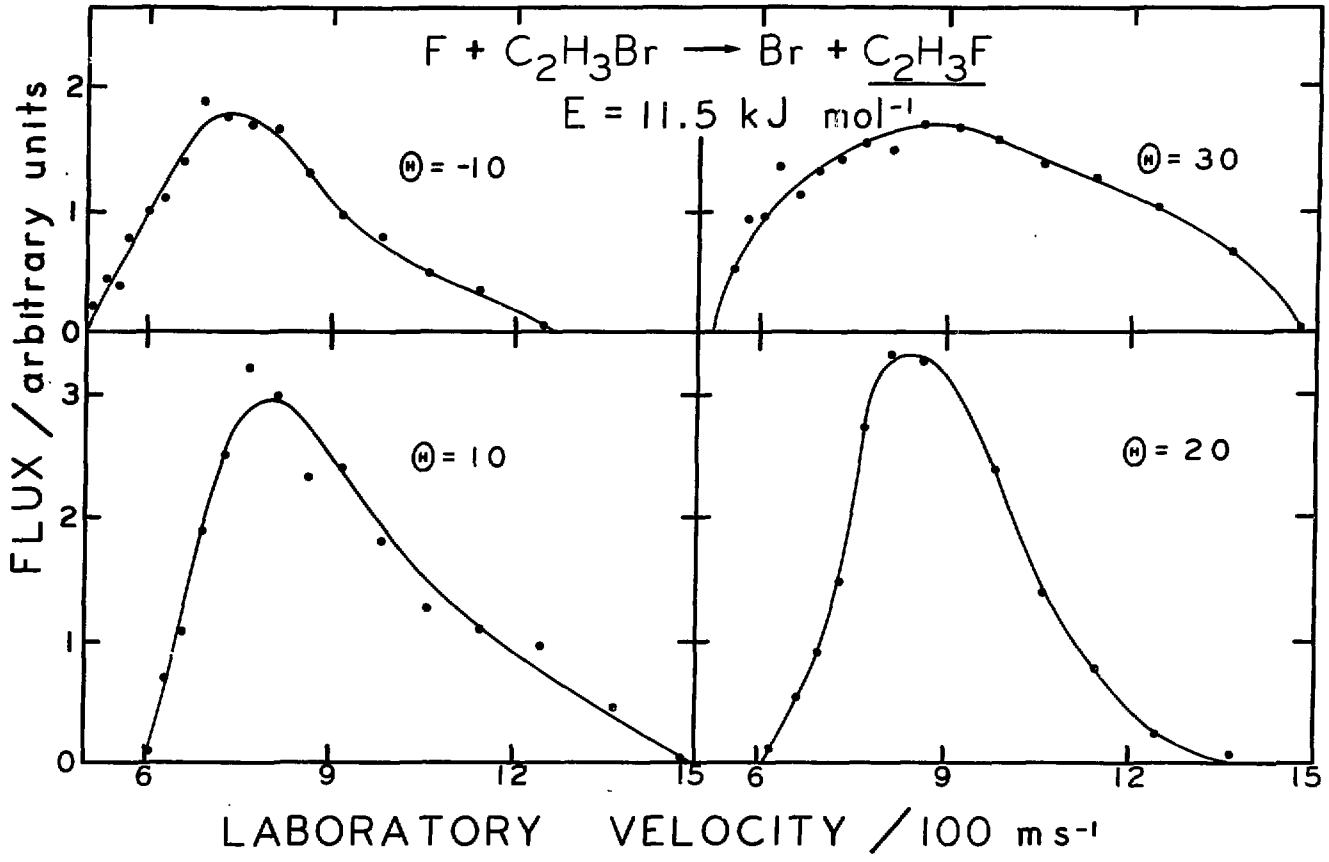

XBL 7811-13181

Fig. 3

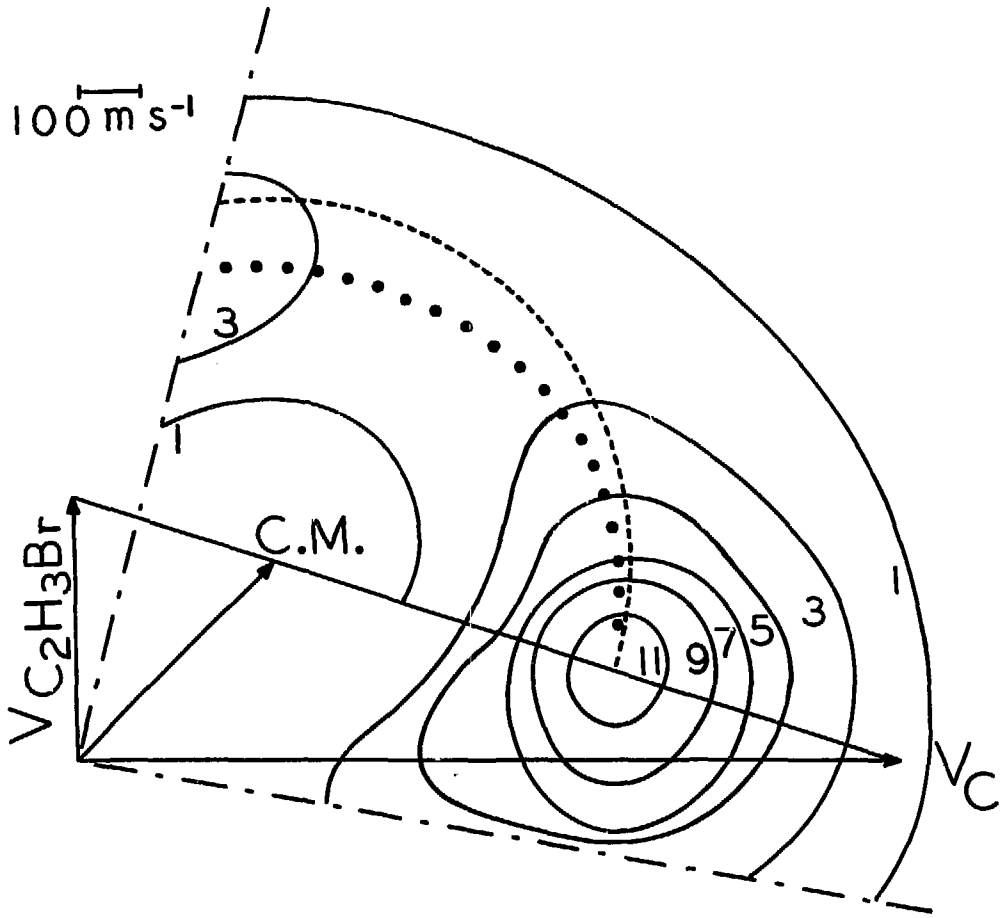

XBL 7811-13178

Fig. 4.

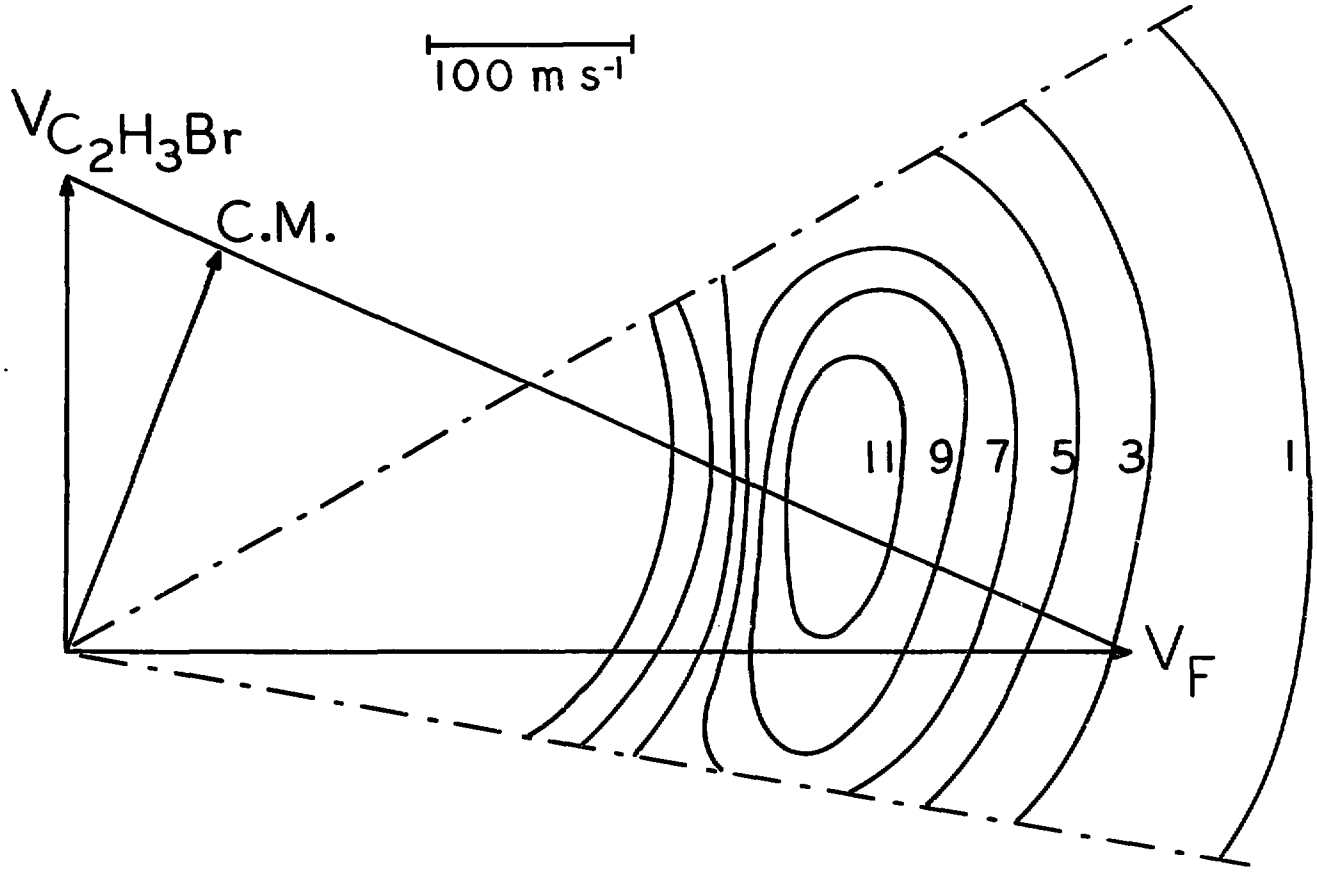

Fig. 5

XBL 7811-13179

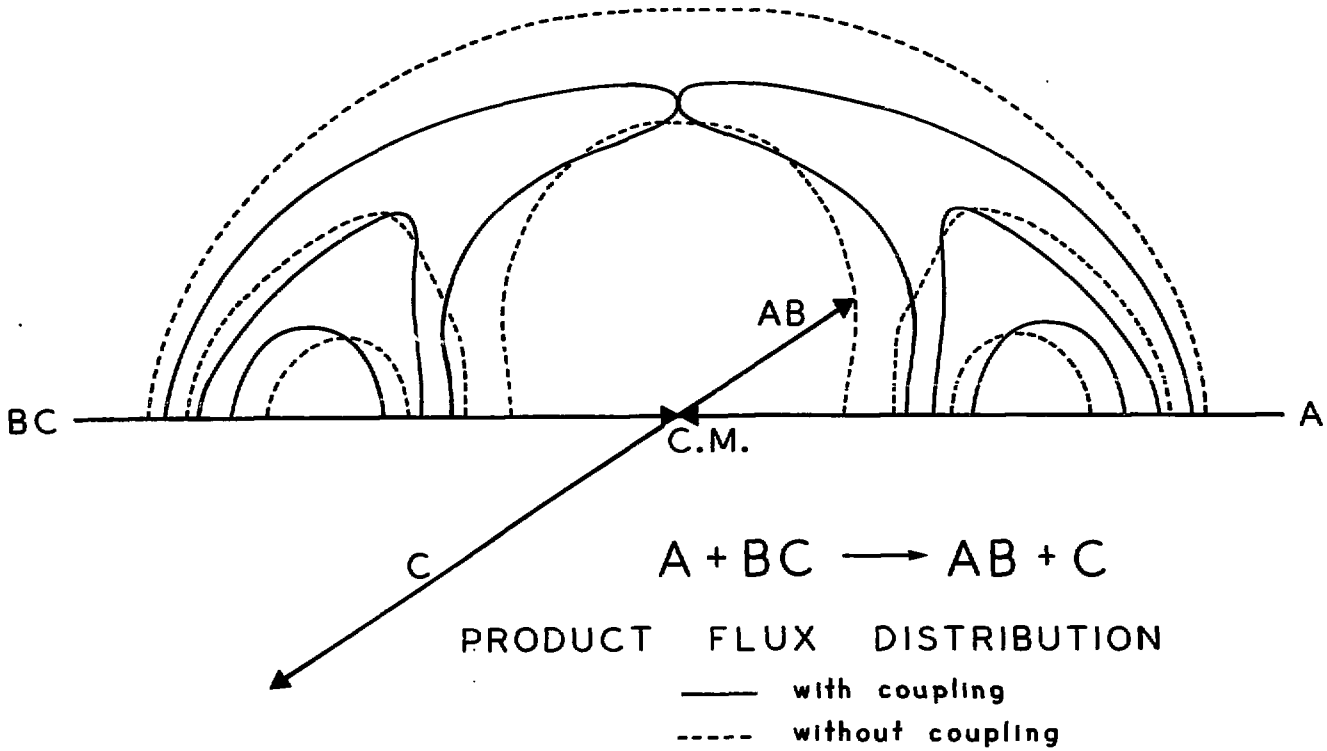

XBL 7812-13196

Fig. 6

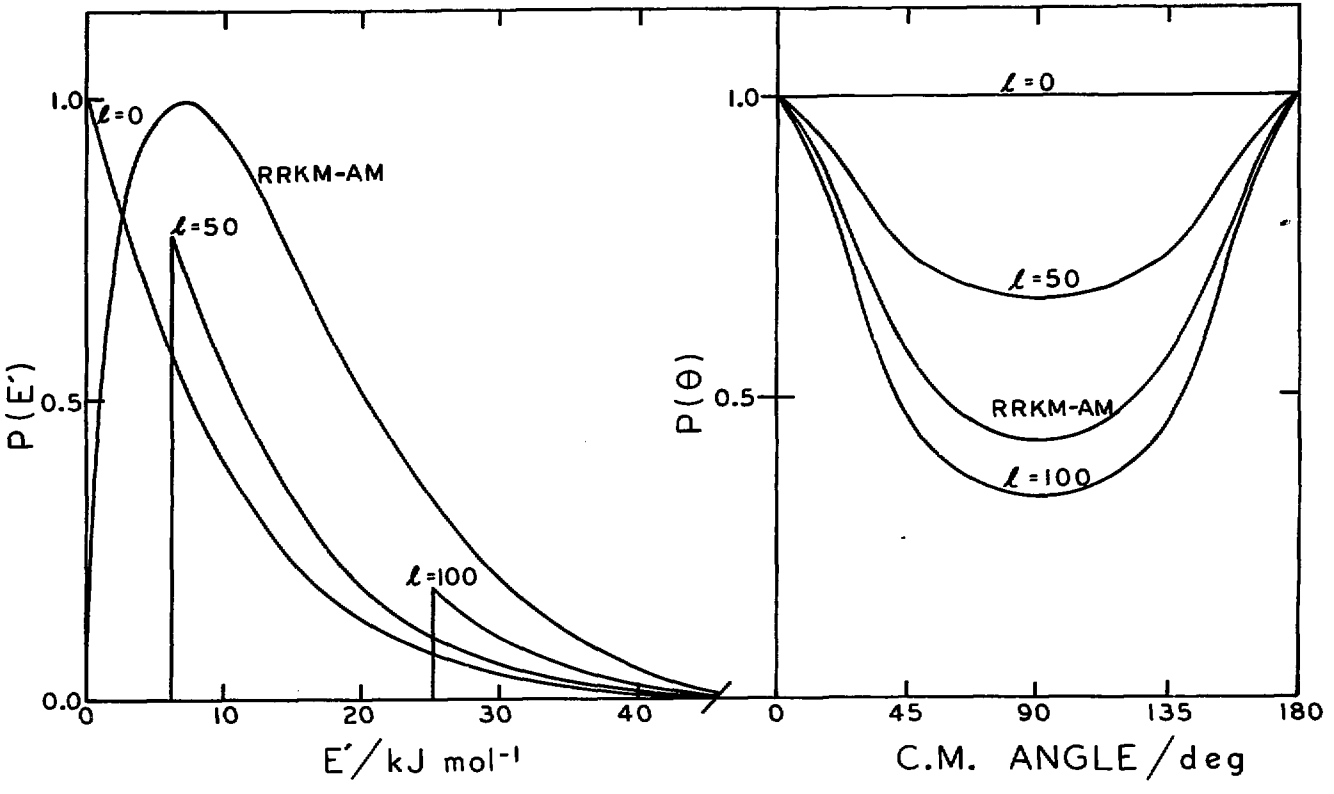

Fig. 7

XBL 7812-13224

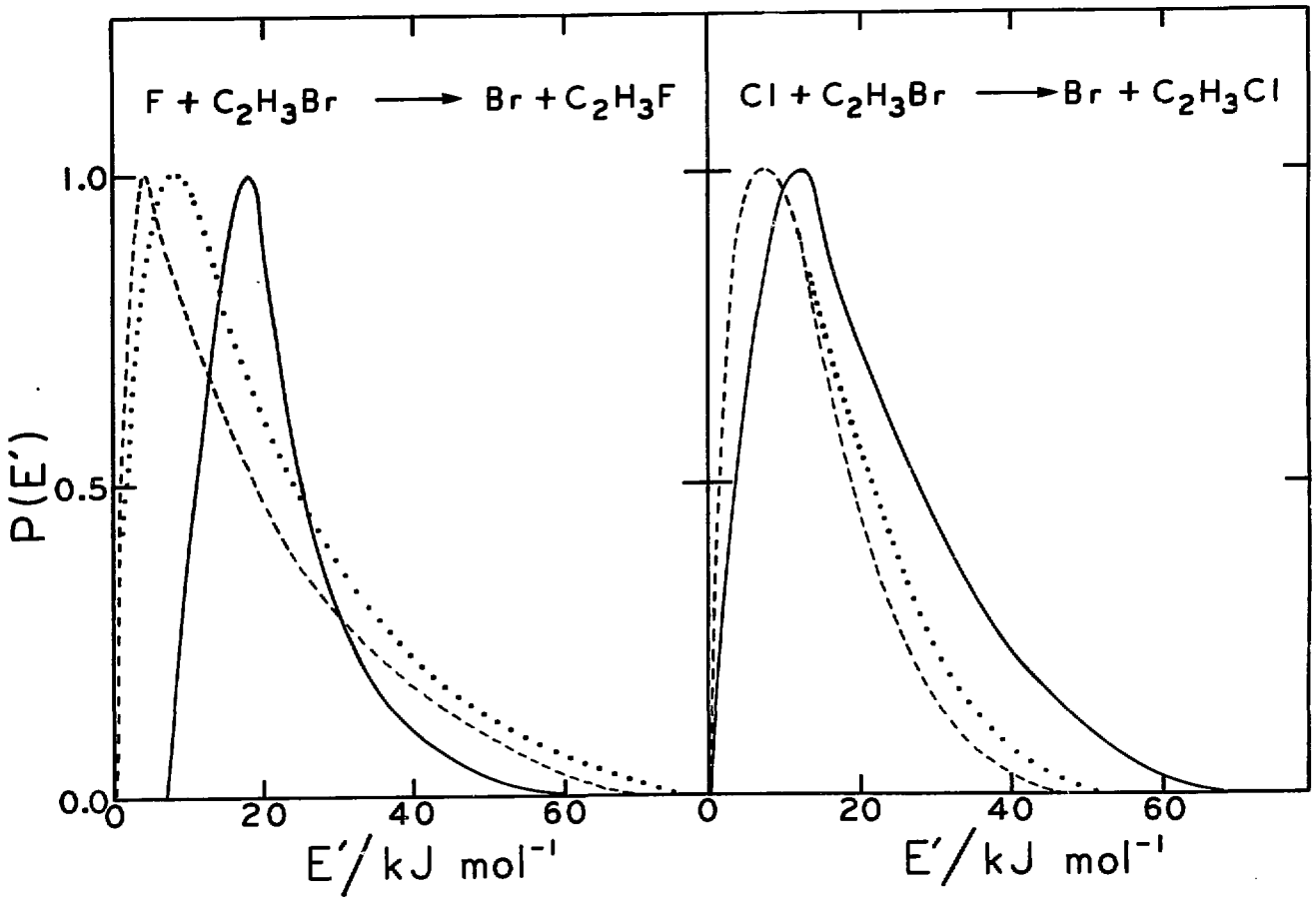

Fig. 8

XBL 7812-13225

III. THE REACTIONS OF Cl WITH 1, 2 AND 3-BROMOPROPENE

INTRODUCTION

The addition of chlorine atoms to unsaturated hydrocarbons has received considerable attention in recent years both in bulk phase experiments and with molecular beams. The radical formed in these reactions is more stable than the reactants by about 20 kcal mol^{-1}, making the lifetime sufficient to allow collisional stabilization in the bulk phase. Still, the radical thus formed is highly reactive so that most details of the collision dynamics can only be inferred by careful analysis of the complex mixture resulting from many bulk phase reactive encounters. Rate constant measurements, principally from photochlorination studies,[1] are in general agreement that, for chlorine atom addition to an olefinic hydrocarbon the activation energy is small, less than 1 kcal mol^{-1}. The rate constants are of moderate size, around 2×10^{-11} cc $molec^{-1}$ sec^{-1} and quite insensitive to the nature of the olefin. Attempts to determine the details of the chlorine addition such as preferred site for attack have been mostly inconclusive. Though there has been speculation that the initial attack is at the least substituted carbon[2] the evidence is weak, depending on product identification in bulk phase studies which do not

distinguish the chlorine attack from subsequent rearrangement.

Few bulk phase kinetic studies of chlorine with bromo-olefins have been reported, the rate constants for these reactions are poorly known. Dissociation of the chlorobromoalkyl radical by loss of a bromine atom has a small endoergicity around 9 kcal mol^{-1} so that, with the large energy released by the addition of Cl to the double bond the lifetime is expected to be very short. The use of crossed molecular beams to study these reactions under single collision conditions offers the possibility of gaining knowledge of the mechanistic details. From an initial study of the reaction of chlorine atoms with 1, 2 and 3-bromopropene using an effusive, thermal chlorine beam and a supersonic olefin beam, Cheung et al.[3] drew several interesting conclusions. The total cross sections were estimated to be 25 - 30 $Å^2$, considerably larger than the 0.5 - 3 $Å^2$ measured for chlorine addition to olefins[4] in the bulk phase. The lifetime of the intermediate in the vinylic reactions, that is, Cl + 1-, and 2-bromopropene, was found to exceed those calculated by RRKM theory and this was interpreted by postulating a mechanism involving chlorine attack on the carbon atom furthest from the bromine and a rate-limiting chlorine atom migration

before unimolecular decay. The allylic reaction, Cl + 3-bromopropene was interpreted differently as a direct attack of chlorine on the 1-carbon followed by rapid bond migration before bromine elimination. Their product translational energy distributions, P(E'), suggested that the vinylic reactions proceed via a statistical complex while the allylic reaction is nonstatistical. Additionally, analysis of product fragmentation in the mass spectrometer was used to determine the final site of the chlorine atom which appears to be at the carbon at which the bromine was originally located in the vinylic reactions and at the opposite end of the molecule for the allylic reaction.

The infrared chemiluminescence from these reactions has been measured under essentially single collision conditions by Durana and McDonald.[5] The vibrational energy distributions they obtain are quite nonstatistical for all three reactions, with the relative population of various vibrational modes differing strongly from the calculated distributions.

In order to clarify the question of product energy partitioning we have undertaken a high resolution study of the vinylic reactions

$$Cl + 1 \text{ and } 2\text{-}C_3H_5Br \rightarrow Br + 1 \text{ and } 2\text{-}C_3H_5Cl \qquad (1),(2)$$

and the allylic reaction

$$Cl + 3\text{-}C_3H_5Br \rightarrow Br + 3\text{-}C_3H_5Cl \qquad (3)$$

The experimental P(E') we have obtained differ dramatically from those of Cheung et al., being decidedly non-statistical, thus substantiating the findings of Durana and McDonald that the product partitioning of energy does not reflect equilibration of the energy among the internal modes of the complex. We find the P(E') for the three reactions to be quite similar.

EXPERIMENTAL

The experiment consisted of crossing two supersonic nozzle beams at right angles in a chamber equipped with a rotatable mass spectrometric detector. The pressure in the scattering chamber was maintained at 1×10^{-7} torr with a Varian oil diffusion pump and liquid nitrogen cooled chamber walls which are particularly effective in

reducing the background of the condensable products. Further details of the apparatus are discussed elsewhere.[6] The chlorine atoms were produced in a resistively heated graphite oven[7] from 1100 torr of a 5% Cl_2 in argon mixture. The peak of the chlorine velocity distribution was found to be 1330 m s^{-1} with a 30% FWHM. The olefins, 1, 2 and 3-bromopropene, obtained from Aldrich Chemical Company, Inc., were placed in a flask immersed in an ice/water bath. Argon gas was bubbled through the olefin to bring the total pressure to 400 torr and the mixture was expanded from a 0.1 mm nozzle at room temperature. The velocity distributions were characterized by time of flight analysis, the parameters describing the beams are given in Table I. The peak velocities were about 520 m s^{-1} with a spread of 20% FWHM.

All three bromopropene reagents were found to be contaminated by an impurity which fragmented in the ionizer to yield m/e = 76 which is the product chloropropene mass. The 3-bromopropene, which exhibited the worst contamination, was fractionally distilled but only minor improvement was obtained.

Angular distributions of total scattered intensity were measured by repeated scans of 100 second counts at

an angle with 150 hz mechanical chopping of the olefin beam and subtraction of the beam-flagged counts from the beam-open signal. Product velocity distributions at four laboratory angles were measured with the cross-correlation time-of-flight method[7] with 12 μs dwell time on each channel.

RESULTS AND ANALYSIS

The laboratory angular distributions of product intensity are shown in Fig. 1 for the three reactions. The error bars are one standard deviation of the mean of 10 measurements at each angle. Elastic scattering of impurity from the olefin beam made the product intensity nearer that beam unobtainable. Although the contaminant probably constituted less than 2% of the secondary beam, the elastic scattering occurs from both chlorine and argon, that is, 100% of the primary beam and has a greater cross section than does the reactive scattering.

The product velocity distributions are shown in Figs. 2, 3 and 4. The time-of-flight and angular data were deconvoluted by the ratio method of Siska[8] to remove the effect of the reactant velocity and angular spread. The procedure is to assume an initial two dimensional

laboratory flux distribution, $I_{LAB}(\Theta,v)$ and then smooth this function over a discrete number of Newton diagrams. The resulting averaged distribution $\overline{I}_{lab}(\Theta,v)$ is then compared to the experimental flux, $I_{EXP}(\Theta,v)$ and the initial guess is corrected by multiplying by the ratio $I_{EXP}(\Theta,v)/\overline{I}_{LAB}(\Theta,v)$. This procedure is repeated until convergence is obtained. The deconvolution method has, in common with other procedures, the inability to distinguish signal from noise, hence smoothing of the initial flux distributions is required in order to prevent extraneous features in the deconvoluted flux map. The resulting contour maps of product flux are shown in Figs. 5 and 6, superimposed on the most probable Newton diagram. The contour maps for reactions 1 and 2 are identical within the experimental error, and that for reaction 3 is only marginally different. The product flux in reaction 3 has a somewhat broader angular distribution and the velocity distribution along center of mass angle 0° is more sharply peaked.

From the deconvoluted flux distribution, the product translational energy distribution at each center of mass angle can be obtained. These are shown for 90° and 0° in Figs. 7 and 8 respectively and it is apparent that there is strong coupling of the angular distribution

T(Θ) and energy distribution similar to that obtained for the reactions of F and Cl with C_2H_3Br and the reactions of O with ICl and CF_3I, as described in chapters 2 and 4. The energy of the forward scattered product at 0° in the center of mass reference frame peaks around 5 kcal mol^{-1} while the P(E') at 90° is narrower and peaked at 1.5 kcal mol^{-1}. Calculations with assumed distributions for P(E') and T(Θ) smoothed over the velocity and angular spread of the reactants verified that no simple, uncoupled set of distributions could adequately reproduce the velocity data although the laboratory angular intensity data could be fit quite readily with a range of trial functions.

Calculation of the product P(E') were performed for the three reactions with the RRKM-AM model.[9] Because the energetics and frequencies are similar for all reactions, and the moments of inertia have a weak effect on the P(E'), no difference was observed in the calculated distribution for the three reactions. The RRKM calculation was performed at five collision energies spanning the experimental range and a single P(E') curve was obtained by integrating over the distribution of collision energies. The parameters used in the 2-bromopropene calculations are given in Table 2. The frequencies of the bromo-chloropropyl radical complex and of the critical configuration were estimated

by the BEBO method[10] using the published values of the fundamentals for the bromopropene and chloropropene molecules.[11]

With the absence of a potential barrier in the exit channel, the critical configuration was taken to be the maximum in the effective potential, V_{eff}. V_{eff} was approximated by the sum of the long-range attraction and the centrifugal energy:

$$V_{eff} = \frac{-C_6'}{r^6} + \frac{J(J+1)\hbar^2}{2\mu' r^2}$$

where μ' is the reduced mass of the products. Setting $dV_{eff}/dr = 0$, the location of the maximum in the effective potential is given by the relation:

$$r_m = \frac{6\mu' C_6'}{J(J+1)\hbar^2}$$

where the mean value of the angular momentum number J is estimated from the mean collision energy and the mean entrance channel impact parameter. The van der Waals C_6 constants for the entrance and exit channels were estimated by the method of Slater and Kirkwood[12] from the polarizabilities. Values of the chlorine and bromine atomic polarizabilities are available,[13] but those of the olefins

were estimated using additivities of bond polarizabilities.[14]

Angular momentum conservation was treated according to the method of Safron et al.[9] for loose complexes. The maximum centrifugal barrier, B'_m, given in equation 3-2, was obtained at each collision energy and was found to vary from 3 - 7 kcal mol^{-1} over the experimental range. When B'_m is significantly greater than the energy at which the P(E') curve peaks, as in this case, further increasing its value has only a small effect on the calculation.[9]

The bromo-chloro-propyl radical was estimated to be stable with respect to reactants by 22 kcal mol^{-1} using group contributions to the ΔH_f.[19] The total energy of the complex was taken to be the sum of the collision energy, the exoergicity of the chlorine addition, and the internal energy of the bromopropene reactant, which is estimated to be 1.5 kcal mol^{-1} after the supersonic expansion.

Calculations were performed with the RRKM program of Bunker with modification of the P(E') calculation to account for angular momentum conservation. Densities and sums of states were estimated using the semiclassical Whitten-Rabinovitch approximation[16] which should be excellent for these reactions in which the density of states is around 10^7 per wavenumber.

The two calculations shown in Fig. 7 differ in the number of frequencies assumed present in the complex. The dotted curve is the complete RRKM calculation with all 24 modes assumed to be active in energy exchange, while the dashed curve was calculated with only the nine skeletal modes active.

DISCUSSION

In the reaction of chlorine atoms with bromopropene, at our collision energy of 4 to 10 kcal mol^{-1}, five reactions are energetically possible.

		ΔH	
$Cl + C_3H_5Br \rightarrow$	$Br + C_3H_5Cl$	-14.5	2-1a
	$HCl + C_3H_4Br$	-15.0	2-1b
	$HBr + C_3H_4Cl$	-14.0	2-1c
	$BrCl + C_3H_5$	5.5	2-1d
	$CH_3 + C_2H_2ClBr$	8.7	2-1e

Chloropropene from reaction 2-1a was the only detectable product though little can be stated concerning the four center elimination reactions 2-1b and 2-1c because fragmentation of the parent molecules and high background make the product difficult to detect. The undissociated

Cl_2 molecules have several reactive channels which are exoergic and potentially observable.

		ΔH kcal mol^{-1}	
$Cl_2 + C_3H_5Br \rightarrow$	$HCl + C_3H_4BrCl$	-30	2-2a
	$HBr + C_3H_4Cl_2$	-29	2-2b
	$CH_3Br + C_2H_2Cl_2$	-17	2-2c
	$CH_3Cl + C_2H_2BrCl$	-16	2-2d
	$BrCl + C_3H_5Cl$	-9	2-2e

Product from the last reaction would interfere with detection of the Cl atom substitution products but lowering of the chlorine oven temperature to 1000°K was accompanied by loss of all mass 76 signal. No product from any of the four center reactions of Cl_2 with bromopropene were observed, probably because the barriers to reaction exceed the available energy.

The product translational energy distributions we obtain for the three reactions differ substantially from those obtained by Cheung et al.[3] Whereas the P(E') which they obtain for reaction 1 and 2 agree well with their statistical calculations, our results show far more energy in translation, peaking at greater energies and decaying gradually to zero at 25 kcal mol^{-1}. We observe a similar P(E') for the three bromopropene reactions in contrast to

Cheung's observations that the 3-bromopropene is exceptional in being nonstatistical. Comparison of our raw data with that of Cheung et al. does not reveal any strong discrepancies which would account for the difference in interpretation. The major disagreement occurs in the laboratory angular distribution of product near the center of mass angles where our signal is a factor of two greater than theirs. This unexplained difference is disconcerting but the intensity of the angular distribution near the center of mass is most strongly influenced by low energy product for these reactions. Slight modification of the shape of P(E') below 1 kcal mol^{-1} from the statistical curve is sufficient to fit our observed distribution near the center of mass. The shape of the high energy fall off in the P(E') curve is most directly related to the high velocity product and the angular intensity far from the center of mass. In these respects our data are quite similar to those of the previous study and the difference in conclusions is principally the result of higher resolution in our experiment. The supersonic chlorine beam, with its narrow velocity distribution allows careful specification of the collision energy and the location of the center of mass. The object of the deconvolution procedure is to find a product energy and angular distribution which, when averaged over the

reactant velocity and angle spreads, will reproduce the observed laboratory data. There will be a range of P(E') and T(Θ) which fit the data within experimental error. If extensive averaging is necessary, as is the case with a thermal reactant beam, the data become quite insensitive to the shape of the P(E'). Whereas with a Maxwell-Boltzman distribution of chlorine velocities, a narrow statistical P(E') may be broadened sufficiently to fit the high velocity tail in the flux distribution, the higher resolution obtained with the nozzle expansion allows the non statistical effects to be identified. In Figs. 7 and 8, error bars have been placed on the derived P(E') in order to indicate the accuracy which can be ascribed to the curves. These are estimated by combining the uncertainty in the data with the sensitivity of the calculation to the different parts of the energy curve. Assessing the accuracy of the P(E') produced from the crossed molecular beam experiment is a difficult procedure and the practice of reporting a range for the P(E') obtained appears unprecedented. In view of this, great care is necessary in interpreting the implications of the P(E') reported from crossed beam experiments, particularly when the experiment involves the use of thermal beams.

Our experimental P(E') are seen to be quite different from those calculated by statistical theory. This difference is most likely indicative of a quasi-direct mechanism in which the lifetime of the intermediate is so short that the dynamics of the reaction can not be well approximated by a treatment in which all vibrational degrees of freedom share the available energy. One simple method of introducing some dynamics into the statistical theory is the adjustment of the number of oscillators, S, in the complex. In the earlier formulation of unimolecular rate theory,[17] S was treated as a variable to achieve best fit to experimental rate constants. Later in the more complete treatment, S was identified with the sum of all vibrational modes of the complex and any active rotations, so that the statistical calculation truly reflected the assumption of complete energy randomization in the molecule. In the calculation of P(E') with the statistical theory a reduction in the effective complexity of the molecule will increase the fraction of energy partitioned to translation. When the experimental P(E') exhibits an excess of energy over the statistical calculation, as in these reactions, it is hoped that the dynamical effects can be accurately represented by a semi-statistical treatment in which a set of modes are separated as inactive in energy sharing.

When this is successful it remains speculative whether the agreement is fortuitous or if this is an accurate picture of the dynamical mechanism of reaction. In the chlorine reaction with bromopropene, removal of all hydrogen modes from the calculation is not sufficient to give agreement with the experimental P(E'). In addition to the extent of energy randomization in the complex, there are several other features of a reaction which can result in greater product translational energy. Classical trajectory studies have indicated that a potential barrier in the exit channel can profoundly alter the relative velocity distribution of the products as they separate. Sloane and Hase[18] have shown that, in the decomposition of excited C_2H_5 with a 3 kcal mol^{-1} barrier in the exit channel, the hydrogen velocity distribution, though statistical at the critical configuration is broadened and shifted after separation from the ethylene. Though little information has been obtained about addition of bromine atoms to a double bond, the few kinetic studies[19] suggest that this proceeds with negligible barrier as does fluorine and chlorine addition. The exit channel effects on the bromine velocity distribution should not be large, then, since there will be little repulsive force exerted between the separating fragments.

In the RRKM-AM statistical calculations, angular momentum conservation is treated in an approximate fashion. The distribution of angular momentum in the reacting complexes is an unknown but has a large influence on the product distributions including the energy partitioning. In reactions such as these, in which two massive rotationally cooled reactants collide forming a complex which dissociates into two massive products, the initial and final orbital angular momentum, L,L', strongly dominates the molecular angular momentum J,J' of the reactants and products. One visible consequence of this is the strong peaking of product on the relative velocity vector. This arises because the products are restricted to leave in or near the plane of rotation of the complex which, for every collision, contains the relative velocity vector. Contribution to product intensity at any other direction can come only from a fraction of the complexes. The forward-backward peaking becomes less distinct if the magnitude of J or J' is large compared to L or L' because the restriction that the product lie in the plane defined by the initial orbital angular momentum L is relaxed. Another consequence of the domination of J by L is the increase in product translation which arises because some of the

energy in the complex becomes fixed in rotation and is deposited in relative kinetic energy of the fragments. While the product flux from a molecule undergoing unimolecular decay would be expected to peak at zero energy in the absence of high rotational excitation, in these high angular momentum reactions the energy distribution is always found to peak at a non-zero energy. Though the distribution of angular momenta in the complexes is recognized to have a large effect on the product translation, little is known concerning the range of impact parameters which contribute to formation of complexes. The RRKM-AM treatment assumes that the reactants are spherically symmetric with the probability for formation of a collision complex being directly proportional to impact parameter, b, up to a maximum b_m which is determined by the long range forces. The validity of this assumption should be best for reactions in which there is no orientation dependence of the reaction probability and then only if the orbiting collision is similar in its reactivity to collisions at small impact parameters. If in fact, the chlorine atom must attack the bromopropene molecule at a special site or orientation, the distribution of angular momenta may be peaked about some value corresponding to the most probable impact parameter.

Cheung et al.[3] justify the assumption of a loose complex in these reactions by their large experimental total cross sections, 25 - 30 $Å^2$, which would suggest no orientation dependence. Bulk phase additions of chlorine atoms to olefins have generally indicated a much smaller cross section 0.5 - 2 $Å^2$ which would probably be indicative of preferential addition at a specific site. This discrepancy in total cross section is not explainable in terms of dynamical effects. The relation between Arrhenius pre-exponential factor and the molecular beam cross section is neither simple nor well understood.[20] For reactions with a large barrier, the magnitude of the thermal rate constant is governed largely by the tip of the Maxwell-Boltzmann distribution of collision energies and a sizeable fraction of the reaction occurs just above threshold. The pre-exponential factor in this case will reflect the reaction cross section near the threshold and cannot be compared easily with a molecular beam cross section determined at larger collision energies. In a reaction with negligible activation energy, such as those under consideration here, the pre-exponential factor will approximate a Boltzmann average of the cross section. If the cross section has little energy dependence the agreement between the Arrhenius pre-exponential and the molecular

beam cross section should be good. For the reaction with low activation energy, even if the energy dependence of the cross section is strong, the molecular beam result should be similar to the Arrhenius pre-exponential determined over the same energy range. Ordinarily, in a reactive scattering experiment, total cross sections, σ_{TOT} are obtained by comparing the elastic scattering of a reactant with elastic cross section calculations based on an assumed potential. The σ_{TOT} thus derived is rarely of high accuracy but would not be expected to be in error by more than a factor of 2. Cheung et al. used a different procedure based on attenuation of a beam contaminant at an angle 10° beyond the bromopropene beam. They assume that the intensity decrease at this angle when the chlorine beam is scattering can be related solely to the calculated total elastic scattering of the original contaminant out of this angle by chlorine atoms and molecules. This ignores the large effect of elastic scattering of contaminant into this angle from other angles greater than 10° beyond the beam. The result of this approximation would be a significant overestimate of the cross section, particularly if the angular spread of contaminant is broad which appears to be the case. If it is true that

the chlorine atom must attack at a carbon removed from the center of mass, which is located near the bromine atom, and the bromine tends to separate with small impact parameter, then the average centrifugal barrier for reacting molecules may be much higher than expected for a loose complex. The result would be a channeling of energy into product translation but the magnitude of the effect for these reactions is estimated from the geometries to be at most 6 kcal mol^{-1} extra energy. This is not sufficient to account for the deviations in the experimental P(E') from the statistical calculations. The strongly non-statistical behavior of these systems can only be attributed to dynamic effects which are observable because the lifetime is not long enough to allow energy randomization.

The distribution of product from these reactions can not be well represented by a separated center of mass angular and energy distribution, as there is a shift of product to smaller average energy in moving from 0° to 90°. The magnitude of this effect is similar to that observed in the reaction Cl + C_2H_3Br and probably arises from angular momentum conservation. The small impact parameter collisions produce complexes with low angular momentum and thus have negligible centrifugal

barrier to decomposition and no product angular constraints. In contrast the collisions with large impact parameter and high angular momentum have a centrifugal barrier and the products are strongly constrained to be in the plane perpendicular to the angular momentum vector. Because we measure the average of all impact parameters, we observe an energy distribution at 0° which is dominated by high angular momentum complexes and, at 90° one with large contributions from complexes formed with low impact parameters.

CONCLUSION

The reaction of chlorine atoms with 1, 2 and 3-bromopropene at about 6 kcal mol^{-1} collision energy, proceeds principally by the bromine substitution channel producing chloropropene. Although there is little or no barrier in the exit channel, the products exhibit a nonstatistical translational energy distribution. While some of the extra energy appearing in translation may be attributable to angular momentum effects, the major deviation from statistical theory is probably the result of a failure of the energy released in carbon-chlorine bond formation to redistribute among the internal degrees of freedom

before decomposition. These observations are consistent with the findings of Durana and McDonald that the products have a nonstatistical vibrational energy distribution. They also support the conclusions from the Cl + C_2H_3Br reaction that energy randomization is poor in halogen substitution reactions in which the statistical lifetime would be much less than a picosecond.

REFERENCES

1. F. S. Dainton, D. A. Lomax, and M. Weston, Trans. Faraday Soc., 1962, 58, 308; P. B. Ayscough, F. S. Fainton, and B. E. Fleischfresser, Trans. Faraday Doc., 1966, 62, 1846.

2. R. Kh. Freidlina, V. N. Kost, and M. Ya. Khorlina, Russian Chemical Review, 1962, 31, 1.

3. J. T. Cheung, J. D. McDonald, and D. R. Herschbach, J. Am. Chem. Soc., 1973, 95(23), 7887; see especially, J. T. Cheung, Ph.D. dissertation, Harvard University, Cambridge, Massachusetts, 1974.

4. P. B. Ayscough, F. S. Dainton, and B. E. Flieschfresser, Trans. Faraday Soc., 1966, 62, 1838.

5. J. F. Durana and J. D. McDonald, J. Chem. Phys., 1976, 64(6), 2518.

6. Y. T. Lee, J. D. McDonald, P. R. LeBreton, and D. R. Herschbach, Rev. Sci. Instrum., 1969, 40, 1402.

7. J. J. Valentini, Ph.D. dissertation, University of California, Berkeley, California, 1976.

8. P. E. Siska, J. Chem. Phys. 1973, 59, 6052.

9. For discussion of RRKM theory see W. Forst, Theory of Unimolecular Reactions, Academic Press, New York, 1973. For angular momentum treatment see S. A. Safron, N. D. Weinstein, D. R. Herschbach and J. C. Tully, Chem. Phys. Lett., 1972, 12, 564.

10. H. S. Johnston, Gas Phase Reaction Rate Theory, the Ronald Press Co., New York, 1966.

11. Vibrational frequencies for 1-C_3H_5Br: R. Elst, G. C. Van den Berg, and A. Oskam, Recl. Trav. Chim. Pays-Bas, 1972, 91(3), 417. For 1-C_3H_5Cl: G. C. Van den den Berg and R. Elst, Recl. Trav. Chimi. Pays-Bas, 1972, 91(1), 105. For 2-C_3H_5Br: R. Meyer and Hs. H. Günthard, Spectrochimica Acta, 1967, 23A, 2341. For 2-C_3H_5Cl: R. Meyer and Hs. H. Günthard, J. Chem. Phys., 1969, 50(1), 353. For 3-C_3H_5Br and 3-C_3H_5Cl: Yu. A. Pentin, E. V. Morozov, and Z. Sharipov, Vestn. Mosk. Univ. Ser. II, Khim., 1966, 21, 23.

12. J. C. Slater and J. G. Kirkwood, Phys. Rev. 193, 37, 682.

13. T. M. Miller and B. Bederson, Adv. in Mol. Phys., 1977, 13, 1.

14. J. O. Hirschfelder, C. F. Curtiss, and R. B. Bird, Molecular Theory of Gases and Liquids, John Wiley and Sons, Inc., New York, 1954, p. 947-951.

15. S. W. Benson, Thermochemical Kinetics, John Wiley and Sons, Inc., New York, 1968.

16. G. Z. Whitten and B. S. Rabinovitch, J. Chem. Phys., 1963, 38, 2466.

17. L. S. Kassel, Kinetics of Homogeneous Gas Reactions, Chemical Catalog Company, New York, 1932.

18. W. L. Hase, private communication.

19. J. A. Kerr and M. J. Parsonage, Evaluated Kinetic Data on Gas Phase Addition Reactions, The Chemical Rubber Company, Cleveland, 1972.

20. M. Menzinger and R. Wolfgang, Angew. Chem. Internat. Edit., 1969, 8, 438.

Table I.

	Peak Velocity x 10^4 cm/sec	Mach #	Mean Collision Energy	Energy Spread FWHM kcal mol^{-1}
Cl	13.3	6.0		
1-C_3H_5Br	5.24	10.5	6.62	3.3
2-C_3H_5Br	5.10	10.5	6.58	3.3
3-C_3H_5Br	5.34	10.5	6.63	3.3

Table II.

		$C_3H_5BrCl^*$	$C_3H_5BrCl^+$
Bond lengths Å	$r_{C=C}$	1.43	1.36
	r_{C-C}	1.49	1.49
	r_{C-Br}	1.96	2.67
	r_{C-Cl}	1.81	1.74
	r_{CH}	1.08	1.08
Angles(degrees)	<CCH	120.	120.
	<HCH	109.5	109.5
	<CC*	120.	120.
	<Cl-CBr	110.	110.
Frequencies cm^{-1}	V_{CH}	3116., 3012., 2986., 2970., 2940.,	3119., 3018., 2989., 2976., 2940.
	$V_{C=C}$	1423.	1633.
	∂_{HCH}	1444., 1444., 1413., 1378.	1447., 1447., 1418., 1380.
	V_{C-C}	1175.	1180.

Table II. (Continued)

	δ_{CCH}	1058., 1005., 928., 985., 685.	1052., 1002., 927., 982., 688.
	ν_{C-Cl}	555.	608.
	ν_{C-Br}	486.	R.C.
	δ_{CCCl}	375.	430.
	δ_{CCBr}	354.	91.
	δ_{CCCl}	343.	376.
	δ_{CCBr}	295.	67.
	δ_{ClCBr}	265.	70.
	τ	197.	196.
Moments of Inertia AMU Å^2		478.5	588.1
		355.1	475.1
		136.3	126.0

Table II. (Continued)

Energetics (kcal mol^{-1})		Polarizabilities ($Å^3$)	
ΔH = -14.5		Cl	2.18
E_C = 4.0 - 10.0		Br	3.05
E^* = 30.0 → 36.0		C_3H_5Cl	8.16
E° = 10.0		C_3H_5Br	9.15

$$C_6 = 6125 \text{ kcal } Å^6 \text{ mol}^{-1}$$

$$C_6' = 7239 \text{ kcal } Å^6 \text{ mol}^{-1}$$

$$B_m' = 0.54^* E_C$$

FIGURE CAPTIONS

Fig. 1. Laboratory angular distributions of chloropropene product from the reaction of Cl + 1, 2 and 3 bromopropene. Errors bars are one standard deviation of the mean of 10 measurements.

Fig. 2. Product flux distributions at different laboratory angles as determined from time of flight measurements for reaction 1.

Fig. 3. Product flux distributions at different laboratory angles as determined from time of flight measurements for reaction 2.

Fig. 4. Product flux distributions at different laboratory angles as determined from time of flight measurements for reaction 3..

Fig. 5. Contour map of product flux in the center of mass reference frame for reactions 1 and 2 shown with the most probable Newton diagram.

Fig. 6. Contour map of product flux in the center of mass reference frame for reaction 3 shown with the most probable Newton diagram.

Fig. 7. Product translational energy distributions. Solid line is the experimental curve along the center of mass angle Θ = 90 degrees. Dotted curve is the RRKM-AM calculation with all 24 vibrational

modes of the complex. Dotted curve is the same calculation with only 9 modes.

Fig. 8. Product translational energy distribution. Solid line is the experimental curve along $\theta = 0$ degrees, for reactions 1 and 2. Dashed curve is the same for reaction 3. Dotted curve is the complete RRKM-AM calculation.

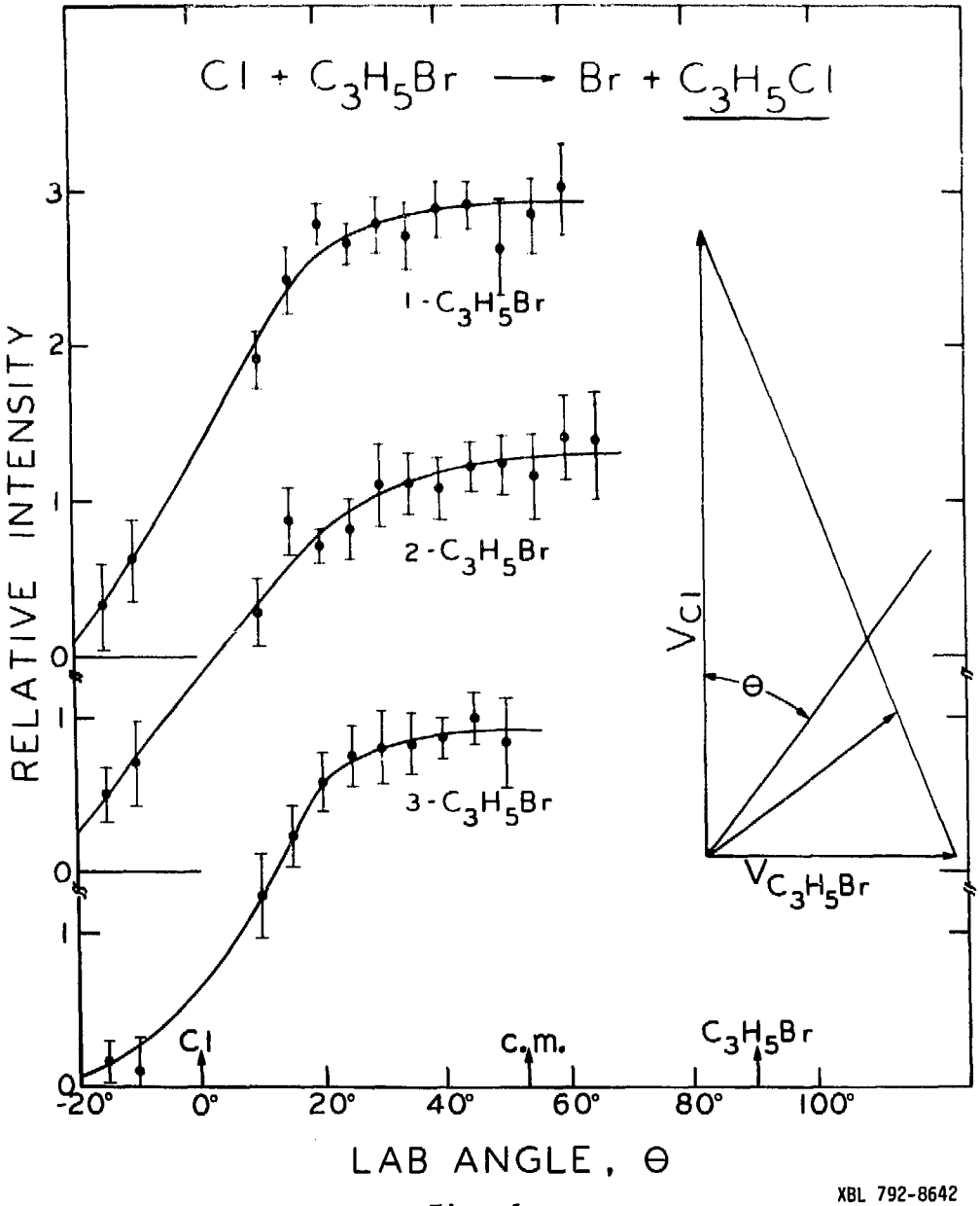

XBL 792-8642

Fig. 1

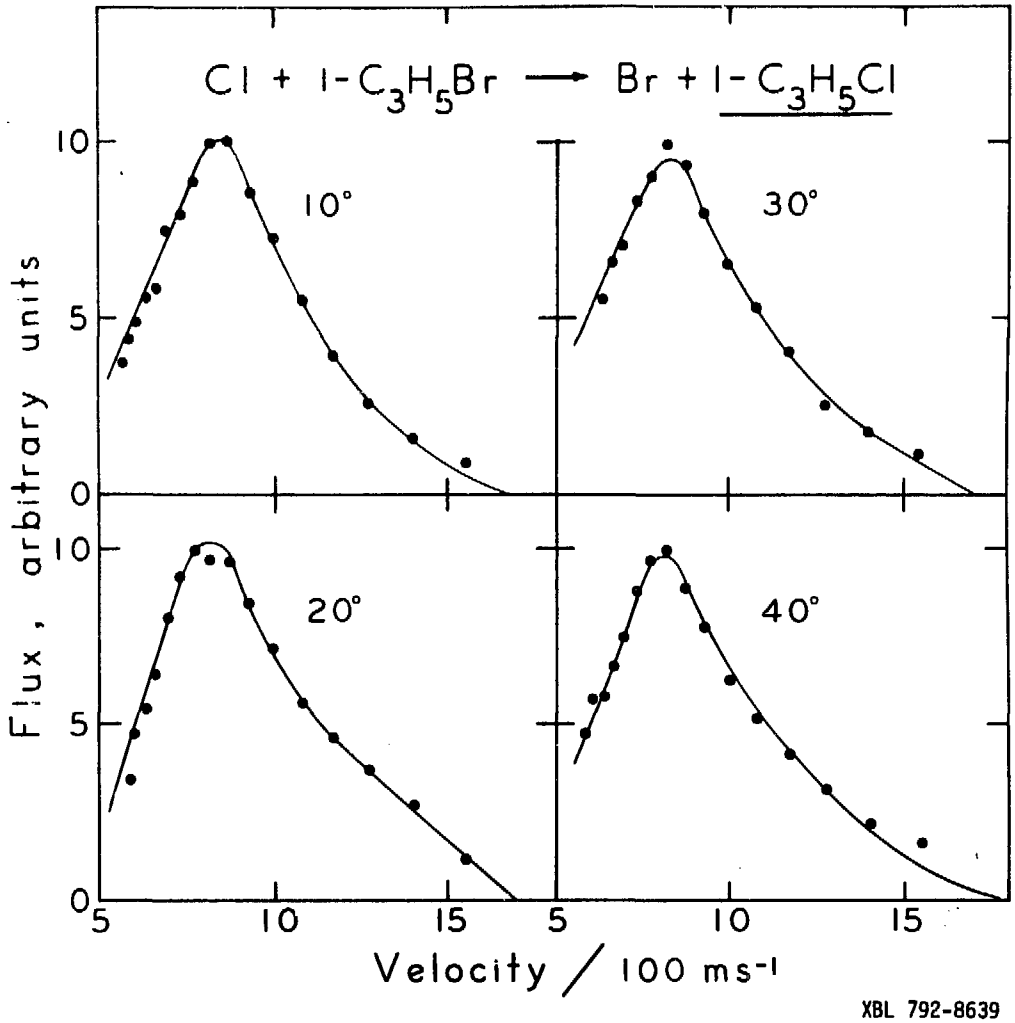
Cl + 1-C3H5Br → Br + 1-C3H5Cl
10°
30°
20°
40°
Flux, arbitrary units
Velocity / 100 ms-1
0
5
10
15
XBL 792-8639

Fig. 2

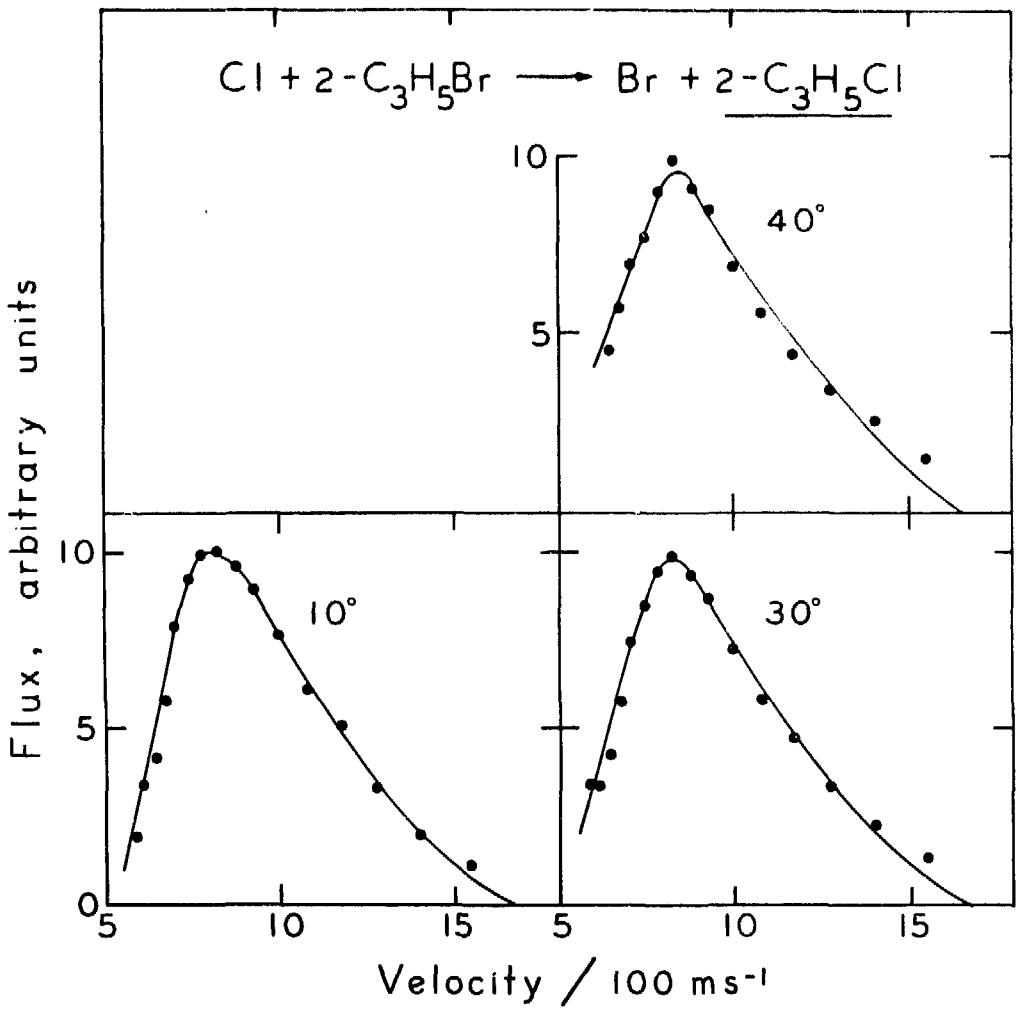

Fig. 3

XBL 792-8640

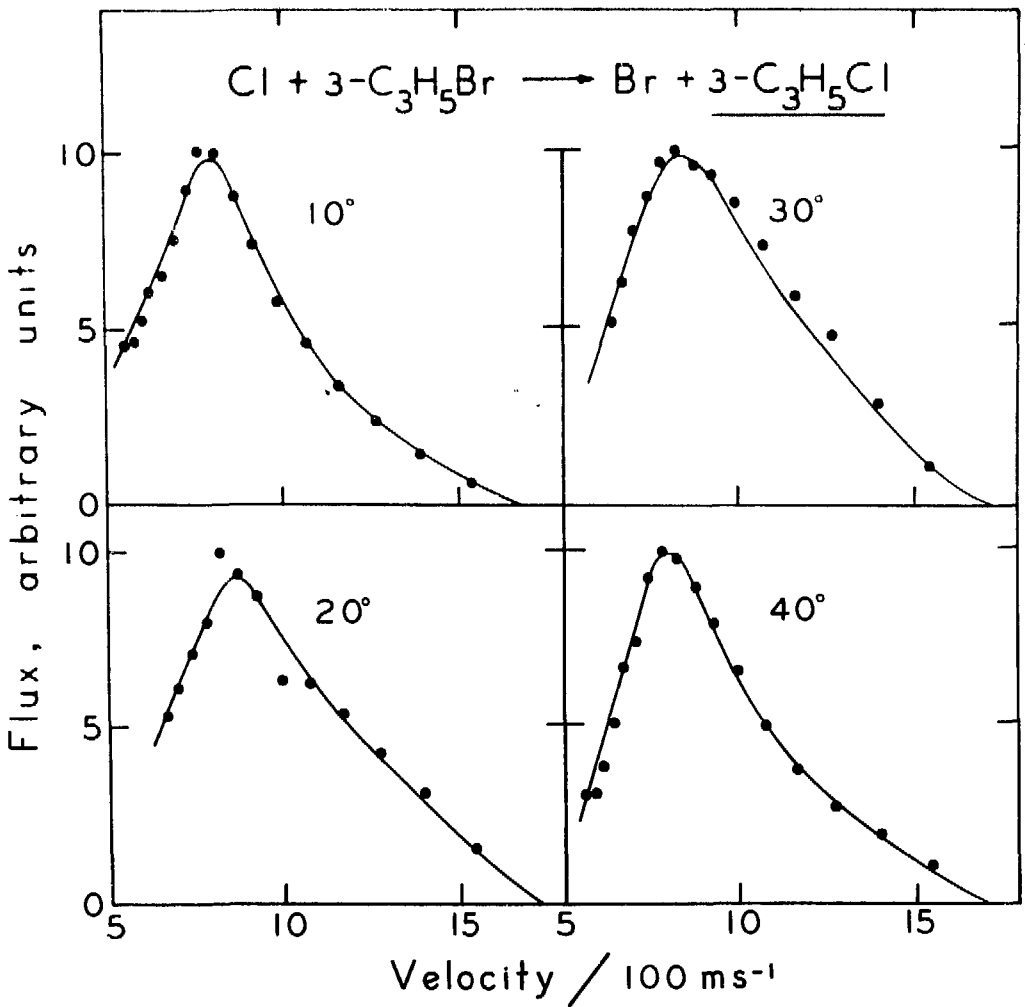

XBL 792-8641

Fig. 4

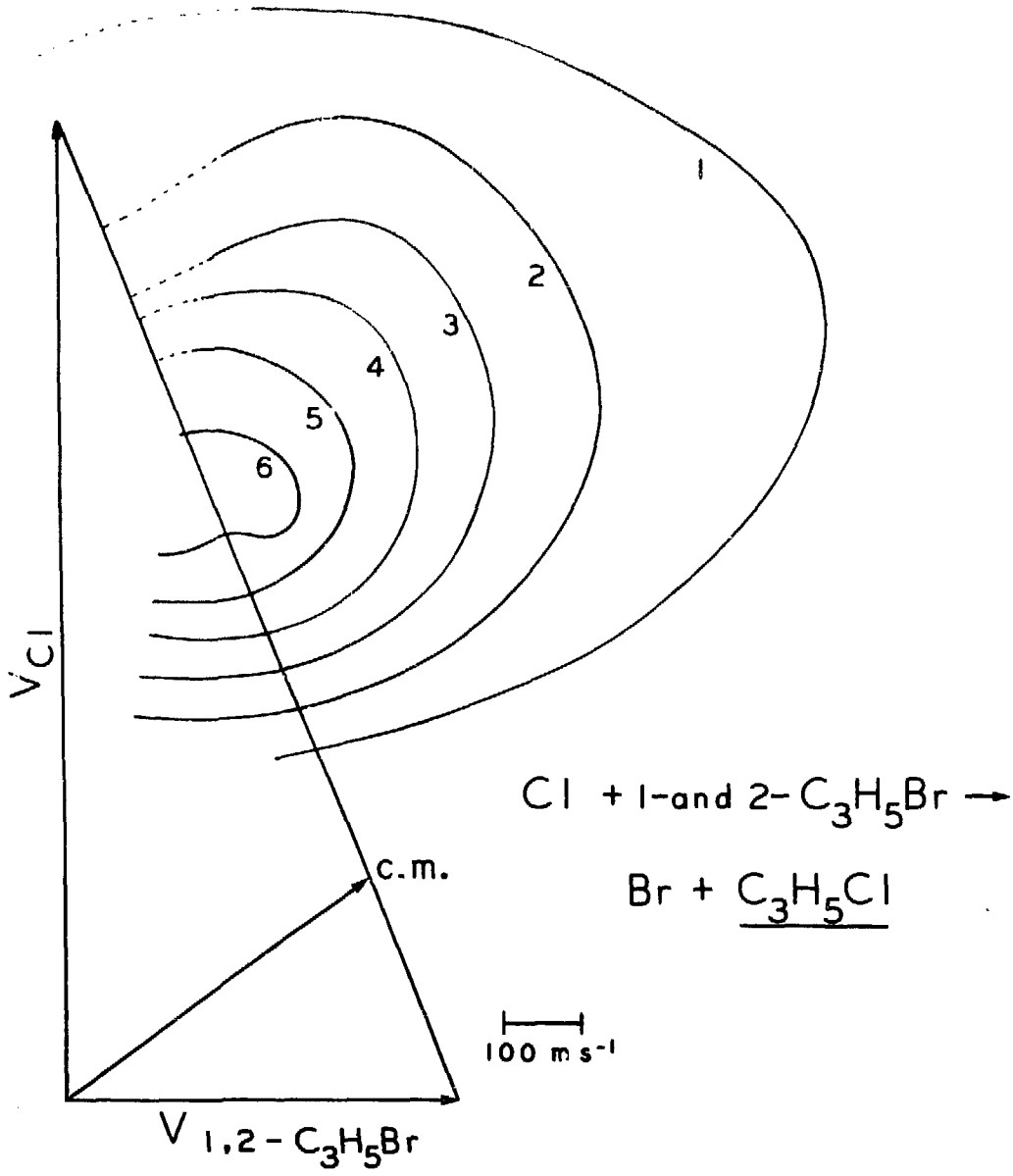

XBL 792-8644

Fig. 5

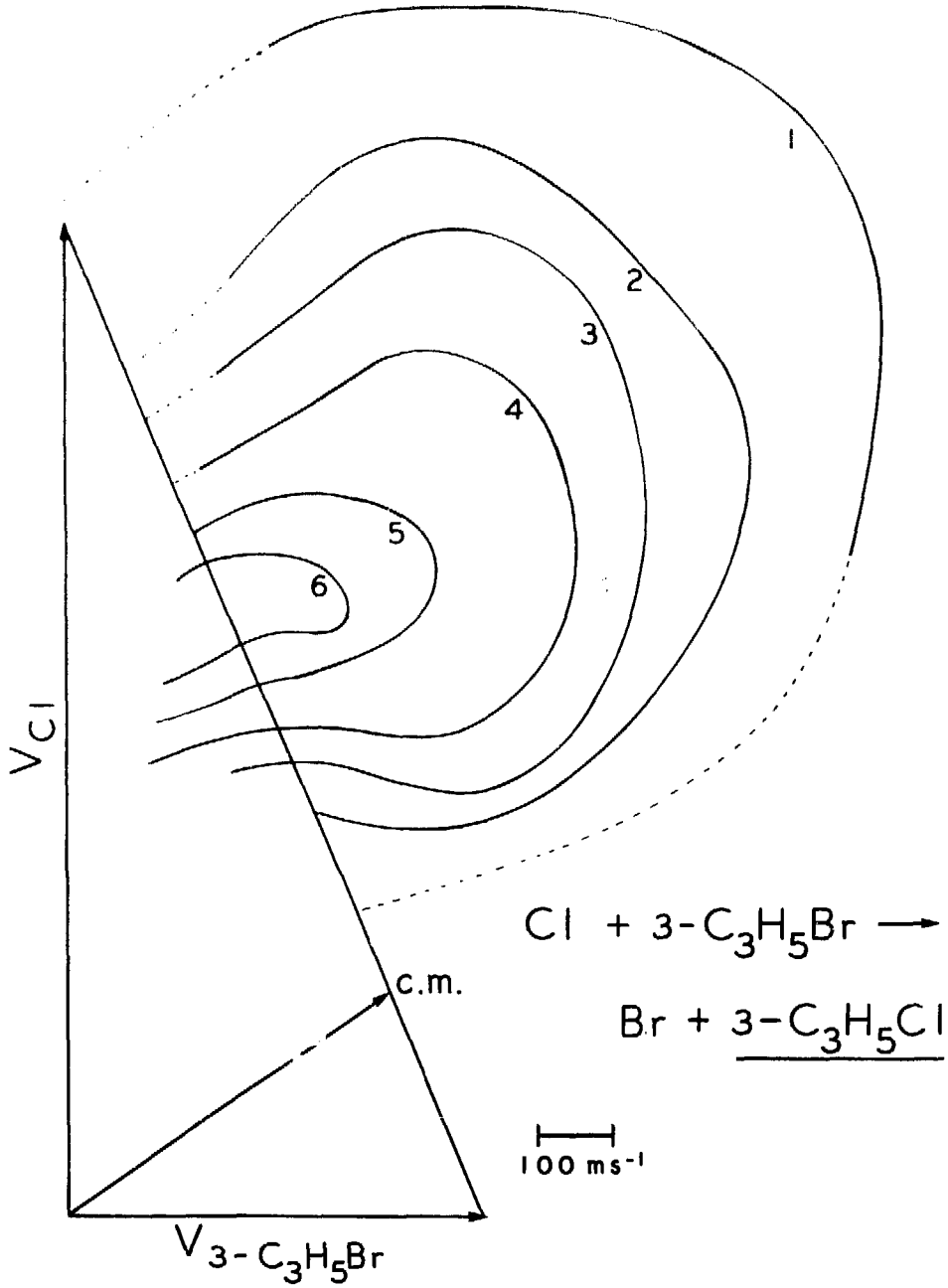

Fig. 6

XBL 792-8643

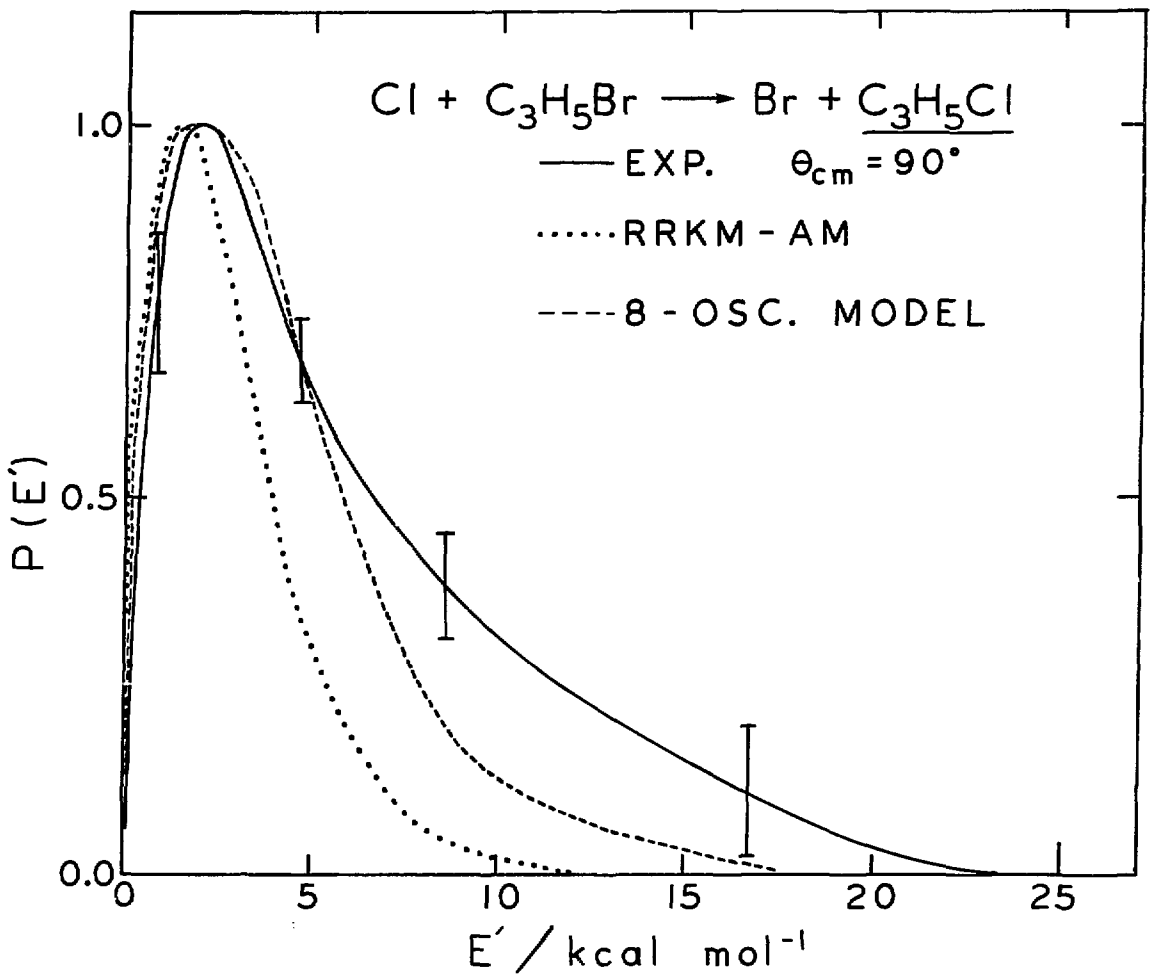

Fig. 7

XBL 792-8646

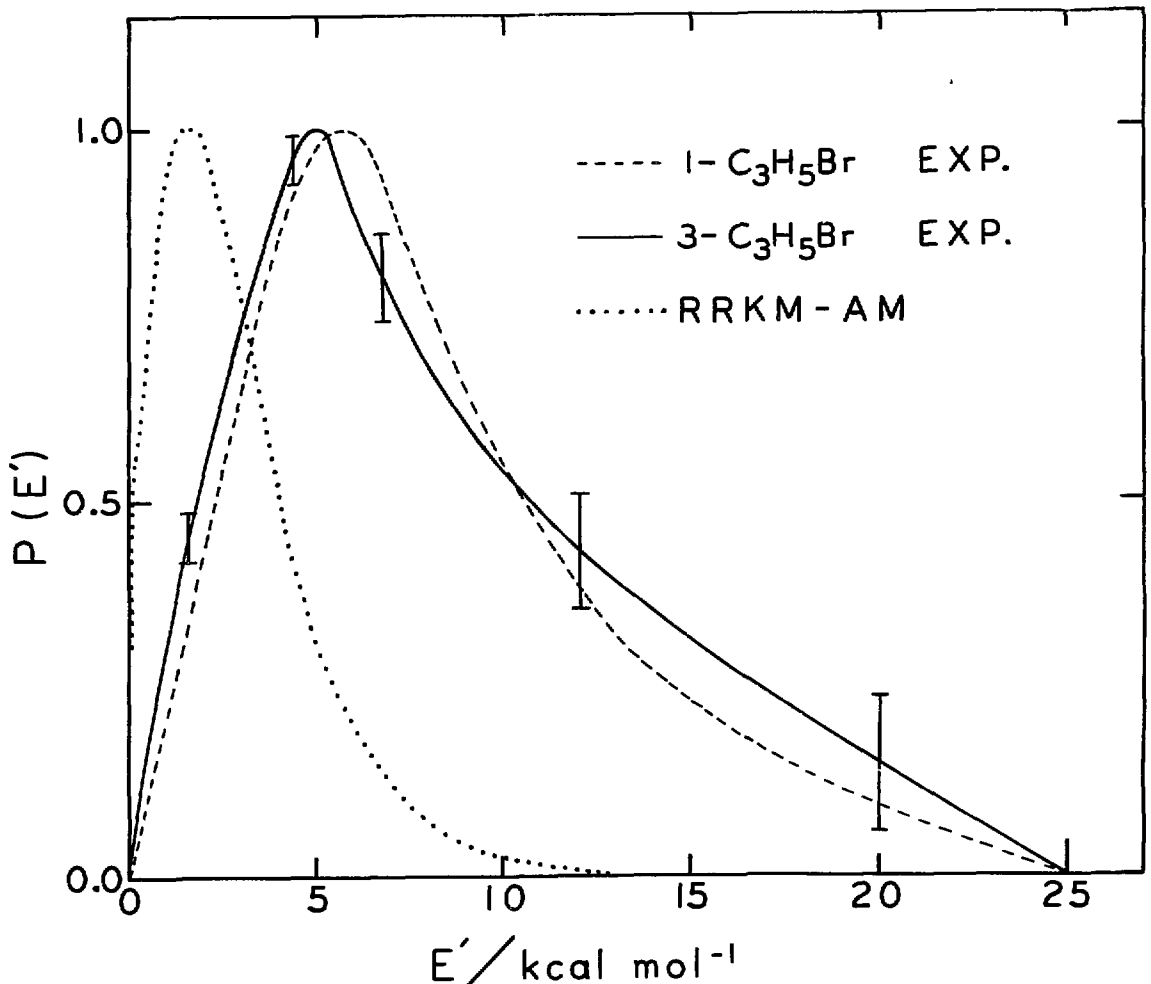

Fig. 8

XBL 792-8645

IV. THE CROSSED BEAM REACTION OF ATOMIC OXYGEN WITH ICl AND CF_3I

INTRODUCTION

The development of atomic oxygen beam sources in several laboratories has enabled the crossed molecular beam method to be applied to the study of oxygen reactions. Though relatively few oxygen atom reactions have been studied in beams to date, the activity is expected to increase rapidly as a consequence of the great importance of these reactions in understanding combustion processes as well as their significance in the upper atmosphere. For many reactions of oxygen atoms with hydrocarbons, the simple identity of the primary products of the bimolecular reaction is difficult to determine in the bulk phase because of the high reactivity of the radicals produced. Application of the molecular beam technique to the investigation of these reactions completely eliminates the problem of secondary reactions, allowing unambiguous identification of the primary pathway. Competing channels can be studied individually by mass selection of the products to derive branching ratios. Molecular beams have been used[1] to resolve the question of primary products in the $O + C_2H_4$ reaction by demonstrating that CHO and not CH_2O is the major product of the simple bimolecular reaction. Measurement of the angular and velocity distribution of product intensity can provide detailed dynamical information which may be very difficult or impossible to extract from

bulk phase experiments. For example, the crossed beam study[2] of F + I_2 suggested the existence of an attractive well in the potential energy surface for the reaction. This was verified by isolation of a stable I_2F molecule in the crossed beam reaction of F_2 with I_2.[3] The application of beams to oxygen atom reactions with hydrocarbons is not free from its own complications, though. For many interesting reactions, such as O + butene, the primary pathway may involve hydrogen atom abstraction, or methyl radical elimination, either of which results in serious product detection problems. The use of isotopically enriched reactants, though costly, should alleviate these problems.

The reactions with halogen diatomics have been among the first systems studied with the atomic oxygen sources. These are chemically interesting reactions in that the ground state reactants approach on a triplet potential energy surface which is an excited state of the triatomic intermediate with one electron promoted from the $3\pi^*$ to the $3\sigma^*$ orbital. The atom arrangement in the ground singlet state of the X_2O cannot be predicted easily from the electronegativity rule which states that the most electronegative atom will be located in the position of highest electron density. For these 20 electron systems, the 3π

molecular orbital which has greatest electron density on the end atoms and the $3\pi^*$, located principally on the center atom are all completely filled in the ground state. F_2O, Cl_2O and Br_2O are all found to have an XOX arrangement although the relative electronegativity of oxygen has changed from most positive in F_2O to most negative in Cl_2O and Br_2O. In the triplet state, in which one electron has been promoted to a $3\sigma^*$MO, the highest electron density should now be on the end atoms, directing the most electropositive atom, iodine, to the center position. The intermediate in the O + ICl reaction should then have an OXY arrangement unless an electronic transition to the singlet surface causes a geometrical rearrangement to XOY. In addition to their chemical interest, these reactions are attractive for their large cross sections and easy product detectability. Only the data for the reactions of O + ICl and I_2 by Grice et al.[4] have appeared in the literature, but papers summarizing results of O + Cl_2,[5] Br_2 and IBr[6] have been published. In all of these studies it is reported that the center of mass angular distributions of product flux are forward backward symmetric with the exception of the Cl_2 reaction in which Grice and coworkers[5] observe a shift to more forward scattering with increasing collision energy. In order to account for these long

lifetimes implied by forward backward symmetry, with a statistical theory, it is necessary to assume that the triatomic intermediate is very stable with respect to decomposition, by 20 kcal mol^{-1} for the Br_2 reaction.[6] The similar FICl complex has been found to be stable by 16 kcal mol^{-1}.[7]

The reactions of O with ICl and IBr provide the most direct test of the possibility for reaction on the singlet surface, in which event the production of OCl or OBr is highly favored energetically. Instead, it is reported that IO is the sole observed product in both cases. While ClOCl and BrOBr are well-known, stable species, a large barrier to rearrangement of the initially formed OXX probably exists. We report here our recent studies of the reactions of oxygen atoms with ICl and CF_3I carried out at higher resolution using a supersonic oxygen atom beam source. In the previous study of O + ICl by Grice and coworkers, with an effusive oxygen beam source,[4] they applied a long-lived collision complex model to deduce a bond energy for the IO product, but the applicability of the long-lived complex model for this reaction is not convincing. In particular the recent laser induced fluorescence studies of the similar F + ICl reaction[8] has shown that the IF vibrational distribution is highly

inverted in contradiction to a statistical long-lived model. Grice and coworkers have also studied the iodine abstraction reaction O + CF_3I.[9] The product from the reaction at two collision energies shows no evidence of the strong peaking on the relative velocity vector which is expected from the domination of orbital angular momentum in a reaction with a relatively large cross section and expected to go through a long-lived complex. At both collision energies, some product is observed with energy in excess of the total available for translation, and hence the comparison with statistical theory is very poor. Their model calculation in which they have reduced the number of oscillators which share the available energy from 12 to 6 and have increased the available energy to well over twice its maximum possible value, still fails to account for the high energy product they observed. Our investigation of the O + ICl reaction with a supersonic oxygen atom beam is generally in agreement with the results of Grice and coworkers. The lifetime of the complex appears to be somewhat shorter and we obtain a slightly higher IO bond energy, though not inconsistent with their value in view of the uncertainties in the determination. On the other hand, our results for the reaction of O + CF_3I are not in line with the conclusions of the previous study of Grice and

coworkers. They are, actually, found to be quite similar to the results of the F + CH_3I reaction.[10]

EXPERIMENTAL

The crossed beam apparatus and data acquisition techniques were similar to those described previously.[11] The oxygen atom source, described in detail elsewhere,[12] employs a high pressure RF plasma, carefully localized at the nozzle, to achieve a high oxygen flux with reasonably narrow velocity spread and 80% dissociation. With a 5% O_2 in argon mixture at 100 torr pressure, we produced a peak velocity 1050 ms^{-1} with a FWHM velocity spread of 40%. This velocity distribution, while considerably narrower than an effusive source is still substantially poorer than that obtained in low temperature and high pressure supersonic expansions. The narrowness of the velocity distribution has been found[13] to depend principally on the Knudsen number, that is the ratio of viscosity-based mean free path behind the nozzle to the nozzle diameter. The high temperature, ~1400 K, of the oxygen atom nozzle combined with the low stagnation pressure required for plasma stability result in a relatively low Knudsen number. The principal pressure limitation was imposed by the pumping

speed of the Varian VS-10 oil diffusion pump on the source chamber. If the pressure in this region exceed 4×10^{-5} torr, the RF power will be dissipated through gaseous discharge of the entire chamber. Subsequent development of the source, including the change to a Varian VHS-400 diffusion pump with approximately twice the pumping speed, has resulted in improved Mach numbers. The ICl, practical grade from Matheson Coleman and Bell, at its vapor pressure of 70 torr in an oil bath at 310°K was mixed with argon to bring the total pressure to 240 torr. The increased velocity which results from the argon seeding does not significantly alter the collision energy because the magnitude of the relative velocity vector is determined mainly by the substantially higher oxygen atom velocity. The entire glass gas line was heated at least 10°K above the bath temperature to prevent condensation of the ICl. This mixture, approximately 30% ICl, was expanded from a 0.1 mm quartz nozzle at 329°K. The ICl beam was measured with the time-of-flight method to have a peak intensity at 502. ms^{-1} and a FWHM velocity spread of 29%. The supersonic CF_3I beam was produced with the same nozzle conditions at 250 torr pressure of CF_3I from PCR Research Chemicals Inc. without further purification. The beam velocity distribution peaked at 266 ms^{-1} with FWHM velocity spread of 30%

corresponding to near complete relaxation of translation, rotation and two low frequency vibrations. Under these conditions the reacting CF_3I should have an average internal energy around 1 kcal mol^{-1}. The mean collision energy for the ICl reaction is 2.36 kcal mol^{-1} with FWHM = 0.8 kcal mol^{-1} while that for the CF_3I reaction is 2.18 kcal mol^{-1} with FWHM = 0.8 kcal mol^{-1}. Laboratory angular distributions of product number density were taken by repeated scans of 100 second counts at each angle. The oxygen beam was modulated at 150 hz with a tuning fork and the signal obtained by subtracting the chopper-closed count from the chopper-open count. The IO product signal intensity at the peak of the angular distribution was approximately 15 counts per second with background 30 counts per second. Velocity distributions at each angle were obtained with the cross-correlation time-of-flight technique[14] with 12 μsec per channel time resolution. Counting time varied from one to three hours at an angle.

RESULTS

The only observed product of the O + ICl reaction was IO. With the increased background at the ClO mass, 51, and uncertainties in relative detection efficiencies we can only

estimate that less than 10% of the reaction goes through the channel producing I + ClO. The laboratory angular distributions of IO product are shown in Fig. 1 with error bars showing standard deviation of the mean of 10 measurements. The product from both reactions is seen to peak near the center of mass though slight bimodality is observed in the ICl reaction. The product velocity distributions are shown in Figs. 2 and 3 together with the best fit calculations using the iterative deconvolution technique of Siska.[15] The contour maps of center-of-mass product flux in Figs. 4 and 5 are deconvoluted distributions, which, when averaged over the reactant beam velocities, will produce the best-fit lines in Figs. 1, 2 and 3. The transformation of center-of-mass flux $I_{cm}(\theta,u)$ to laboratory number density flux, $N(\Theta,v)$ is given by the equation[16]

$$N(\Theta,v) = \frac{v}{u^2} I_{cm}(\theta,u) \qquad (1)$$

The effect of the Jacobian v/u^2 for the coordinate transformation is seen in the strong enhancement of the low energy product about the center-of-mass angle in both reactions. While the product flux actually peaks strongly on the relative velocity vector well-removed from the center-of-mass, as seen in Figs. 4 and 5, the observed

laboratory intensity falls off rapidly away from the center-of-mass angle. At angles greater than 20 degrees from the center-of-mass, the time necessary for obtaining an acceptable signal to noise ratio in the time of flight measurements became prohibitive, even with use of the cross correlation technique which gives a data acquisition advantage of a factor of 20 over the conventional time of flight method.

Some backscattered product is observed in both reactions but, in neither case is there sufficient intensity to produce symmetry about 90°. Fitting of the angular and velocity data with an uncoupled center-of-mass energy distribution, P(E') and center-of-mass angular distribution, T(θ), indicates that the ratio of flux at 0° to that at 180° is about 2.0 for the ICl and 2.2 for the CF_3I reaction.

The product velocity and angular distributions in the center-of-mass reference frame, in fact, exhibit rather strong coupling in both reactions as can be seen in Figs. 4 and 5. The velocity at which the flux peaks decreases smoothly as the center-of-mass angle increases from 0° to 90°.

The experimental P(E') shown in Figs. 6 and 7 are the average energy distributions between 0° and 90°. Each theoretical curve was obtained by calculating P(E') with the RRKM-AM model[17] for five collision energies spanning

the experimental range and the P(E') were summed over the distribution of collision energies in the experiment. Parameters used in the calculations are shown in Table I and II. The curves are calculations for three values of the IO bond energy; 53.0, 55.0 and 57.0 kcal mol^{-1} all vibrational modes of the complex are assumed to participate in energy sharing. The OICl complex was assumed to be bent with the least electronegative atom, iodine, in the center and an angle 115 degrees. Simple molecular orbital theory[18] suggests that the ground state of a 20 electron triatomic will be strongly bent, principally because the highest occupied $3\pi^*$ orbital favors a bent geometry. This is observed for F_2O, 103 degrees and Cl_2O, 111 degrees. In the triplet state of the OICl molecule, one of the $3\pi^*$ electrons has been promoted to a strongly linear directing $3\sigma^*$ orbital. The triplet state should be less strongly bent, more like the 19 electron systems, for example ClO_2, 118 degrees. The bond lengths and stretching frequencies are estimated from experimental bond lengths and vibrations of the diatomics ICl and IO using a simple bond energy bond order treatment.[19] The OICl bending frequency has been taken to be similar to the bend for ClO_2 and Cl_2O for lack of more similar molecules. In a similar way, vibrational frequencies and geometries for CF_3 and CF_3I[20] were used to derive estimates of the CF_3IO complex and critical

configuration. The choice of frequencies and the effect of the geometry, which enters the calculation only as the moments of inertia, on the calculated P(E') is miniscule. A calculation was performed for each system with all frequencies of the critical configuration reduced by 10% and, although this increased the calculated rate constants by a factor of 10, the change in the P(E') was extremely slight. The stability of the complexes in both reactions was assumed to be 16 kcal mol^{-1}. The depth of the well, while having no effect on the translational energy distribution, strongly influences the calculated lifetimes. Initially, calculation of the maximum exit-channel centrifugal barrier, B'_m, followed the prescription of Safron et al.,[21] for a loose complex,

$$B'_m = \left(\frac{\mu}{\mu'}\right)^{3/2} \left(\frac{C_6}{C'_6}\right)^{1/2} E_c \qquad (2)$$

where μ, μ' are the reduced masses of the reactants and products, C_6, C'_6 the respective long-range attraction force constants and E_c is the collision energy. The C_6 constants were estimated using the Slater Kirkwood method[22] and the polarizabilities which are available for some of the species. The other polarizabilities were estimated by the additive method.[23] An improved fit to the ICl data was obtained by

increasing B'_m to 0.454 E_c, approximately double the value, 0.26 E_c, calculated with the C_6 constants. The principal effect, here, is to move the calculated peak of the energy distribution from 0.9 to 1.5 kcal mol^{-1} and to increase the high energy tail somewhat.

DISCUSSION

In attempting to deduce the exothermicity of a reaction from analysis of the product in a cross beam experiment, one looks to the high energy fall off to set a lower bound. The accuracy of the determination depends on good specification of the collision energy to reduce uncertainties resulting from energy dependence of the cross section. In their O + ICl study[4] using a microwave discharge generated effusive oxygen atom beam, Grice et al. correctly pointed out that the spread in centroid vector location is most strongly affected by the ICl velocity and is only mildy broadened by the oxygen atom velocity spread. A more important effect of the beam velocity spread, though, is the concomitant uncertainty in collision energy. The collision energy is conveniently expressed in terms of the two masses and energies as $E_c = \frac{m_1E_1 + m_2E_2}{m_1 + m_2}$. With a reaction like O + ICl in which which the mass mismatch is quite large, the

energy of the light particle is the dominant factor in determining the collision energy. Use of an effusive oxygen atom beam, then, leads to large uncertainty in the collision energy. For a reaction which is almost thermoneutral in which the collision energy is a large fraction of the total energy available for translation, the energy spread will make more difficult the interpretations. The use of narrow velocity distributions of the reactants to produce a well-defined collision energy enables one to assign a minimum exothermicity necessary to give the observed product with proper energy conservation. The resolution limitations of the time of flight method introduce the greatest uncertainty for the molecules with highest speed and account has been taken of this in the analysis of the high energy data. For the reaction of O + ICl an approximate lower bound of 3.5 kcal mol^{-1} can be assigned the exothermicity. In general, it might be difficult to obtain a better knowledge of the reaction energetics without additional knowledge of the internal excitation of products, but this specific reaction is particularly well-suited for making a more definitive determination of exothermicity. Although the exact product translational energy distributions depend on both exothermicity and reaction dynamics, for systems with a small number of internal degrees of

freedom the observed fall-off of high energy product is more sensitive to the actual total energy available than to the reaction dynamics. Relying on fitting the fall-off region, we obtain an exothermicity $\Delta H = -5.5 \pm 2.0$ kcal mol^{-1} for the reaction O + ICl → IO + Cl, from which, with the known ΔH_f of the other species,[24] we deduce an IO bond energy 55.0 ± 2.0 kcal mol^{-1}. As demonstrated in Fig. 6, calculations with the RRKM-AM model agree well with these conclusions if the maximum certifugal barrier, B_m', is taken as a variable to achieve best fit.

The value of B_m' specifies the degree to which conservation of angular momentum causes energy to be stored in rotational motion of the complex to be partitioned to translation of the products. If the long-range dispersion force between the reactants determines the maximum impact parameter for capture, then B_m' is related simply to the ratio of entrance to exit channel C_6 constants, as in equation 2. We estimate that the C_6 constant for O + ICl is 1920. kcal $Å^6$ mol^{-1} or about half the C_6' for Cl + IO, 3780. kcal $Å^6$ mol^{-1}. In order to fit the experimental results we have increased the ratio of C_6/C_6' by a factor of four, requiring that the exit channel C_6' be half the entrance channel C_6. This cannot be physically realistic in view of the much greater polarizability of chlorine,

2.14 $Å^3$ than that of oxygen, 0.77 $Å^3$. Considering the uncertainties in reaction energetics, it is not clear that the improved fit with B_m' increased indicates a nonstatistical translational energy distribution. Nonstatistical effects have been observed in measured chemiluminescence from the reaction of F + ICl,[8] in which the vibrational population of the IF product was found to be strongly inverted, while the rotational distribution of energy appeared statistical. This implies that the partitioning of energy to translation is less than statistical.

Our slightly higher IO bond energy is not inconsistent with 53 ± 3 kcal mole obtained by Grice and coworkers[25] although reliance on the statistical calculation to derive this value by comparing the overall features is questionable for this reaction. The RRKM lifetime is calculated to be exceedingly short, 0.3 ps, a region in which nonstatistical effects have been observed in several other reactions.[20] The density of states in the complex at the dissociation energy is very low, approximately 1 per cm^{-1}, hence the products might be expected to exhibit more dynamical effects. Additionally, the uncertainties in treatment of angular momentum may introduce too much flexibility to the model, making it unreliable for thermodynamic data determination. Finally, the use of the velocity

distribution along the centroid in reference 25 is contra-indicated because the severe Jacobian enhancement at this angle tends to overwhelm the information contained in the high energy tail.

The product from the CF_3I reaction is shown in Fig. 7 to agree well with statistical calculations using the IO bond energy determined above. The density of states for the CF_3I-O complex at the dissociation energy is about 10^7 per cm^{-1} and the calculated lifetime about 2 ps, although uncertainties in the energetics of the complex as well as its frequencies reduce the significance of these figures. Grice and coworkers[9] report their study of this reaction at two higher collision energies in which they observe high energy product far exceeding the total available for translation. The conditions of the reactants are too well specified to attribute this to uncertainty in internal energy, thus the explanation must lie in some systematic error. Their reported center-of-mass angular distribution shows no peaking on the relative velocity vector though the kinematics of the reactions almost require this. The contour map in Fig. 5 shows the strong forward scattered product observed in our experiment. Although Jacobian enhancement of the product has produced strong peaking at the center-of-mass angle, transformation

to the CM reference frame demonstrates the peaking on the relative velocity vector away from the center-of-mass.

The asymmetry of product about 90° in both reactions is not inconsistent with the statistical calculations if the intermediates in both reactions are assumed to be stable by 16 kcal mol^{-1} with respect to the products. The rotational period is estimated to be 0.8 - 3.0 ps for the ICl and 1-5 ps for the CF_3I reactions, in each case comparable to the calculated lifetime. While at a lower collision energy, 0.81 kcal mol^{-1} Radlein et al.[4] observed forward backward symmetry in the O + ICl reaction, given the uncertainties in rotational period, stability of the intermediate, and collision energy, we do not consider this a point of disagreement.

The coupling of product energy and angular distributions which is observed here can arise from several dynamical effects. The observation of such coupling in direct reactions with product repulsion has been reported,[26] but the energetics of these two reactions preclude this mechanism as an explanation. The exoergicity is not large enough for there to be strong repulsion forces in the exit channel. More pertinent is the coupling which should arise even in long lived complexes from the distribution and the disposal of angular momentum.[27] Because both the product

energy and angular distributions vary with impact parameter, the observed distributions, averaged over all possible impact parameters will retain the coupling. Grice and coworkers[5] have reported observing strong coupling of P(E') and T(θ) in the O + Cl_2 reaction and have suggested that this may result from the lifetime shortening of complexes with large angular momentum. Such an effect should occur to some degree and, if it is the dominant cause of the coupling, will give qualitatively different product distributions from the mechanism described above. The lifetime shortening effect of angular momentum should cause the forward scattered product to exhibit a markedly different P(E') than the backscattered product. The coupling described in chapter 2 for long lived complexes will be observed as an increase in translational energy of both forward and backward scattered product relative to the side-scattered product.

CONCLUSION

We have used the reaction of O + ICl to obtain an improved value of the IO bond energy by analysis of the high energy fall off in the translational energy distribution. The experimental P(E') did not deviate strongly from

calculations with a long-lived complex model though a good fit required increasing the exit channel centrifugal barrier to a physically unrealistic value. The reaction of oxygen atoms with CF_3I appears to proceed through a complex with a mean lifetime comparable to the rotational period. The product translational energy for this system agrees quite well with the RRKM-AM calculations.

REFERENCES

1. J. R. Kanopky and D. Gutman, Chem. Phys. Lett., 1972, 15(2), 236.

2. Y. C. Wong and Y. T. Lee, Disc. Faraday Soc., 1973, 55, 383.

3. M. J. Coggiola, J. J. Valentini and Y. T. Lee, Int. J. of Chem. Kin., 1976, 8, 605.

4. D. St. A. G. Radlein, J. C. Whitehead, and R. Grice, Mol. Phys., 1975, 29, 1813.

5. P. A. Gorry, C. V. Nowikow and R. Grice, Chem. Phys. Lett., 1977, 49(1), 116.

6. D. D. Parrish, D. R. Herchbach, J. Am. Chem. Soc., 1973, 95(18), 6133.

7. J. J. Valentini, M. J. Coggiola, Y. T. Lee, Faraday Disc., 1977, 62, 232.

8. J. Wanner, private communication.

9. P. A. Gorry, C. V. Nowikow and R. Grice, Chem. Phys. Lett. 1978, 55(1), 24.

10. J. M. Farrar and Y. T. Lee, J. Chem. Phys. 1975, 63(8), 3639.

11. Y. T. Lee, J. D. McDonald, P. R. LeBreton and D. R. Herchbach, Rev. Sci. Instrum., 1969, 40, 1402. For data acquisition, see J. J. Valentini, Ph.D. dissertation, University of California, Berkeley, California, 1976.

12. S. J. Sibener, R. J. Buss, and Y. T. Lee, XIth International Symposium on Rarefied Gas Dynamics, Cannes, France, 1978 (also to be published S. J. Sibener, R. J. Buss, and Y. T. Lee, Rev. Sci. Instr.).

13. J. B. Anderson and J. B. Fenn, Phys. Fluids, 1965, 8, 780.

14. V. L. Hirschy and J. P. Aldridge, Rev. Sci. Instr. 1971, 42, 381. Also see J. M. Farrar, Ph.D. dissertation, University of Chicago, Chicago, Illinois, 19 .

15. P. E. Siska, J. Chem. Phys., 1973, 59, 6052.

16. E. A. Entemann, Ph.D. dissertation, Harvard University, Cambridge, Mass., 1967, also T. T. Warnock and R. B. Bernstein, J. Chem. Phys., 1968, 49, 1878.

17. P. J. Robinson and K. A. Holbrook, Unimolecular Reactions, Wiley-Interscience, New York, 1972. See also reference 21 for angular momentum treatment.

18. R. J. Bunker and S. D. Peyerimoff, Chem. Reviews, 1974, 74(2), 127.

19. H. S. Johnston, Gas Phase Reaction Rate Theory, The Ronald Press Co., New York, 1966.

20. Vibrational spectrum for CF_3I: L. H. Ngai and R. H. Mann, J. Mol. Spect., 1971, 38, 322; for CF_3: D. E. Milligan and M. E. Jacox, J. Chem. Phys., 1968, 48(5), 2265; for ICl: G. Herzberg, Spectra of Diatomic Molecules, D. Van Nostrand Company Inc., New York, 1950.

21. S. A. Safron, N. D. Weinstein, D. R. Herschbach, and J. C. Tully, Chem. Phys. Lett., 1972, 12, 564.

22. J. C. Slater and J. G. Kirkwood, Phys. Rev., 1931, 37, 682.

23. J. O. Hirschfelder, C. F. Curtiss and R. B. Bird, Molecular Theory of Gases and Liquids, John Wiley and Sons, Inc., New York, 1954, p. 947-951.

24. H. M. Rosenstock, K. Draxl, B. W. Steiner, J. T. Herron, J. Phys. Chem. Ref. Data, 1977, 6, Suppl. #1.

25. D. St. A. G. Radlein, J. C. Whitehead, R. Grice, Nature, 1975, 253, 37.

26. N. D. Weinstein, Ph.D. dissertation, Harvard University, Cambridge, Mass., 1972.

27. R. J. Buss and Y. T. Lee, Faraday Discussions, Birmingham, England, April 9-11, 1979.

Table I.

		OIC1*	OIC1$^+$
Bond length Å	r_{IO}	2.0	1.87
	r_{IC1}	2.5	3.5
Bond Angles degrees	< OIC1	115	115
Frequencies cm^{-1}	V_{IO}	486	683
	V_{IC1}	271	R.C.
	δ_{OIC1}	250	25
Moments of Inertia AMU·Å^2		175.4	301.3
		132.5	262.8
		43.0	38.5

Energetics (kcal mol^{-1})

ΔH	-5.5
E_c	1.0 - 4.0
E*	23.0 - 27.0
E°	16.0

Polarizabilities (Å^3)

C1	=	2.18
O	=	0.802
IC1	=	7.5
IO	=	6.02

C_6 = 1981. kcal Å^6 mol^{-1}

C_6' = 3831. kcal Å^6 mol^{-1}

B_m' = 0.268 E_c

Table II.

		CF_3I-O*	CF_3I-O^+
Bond length Å	r_{IO}	2.0	1.87
	r_{CI}	2.54	2.82
	r_{CF}	1.33	1.33
Angles	<CIO	115	115
Degrees	<ICF	109	
Frequencies cm^{-1}	V_{IO}	486	683
	V_{CF}	1195, 1195, 1067	1223, 1223, 1077
	V_{CI}	202	R.C.
	δ_{CF}	730, 529	715, 521
	δ_{CI}	132, 132	26, 26
	δ_{CIO}	200, 200	40, 40
	τ	150	30
Moments of Inertia AMU·Å^2		334.8	1091
		333.8	1091
		89.6	99.4

Energetics (kcal mol^{-1})		Polarizabilities (Å^3)		
H	-2.0	CF_3I	=	7.33
E_c	1.0 - 4.0	CF_3	=	3.43
E*	20.0 - 24.0	O	=	0.802
E*	16.0	IO	=	6.02

Table II. (Continued)

$$C_6 = 2440.\ \text{kcal}\ \text{Å}^6\ \text{mol}^{-1}$$

$$C_6' = 7104.\ \text{kcal}\ \text{Å}^6\ \text{mol}^{-1}$$

$$B_m' = 0.105\ E_c$$

FIGURE CAPTIONS

Fig. 1. Laboratory angular distribution of IO intensity from the reactions of O + ICl, CF_3I. Error bars are one standard deviation of the mean of 10 measurements at each angle.

Fig. 2. Product IO flux distribution from the reaction O + ICl at eight laboratory angles. Solid lines are the best fit from the deconvolution procedure.

Fig. 3. Product IO flux distributions from the reaction O + CF_3I at seven laboratory angles.

Fig. 4. Contour map of center of mass product IO flux from the reaction O + ICl with the most probable Newton diagram.

Fig. 5. Contour map of center of mass product IO flux from the reaction of O + CF_3I.

Fig. 6. Product translational energy distributions.
··· experimental, lines are RRKM-AM calculations for three values of the IO bond energy,
- - - - E_{IO} = 53, ——— E_{IO} = 55, and
- —— - —— E_{IO} = 57 kcal mol^{-1}.

Fig. 7. Product translational energy distributions.
··· experimental, lines are RRKM-AM calculations for three values of the IO bond energy,
- - - - E_{IO} = 53, ——— E_{IO} = 55, and
- —— - —— E_{IO} = 57 kcal mol^{-1}.

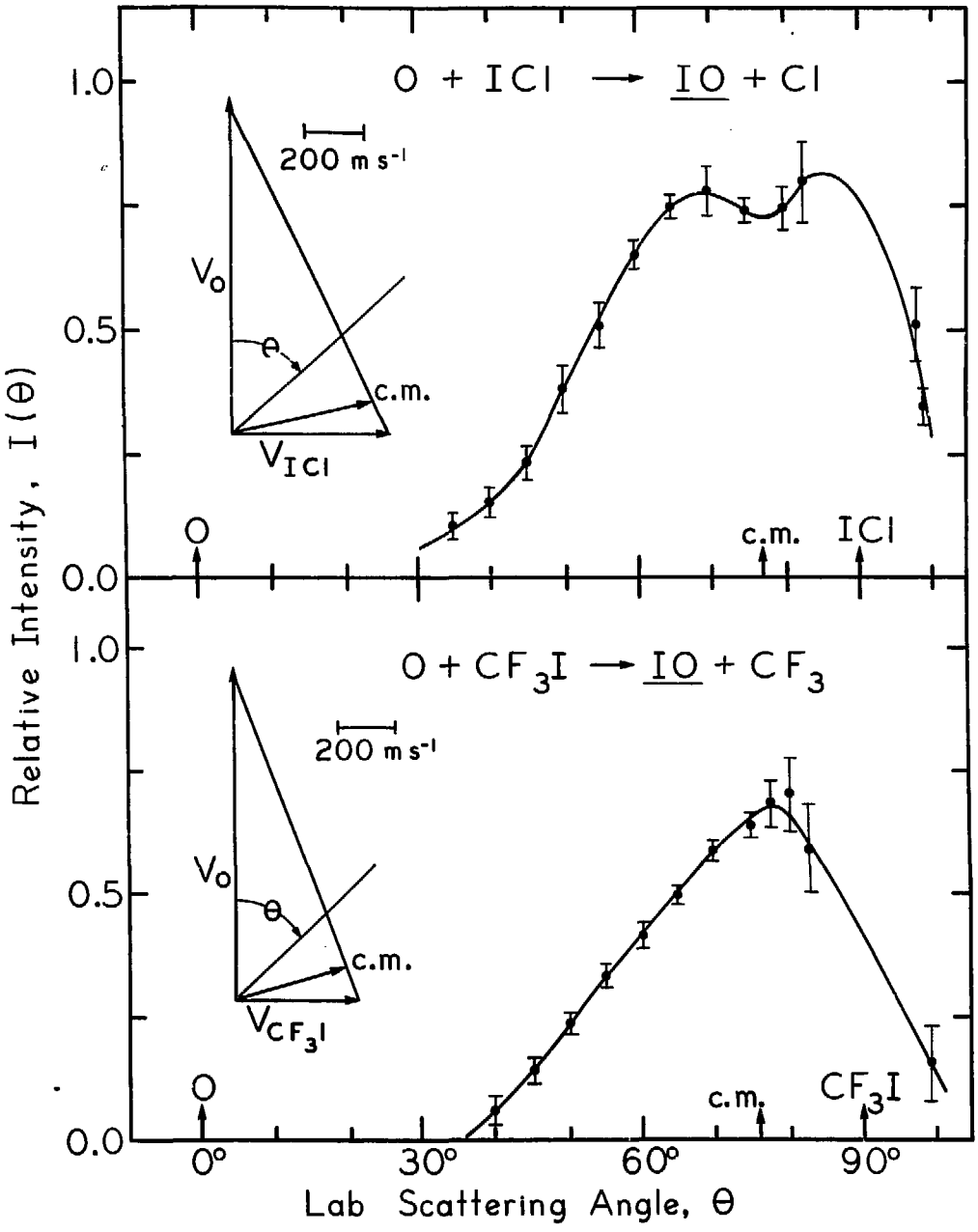

XBL 7812-14076

Fig. 1

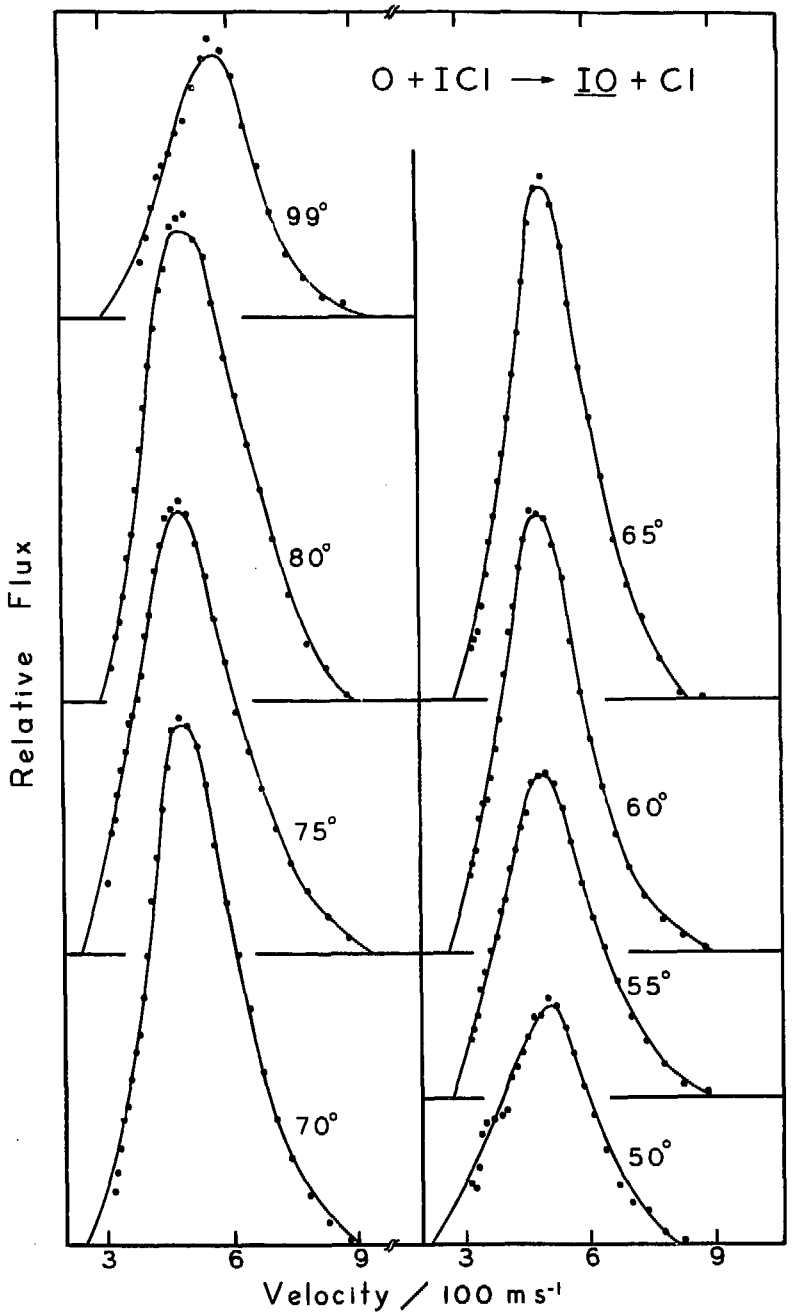

XBL 7812-14053

Fig. 2

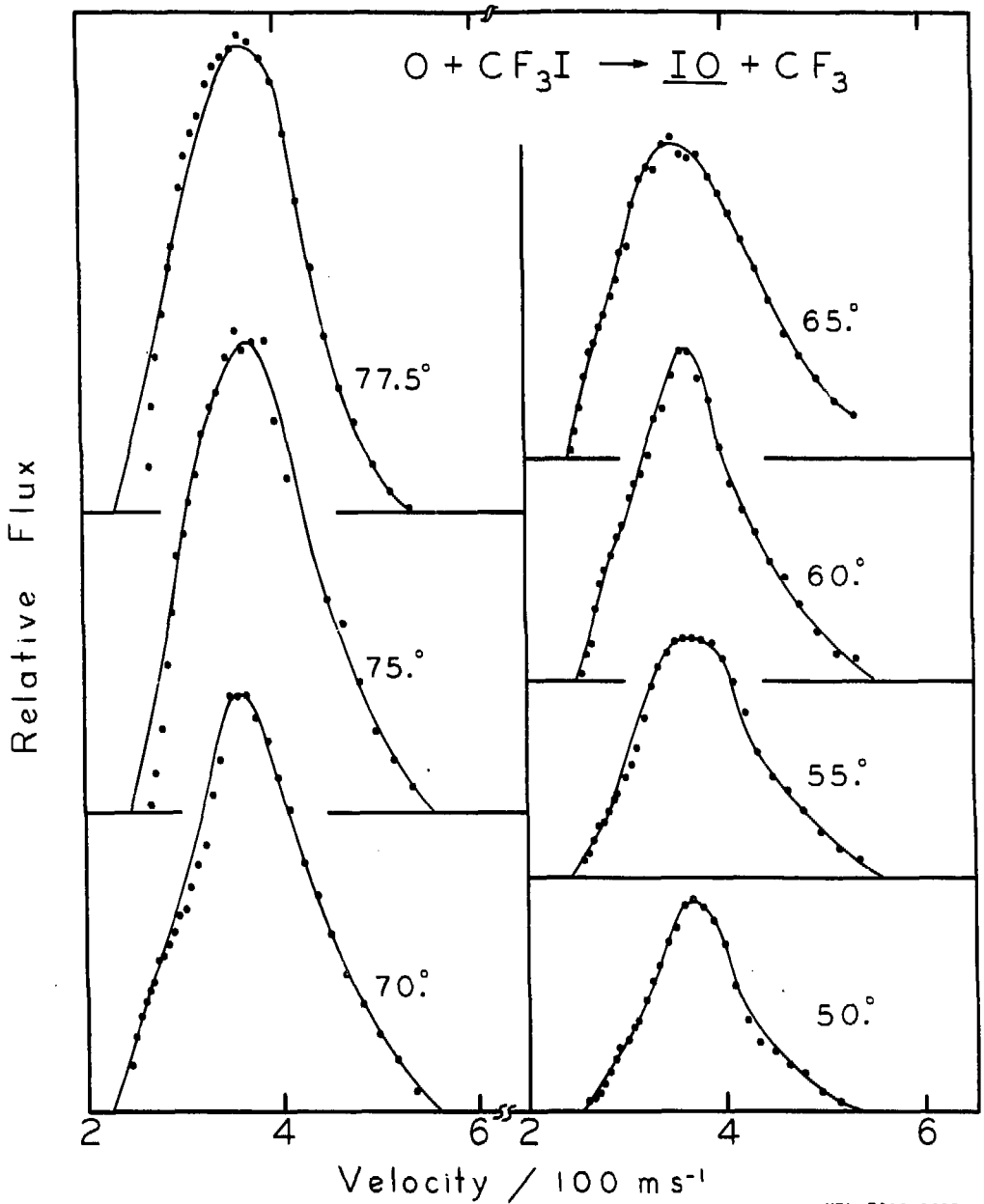

XBL 7812-14052

Fig. 3

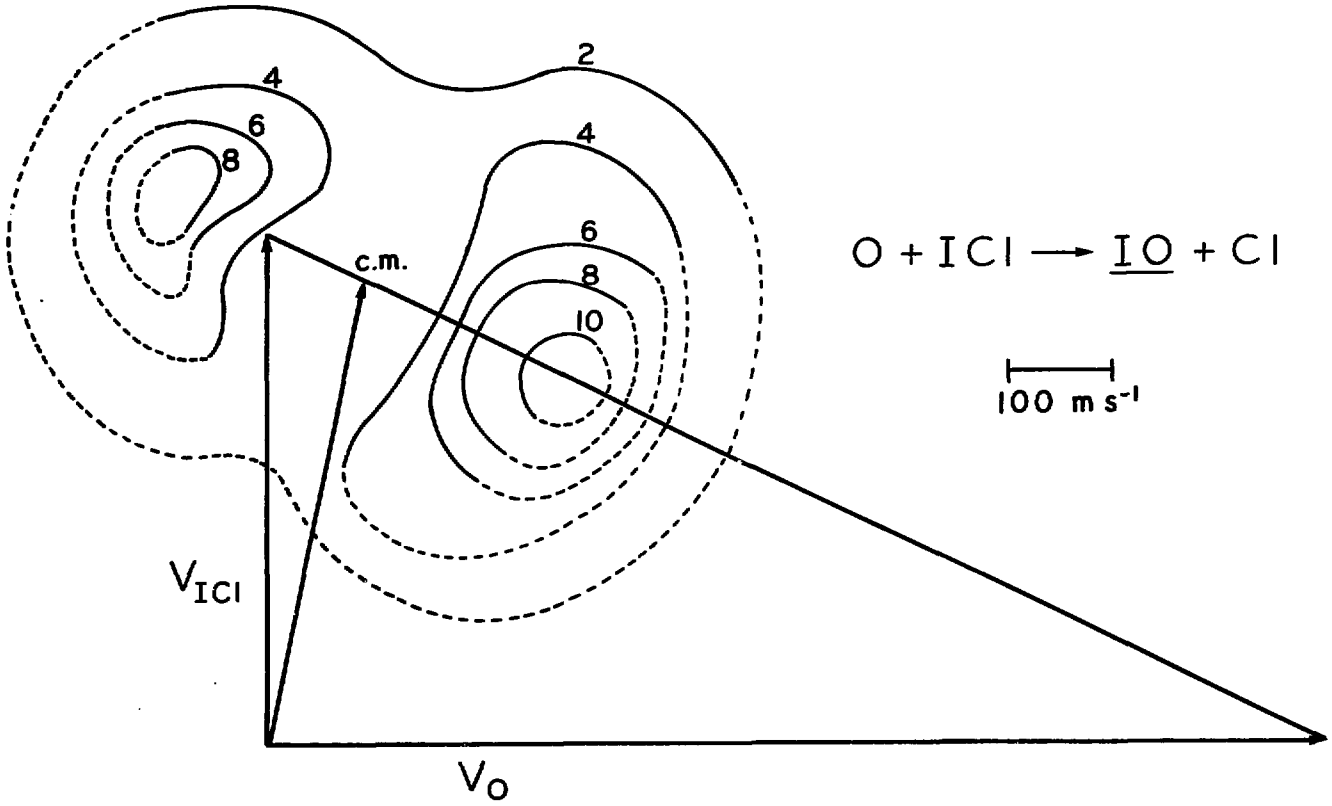

Fig. 4

XBL 7812-14055

$$O + CF_3I \longrightarrow \underline{IO} + CF_3$$

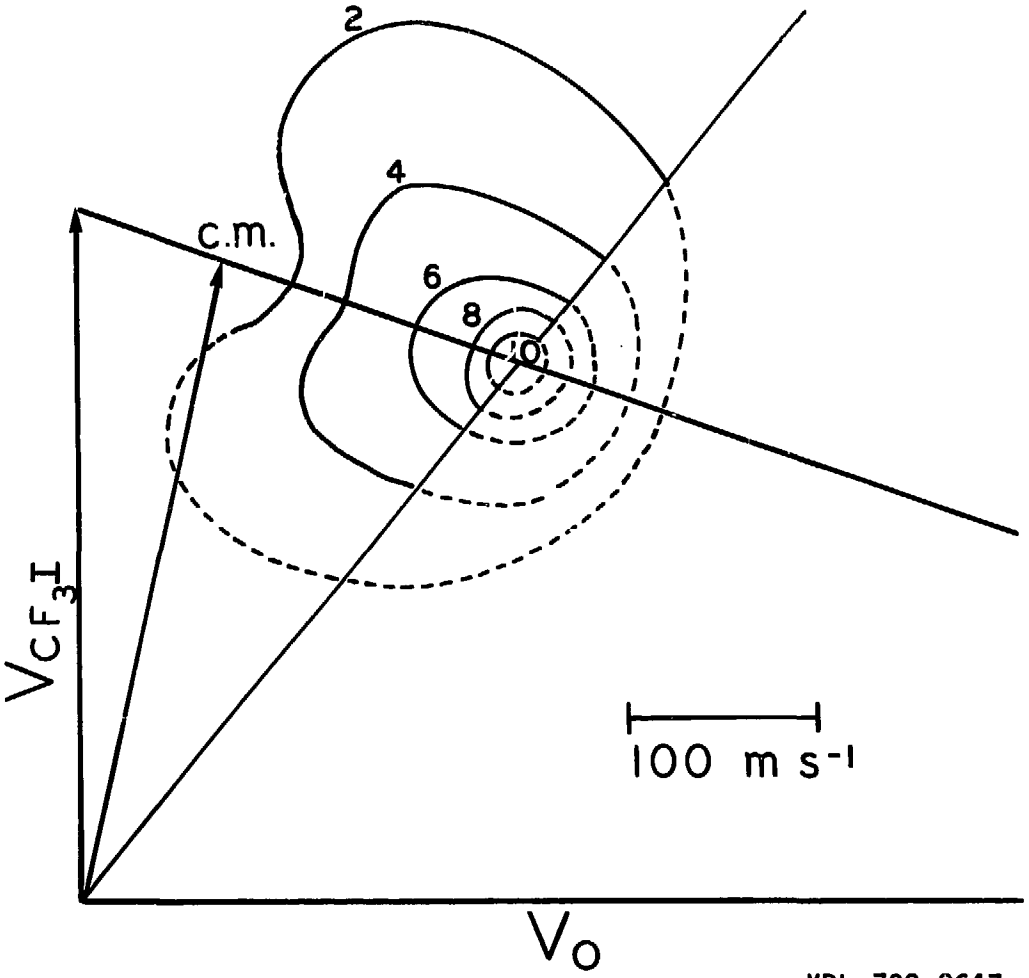

XBL 792-8647

Fig. 5

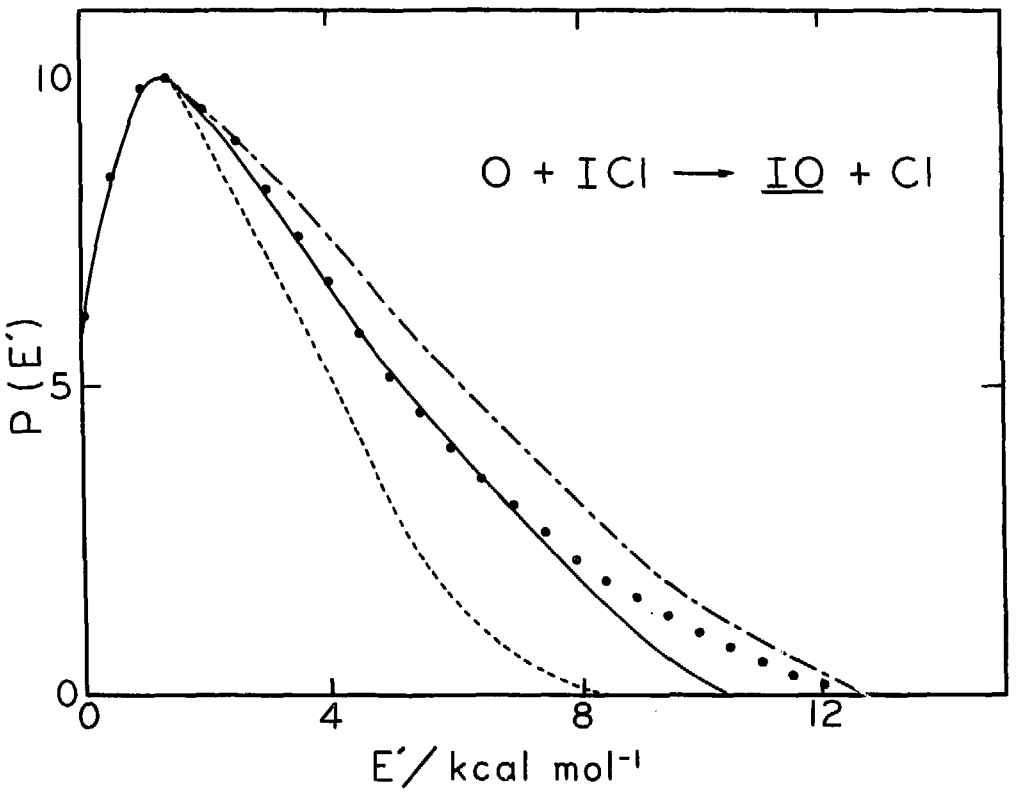

XBL 7812-14051

Fig. 6

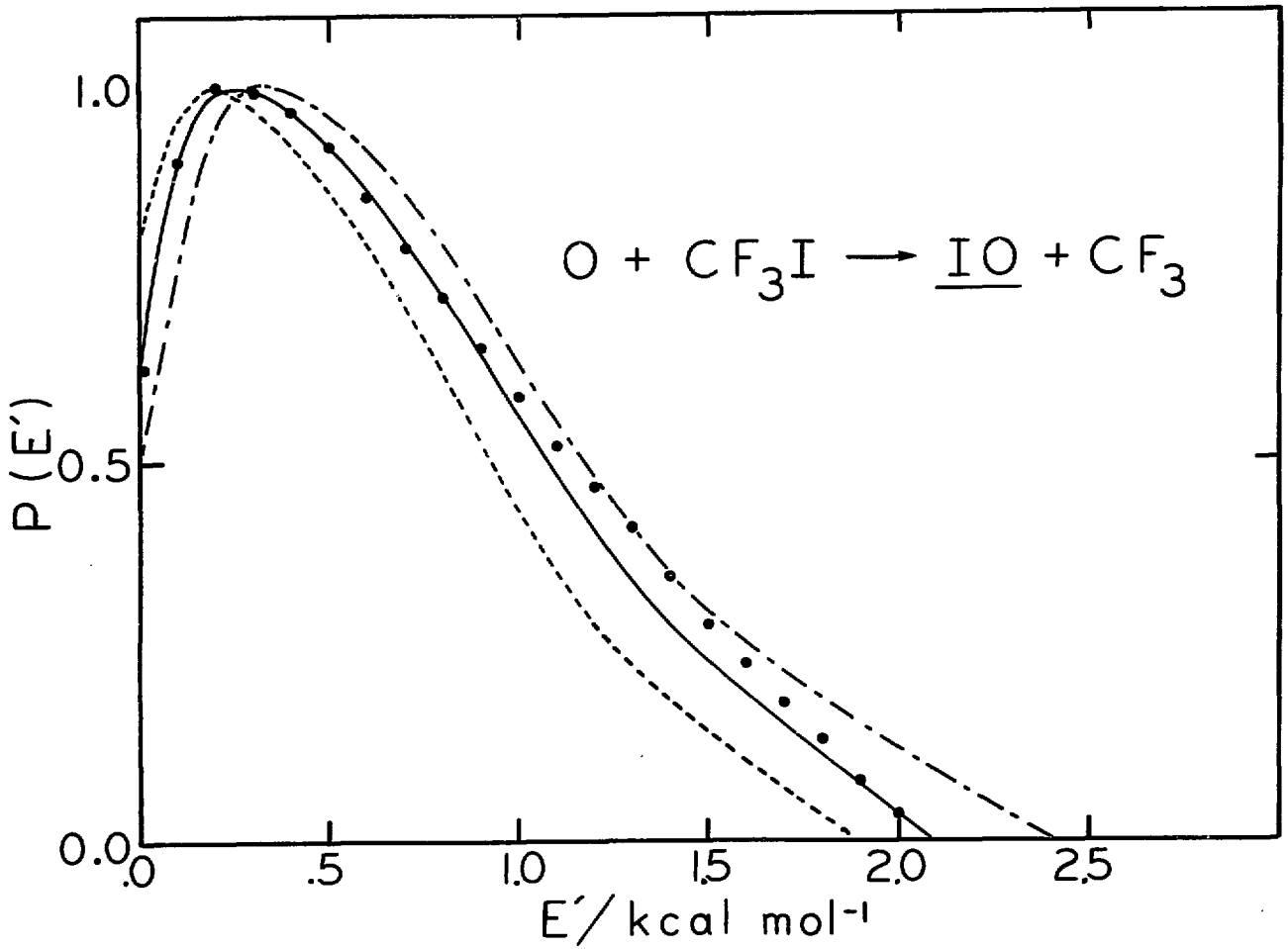

Fig. 7

XBL 7812-14050

APPENDIX

The data obtained in a crossed molecular beams reactive scattering experiment can be a rich source of microscopic dynamical information. The experimental results are most readily understood when transformed to the center-of-mass reference frame, but because the beams can not be made monoenergetic and perfectly collimated, this transformation is not unique. An iterative procedure for deconvoluting the data to remove the effects of the beam spread has been developed by Siska[1] and is widely used for molecular beam data reduction.[2] In common with other unaveraging procedures, this method cannot distinguish real features of the data from noise and thus may produce aberrations in the center-of-mass flux contours unless the input data is subjected to severe smoothing. Because the experimenter, as well, may not be able to distinguish real features from noise, the smoothing operation can distort the data and reduce its information content. The more reliable method, convoluting the theory to compare directly with the experimental results is often desirable, particularly because the measured uncertainty in the data can be used to place error limits on various parameters in the model.

The program CMLB described here was written to allow great flexibility in fitting a product energy distribution P(E') and a center of mass angular distribution T(θ) to

the experimental data. When used in conjunction with the deconvolution program mentioned above, it is a powerful tool for interpreting the molecular beam data. The program generates time of flight spectra and laboratory angular distributions of integrated intensity for direct comparision with experiment, as well as flux distributions and contour maps of product to assist in the fitting operation. The output also contains a calculated integral cross section.

The distribution of product number density $\overline{N}(t,\Theta)$ as a function of time at each laboratory angle, and the integrated intensity, $\overline{N}(\Theta)$, are obtained by summing the contributions from a discrete set of Newton diagrams. For a description of the use of Newton diagrams and in particular the application to molecular beam velocity and angular spreads, see reference 2.

$$\overline{N}(v,\Theta) = \sum_n f_n \, N(v,\Theta) \tag{1}$$

$$\overline{N}(t,\Theta) = \frac{dv}{dt} \overline{N}(v,\Theta)$$

$$= kv^2 \overline{N}(v,\Theta) \tag{2}$$

$$\overline{N}(\Theta) = \int_0^\infty \overline{N}(v,\Theta)dv \tag{3}$$

Here f_n is the distribution function for the Newton diagrams, which includes the weighting for the beam

$$f_n = f(V_1)f(V_2)f(\gamma)(v_1^2 + v_2^2)^{1/2} S(E_c) / \sum_n f(V_1)f(V_2)f(\gamma)(v_1^2 + v_2^2)^{1/2} S(E_c) \quad (4)$$

velocities V, $_iV_2$ and the intersection angle, γ, and also a cross section weighting $S(E_c)$ if the reactivity varies with collision energy, E_c.

The distribution of product flux is assumed to be separable into the product of an energy and angular part,

$$I(E,\theta,E_c) = I(E,E_c)\ T(\theta) \quad (5)$$

which changes for different Newton diagrams only if there is a dependence of the energy part on collision energy. This is particularly likely for thermoneutral or endoergic reactions in which the total energy available to the fragments is strongly increasing with collision energy. Coupling between the energy and angular parts is expected to occur for most reactions, see for example chapter II, but is often not detectable in the molecular beam experiment. Modification of the program to allow coupling should

be quite straightforward and was effected in order to perform the coupling calculation described in chapter II.

The energy distribution is converted to laboratory flux with renormalization.

$$I_c(u,\theta,E_c) = \frac{dE}{dU} I(E,\theta,E_c) \tag{6}$$

$$= k\ u\ I(E,\theta,E_c) \tag{7}$$

$$k = \int_0^\infty I(E,\theta,E_c)dE / \int_0^\infty u\ I(E,\theta,E_c)dU \tag{8}$$

$$I_L(v,\Theta,E_c) = \frac{v^2}{u^2} I_c(u,\theta,E_c) \tag{9}$$

$$N(v,\Theta,E_c) = \frac{v}{u^2} I_c(u,\theta,E_c) \tag{10}$$

The Jacobian for transformation of center of mass flux, I_c to laboratory flux, I_L causes a singularity to occur in the laboratory intensity for many physically realistic energy distributions, for example the RRKM derived P(E') which peaks at zero energy. The finite resolution of the machine performs a physical integration so that the measured intensities are always finite. In order to remove calculational difficulties, the laboratory flux within a small cutoff radius about the center of mass corresponding to the resolution of the machine was evaluated

with the Jacobian held at a constant finite value. That this approximation does not seriously affect the calculated intensities was ascertained by extensive testing with trial P(E'), varying the cutoff radius.

The time of flight spectra, obtained using equation 2 are further smoothed to account for resolution broadening. The wheel and detector slit sizes are used to generate a trapezoidal slit function. The ionizer is taken to be uniform density and rectangular with its length read as an input parameter. These approximations in treating the machine broadening effects are expected to introduce a negligible error and this has been verified by evaluating the magnitude of the broadening for a range of slit functions and ionizer lengths.

The total cross section is found by integrating the flux in the center of mass reference frame after scaling to obtain a best fit to the experimental laboratory angular distribution. The energy distribution is initially normalized at each collision energy so that

$$\int_0^\infty I(E,E_c)dE = 1$$

then $$\sigma_{TOT} = 2\pi\int_0^\pi\int_0^\infty z\ I(E,E_c)T(\theta)\sin\theta dEd\theta$$

$$= 2\pi z\int_0^\pi T(\theta)\sin\theta d\theta$$

where the scaling factor z is given by comparing the experimental data N_E with the calculated:

$$\frac{d}{dz}\sum_i [N_E(\Theta_i) - z\,\overline{N}(\Theta_i)]^2 = 0$$

$$z = \sum_i N_E(\Theta_i)\overline{N}(\Theta_i) / \sum_i \overline{N}(\Theta_i)\overline{N}(\Theta_i)$$

Thus, when an energy and center of mass angular distribution have been found which produce a good fit to the data, one obtains a value for the integrated cross section in units of flux. In order to find the total cross section in $Å^2$ units, an independent measure of the detection efficiency and beam intensities, such as the small angle elastic scattering of reactant, must be found.

The form of the input $T(\theta)$ can be either a distribution of points or a set of Legendre coefficients, a_n so that $T(\theta) = \sum_n a_n P_n$. In the latter case, the program can perform an optimization of selected coefficients to obtain a best fit to the experimental laboratory angular distribution. The use of a Legendre expansion is often convenient because this takes advantage of any inherent symmetry in the product distribution. If the product has forward backward symmetry, only even Legendre coefficients will be necessary to obtain a fit. The energy distribution can be specified by a functional form such as RRK, P(E') =

$(E'/B)^P(E_T-E')^q$ where B is the maximum exit channel barrier and E_T is the total available energy. Alternatively, for greater flexibility, the P(E') can be given in a point form.

In addition to the calculated time of flight spectra and angular distribution, the program can generate contour maps of the experimental flux, the calculated smoothed laboratory flux, or the calculated flux in the center of mass reference frame.

The following is a listing of the program with a sample calculation. The order and description of input parameters is given in the program comments.

REFERENCES

1. P. E. Siska, J. Chem. Phys., 1973, 59, 6052.

2. J. J. Valentini, Ph.D. dissertation, University of California, Berkeley, California, 1976.

```
      PROGRAM CMLB(INPUT,OUTPUT,PUNCH,TAPE5=INPUT,TAPE6=OUTPUT,TAPE7=PUN
     CCH)
C    VERSION M10
C   PROGRAM TO CALCULATE LABORATORY VELOCITY AND ANGULAR DISTRIBUTIONS
C   OF REACTIVELY SCATTERED PRODUCT.
C   INPUT CONSISTS OF BEAM PARAMETERS, TRIAL ENERGY DISTRIBUTION, TRIAL
C   ANGULAR DISTRIBUTION.
C   OUTPUT CAN BE PLOTS OF CALCULATED CM FLUX, CALCULATED LAB FLUX, OR
C   EXPERIMENTAL LAB FLUX/ OR NUMERICAL PRODUCT FLUX DISTRIBUTIONS AT
C   EACH LAB ANGLE, INTENSITY DIST. IN TIME, OR LAB ANGULAR DIST.
C   INPUT FORMAT< ALL INTEGERS = I5, ALL REALS = F10.0
C    ALL ENERGIES ARE IN UNITS OF KCAL/MOLE.
C   INPUT CARDS<
C 1**    TITLE, 8A10 FORMAT
C 2**    OPTIONS, 80I1 FORMAT? THIS SPECIAL CARD IS USED TO SPECIFY ALL
C     INPUT/OUTPUT AND OPERATIONAL OPTIONS.  IT SHOULD LOOK SOMETHING
C     LIKE 101110011010.  A ONE MEANS YES, A ZERO MEANS NO.
C
C   LIST OF OPTIONS IN ORDER
C
C *1* PRINT NEWTON DIAGRAM INFORMATION?  THIS TABLE IS USUALLY OF
C     INTEREST ONLY WHILE BEAM PARAMETERS ARE BEING CHANGED.
C *2* OPTIMIZE ANGULAR FUNCTION?  THE PROGRAM CAN TAKE THE INITIAL
C     LEGENDRE POLYNOMIAL AND OPTIMIZE SPECIFIED COEFFICIENTS TO OBTAIN
C     A BEST FIT TO THE LAB ANGULAR DISTRIBUTION.
C *3* EXPERIMENTAL FLUX INPUT?  WILL YOU BE PROVIDING ANY MEASURED
C     FLUX DISTR?  THESE ARE NOT USED IN THE CALCULATION BUT ARE
C     PRINTED FOR COMPARISON.
C *4* ENERGY DISTR IN POINT FORM?  IF YOU ANSWER NO, THE RRK FORM IS
C     PRESUMED UNLESS CHANGES ARE MADE IN SUBROUTINE ENERGY.
C *5* WEIGHTING OF CROSS SECTION?  IF THE CROSS SECTION IS EXPECTED TO
C     VARY WITH COLLISION ENERGY, A SET OF WEIGHTS CAN BE SPECIFIED.
C *6* PRINT CM ANGULAR DISTR?  THIS WILL SIMPLY WRITE OUT THE TRIAL
C     FUNCTION WHICH YOU CHOSE,  WHETHER LEGENDRE OR POINT FORM.
C *7* LABORATORY FLUX OUTPUT?  THE PROGRAM WILL PRINT CALCULATED FLUX
C     DISTR. AT EACH ANGLE FOR WHICH YOU PROVIDED EXPERIMENTAL DATA.
C *8* NUMBER DENSITY(TIME) OUTPUT?  THE PROGRAM WILL PRINT CALCULATED
C     INTENSITY DATA IN TIME SPACE FOR DIRECT COMPARISON WITH TOF DATA.
C *9* PLOT CALCULATED LAB FLUX?
C *10* PLOT CALCULATED CM FLUX?
C *11* PLOT EXPERIMENTAL LAB FLUX?
C *12* PRINT CALCULATED P(E) ALONG CM ANGLE ZERO?
C
C
C 3**  NVB1,NVB2,NGAM< NUMBER OF VELOCITIES IN EACH BEAM AND NUMBER OF
C    INTERSECTION ANGLES FOR WHICH NEWTON DIAGRAMS ARE TO BE CALCULATED.
C 4** G1,G2,GAMMA,HW< MASSES OF THE TWO BEAMS, MEAN INTERSECTION ANGLE,
C    AND HALF-WIDTH OF SPREAD IN INTERSECTION ANGLE.
C 5** VPAR(I,1),I=1,5< BEAM PARAMETERS> TEMPERATURE,SPECIFIC HEAT RATIO,
C    MACH NUMBER, DUMMY, CODE.  IF CODE<0.   NOZZLE SOURCE, IF CODE=0
C    VELOCITY SELECTED SOURCE, IF CODE>0 PARAMETRIC FORM FOR VEL DISTR.
C 6**VPAR(I,2),I=1,5< PARAMETERS FOR THE OTHER BEAM.
C 7** PMASS,TM< MASS OF DETECTED PRODUCT, MASS OF OTHER PRODUCT.
C 8** NLEG,NANG< IF NANG=0, THEN NLEG IS THE NUMBER OF LEGENDRE COEF-
C    FICIENTS FOR DESCRIBING THE CM ANGULAR DISTR.  IF NANG>0, THEN NLEG
C    IS THE NUMBER OF ANGLES FOR WHICH A CM ANG DISTR WILL BE GIVEN.
C    IF NANG=2, THE DISTR WILL BE ASSUMED SYMMETRIC ABOUT 90 DEGREES.
C 9** TO(I),I=1,NLEG< IF NANG>0, THIS IS A SET OF CM ANGLES FOR WHICH
C    INTENSITIES WILL BE INPUT, MAXIMUM NUMBER IS 20. IF NANG=0 OMIT.
C 10** PO(I),I=1,NLEG< IF NANG>0, THIS IS A SET OF INTENSITIES FOR TO(I)
C    IF NANG=0, THESE ARE LEGENDRE COEF STARTING WITH PO, MAXIMUM=P10.
```

```
C
C   IF YOU REQUEST ENERGY DISTR IN OTHER THAN POINT FORM, REPLACE CARDS
C   11, 12, 13 WITH OTHER CARDS DETERMINED BY SUBROUTINE ENERGY.
C
C 11** NEN< NUMBER OF COLLISION ENERGIES FOR WHICH P(E) WILL BE PROVIDED
C 12** DEN,ENSUB< ENERGY INCREMENT IN P(E), AND A CONSTANT TO BE
C   SUBTRACTED FROM THE COLLISION ENERGY, USUALLY 0.
C 13** EN(I)< FOR EACH OF NEN DISTR, EN(I) IS THE COLLISION ENERGY,
C       NP(I)< THIS IS THE NUMBER OF ENERGIES.  THEN LIST NP(I) VALUES
C       PE(J,I)< OF THE DISTR.  IF ONLY ONE P(E) IS TO BE PROVIDED, EN(I)
C   SHOULD BE SET AT SOME VALUE LESS THAN THE MINIMUM COLLISION ENERGY.
C 14** NA,NV< NUMBER OF LAB ANGLES AND NUMBER OF VELOCITIES AT EACH
C   ANGLE FOR WHICH THE FLUX IS TO BE CALCULATED.
C 15** VZ,DV< BEGINNING VELOCITY(1.0E4 CM/SEC) AND VELOCITY INCREMENT.
C *** FOR NA ANGLES, READ 16 AND 17.
C 16** AA,B(I),IDUM(I)< LAB ANGLE REFERENCED TO THE PRIMARY BEAM,
C   MEASURED INTENSITY, AND AN OPTION.  IF IDUM≠0, NO EXPERIMENTAL FLUX
C   IS TO BE PROVIDED AT THIS ANGLE.  IF IDUM=0, AND, ON THE OPTION
C   CARD ABOVE, EXPT LAB FLUX WAS SPECIFIED, THEN THE FLUX DISTR SHOULD
C   FOLLOW.
C 17** PF(J,I),J=1,NV< MEASURED FLUX DISTR IF SPECIFIED ABOVE.
C
C *** IF THE TOF INTENSITY OPTION WAS REQUESTED, INSERT CARDS 18, 19.
C
C 18** EION,DIST,SIZE,PATH,TIME<  ION ENERGY, ION FLIGHT PATH, IONIZER
C   LENGTH(CM), NEUTRAL FLIGHT PATH(CM), AND TIME PER CHANNEL(USEC).
C 19** HZ,DIA,SA,SB< FREQUENCY OF TOF WHEEL, DIAMETER OF WHEEL(CM),
C   SLIT SIZE IN WHEEL(MM), DETECTOR SLIT SIZE(MM).
C
C *** IF ANG FUNCTION OPTIMIZATION WAS REQUESTED, INSERT CARDS 20, 21,22
C
C 20** NOPT,ITMAX< NUMBER OF PARAMETERS TO BE OPTIMIZED, MAXIMUM
C   NUMBER OF ITERATIONS.
C 21** K(I),I=1,NOPT< LIST THE NUMBER OF THE COEFFICIENTS TO BE VARIED
C   NOTE THAT P0=1, P1=2 ... P10=11.
C 22** RADIUS< PARAMETER TO MEASURE CONVERGENCE OF OPTIMIZATION,
C   TRY .01, THE SMALLER IT GETS, THE LONGER IT TAKES.
C
C *** IF THE CROSS SECTION IS TO BE WEIGHTED ACCORDING TO COLLISION
C   ENERGY, INSERT CARDS 23, 24, 25.
C 23** NEW< NUMBER OF COLLISION ENERGIES TO BE WEIGHTED.
C 24** EW(I)< LIST OF COLLISION ENERGIES
C 25** SIG(I)< LIST OF WEIGHTS IN ARBITRARY UNITS
      COMMON/CENE/MP,CC,S5
      COMMON/CHII/NPUNCH,NV,CHIS,B(15),PM(15),P(100,15),Z,VL(100),PF(100
     C,15),DV
      COMMON/GRA/NA,KPLT,KDAT,A(15),SUMF(15),VZ,PC(100,15),KCMP
      COMMON/LEGE/KLEG,NANG,KPTS,T,THETA,TO(21)
      COMMON/NEWTON/NGAM,NGRID,NVB(2),G1,G2,GAMMA,GG,HW,PMASS,TM,C(400),
     CC2(400),D(400),FABG(400),THC(400),V1A(400),VV(400),VPAR(5,2),V1,V2
     C,CXMP,CYMP,AL(400),CUT(400)
      COMMON/VAL/NEN,NP,NLEG,IJK,CA,DEN,E,PIN,EC(400),EN(10),PE(200,10)
      COMMON/WEIGHT/NEW,KWTS,EW(20),SIG(20),EF,KSTP
      COMMON/TRIP/TIME,HZ,DIA,SA,SB,TTCM,DT,TRP(19)
      DIMENSION PT(100,15)
      DIMENSION IL(8),Q(2),IDUM(15)
      DIMENSION PP(260),NP(15),PO(21),TEM(11),K(11)
      DIMENSION PPSH(260)
      DATA Q/3H NO,3HYES/
      DATA RAD/.0174533/,D2/1.93498/
      DATA FDEG/.0872665/
      DATA CON/1.28485/
```

```
C*** READ INPUT PARAMETERS AND PRINT
      READ(5,1000) IL
      READ(5,1003)KSTP,KOPT,KFIN,KPTS,KWTS,KLEG,KFOT,KTIM,KPLT
     C,KCMP,KDAT,KPOE
      WRITE(6,1121)
      WRITE(6,1019) IL
      WRITE(6,1203)
      WRITE(6,1216)Q(KSTP+1)
      WRITE(6,1204)Q(KOPT+1)
      WRITE(6,1205)Q(KFIN+1)
      WRITE(6,1206)Q(KPTS+1)
      WRITE(6,1207)Q(KWTS+1)
      WRITE(6,1208)Q(KLEG+1)
      WRITE(6,1209)Q(KFOT+1)
      WRITE(6,1210)Q(KTIM+1)
      WRITE(6,1211)Q(KPLT+1)
      WRITE(6,1214)Q(KCMP+1)
      WRITE(6,1215)Q(KDAT+1)
      WRITE(6,1222)Q(KPOE+1)
      READ(5,1001) NVB(1),NVB(2),NGAM
      READ(5,1002)G1,G2,GAMMA,HW
      READ(5,1002) (VPAR(I,1),I=1,5)
      READ(5,1002) (VPAR(I,2),I=1,5)
      READ(5,1002)PMASS,TM
      READ(5,1001)NLEG,NANG
      IF(NANG.EQ.0)GO TO 35
      READ(5,1002)(TO(I),I=1,NLEG)
      TO(NLEG+1)=0.
35    READ(5,1002)(PO(I),I=1,NLEG)
      PO(NLEG+1)=0.
      IF(KOPT.EQ.0)GO TO 16
      DO 15 I=1,NLEG
15    TEM(I)=PO(I)
16    CONTINUE
      WRITE(6,1006)
      WRITE(6,1007)G1,G2
      T1=VPAR(1,1)
      T2=VPAR(1,2)
      VPAR(1,1)=CON*SQRT(T1/G1)
      IF(G2.LE..001)GO TO 98
      VPAR(1,2)=CON*SQRT(T2/G2)
      GO TO  99
98    VPAR(1,2)=0.0
99    CONTINUE
      WRITE(6,1008) T1,T2
      WRITE(6,1009) VPAR(2,1),VPAR(2,2)
      WRITE(6,1010) VPAR(3,1),VPAR(3,2)
      IF(VPAR(5,1)) 110,111,112
  110 IF(VPAR(5,2)) 113,114,112
  111 IF(VPAR(5,2)) 115,116,112
  113 WRITE(6,1011)
      GO TO 112
  114 WRITE(6,1012)
      GO TO 112
  115 WRITE(6,1013)
      GO TO 112
  116 WRITE(6,1014)
  112 WRITE(6,1015) NVB(1),NVB(2)
      WRITE(6,1105)PMASS
      IF(KPTS.EQ.0)GO TO 5
      READ(5,1001)NEN
      READ(5,1002)DEN,ENSUB
```

```
      IF(NEN.LE.0)STOP
      WRITE(6,1100)
      DO 4  I=1,NEN
      READ(5,1002)EN(I)
      EN(I)=EN(I)-ENSUB
      WRITE(6,1101)EN(I)
      READ(5,1001)NP(I)
      NPF= NP(I)
      READ(5,1002) (PE(J,I),J=1,NPF)
C*** NORMALIZE P(E) TO UNIT AREA
      AREA= PE(1,I)+PE(NP(I),I)
      NP1= NP(I)-1
      DO 210 J=2,NP1
  210 AREA=AREA+2.*PE(J,I)
      AREA=AREA*DEN/2.
      DO 215  J=1,NPF
  215 PE(J,I)= PE(J,I)/AREA
      WRITE(6,1106)NP(I),DEN
      WRITE(6,1102) (PE(J,I),J=1,NPF)
4     CONTINUE
      IF(NEN.NE.1)GO TO 445
      NEN=2
      EN(2)=800.
      NP(2)=NP(1)
      DO 444 I=1,NPF
444   PE(I,2)=PE(I,1)
445   CONTINUE
      GO TO 6
5     CALL ENERGY
6     READ(5,1001)NA,NV
      READ(5,1002)VZ,DV
      WRITE(6,1220)NA,NV
      WRITE(6,1221)VZ,DV
      DO 7 IV=1,NV
7     VL(IV)=FLOAT(IV-1)*DV+VZ
      DO 10 IA=1,NA
      READ(5,1004)AA,B(IA),IDUM(IA)
      A(IA)=AA*RAD
      IF(KFIN.EQ.0)GO TO 20
      IF(IDUM(IA).NE.0)GO TO 20
      READ(5,1002)(PF(IV,IA),IV=1,NV)
C*** SCALE THE EXPERIMENTAL FLUX TO GIVE MEASURED INTENSITY
      SUME=0.
      DO 8 IV=1,NV
8     SUME=SUME+PF(IV,IA)/VL(IV)
      Z=B(IA)/SUME
      DO 9 IV=1,NV
9     PF(IV,IA)=PF(IV,IA)*Z
      GO TO 10
20    DO 11 IV=1,NV
11    PF(IV,IA)=0.0
10    CONTINUE
      IF(KTIM.EQ.0)GO TO 13
      READ(5,1002)EION,DIST,SIZE,PATH,TIME
      READ(5,1002) HZ, DIA, SA, SB
      CALL TRAP
      PATH=PATH*100.
      DP=SIZE*5.
      PAT=PATH-SIZE*50.
13    IF(KOPT.EQ.0)GO TO 14
      READ(5,1001)NOPT,ITMAX
      READ(5,1001)(K(I),I=1,NOPT)
```

```
      READ(5,1002)RADIUS
C  READ ENERGY WEIGHTS IF KWTS=YES WAS SPECIFIED.
14    CALL WATE
      WRITE(6,1103)
      WRITE(6,1104)(PO(I),I=1,NLEG)
C*** CALCULATE AND PRINT CM ANG DISTR IF REQUESTED
      KK=KLEG
      KLEG=1
      CA=0.
      TSUM=0.
      THETA=0.
      IF(KK.NE.0)WRITE(6,1120)
      DO 2  I=1,37
      CALL EVAL(PO)
      THE=THETA/RAD
      IF(KK.NE.0)WRITE(6,1119)THE,T
      TSUM=TSUM+SIN(THETA)*T
2     THETA=THETA+.0872665
      TSUM=TSUM*FDEG
      KLEG=0
C*** CALCULATE AND PRINT NEWTON DIAGRAM INFORMATION
       WRITE(6,1242)
      CALL NEWT
C*** PERFORM SMOOTHING OPERATION, CALCULATE LAB ANG DISTR, AND CHI
      CALL CHI(PO)
      CHIT=CHIS
      IF(KOPT.EQ.0)GO TO 56
      IT=1
C*** INCREMENT PARAMETER TO BE OPTIMIZED
51    DO 55 I=1,NOPT
      DP=PO(K(I))*.1+.1
52    TEM(K(I))=  PO(K(I))+DP
      WRITE(6,1241)
      CALL CHI(TEM)
      WRITE(6,1118)(TEM(K(J)),J=1,NOPT)
C*** COMPARE NEW CHI WITH OLD
      IF(ABS(CHIS-CHIT).LT.RADIUS)GO TO 75
      IF(CHIS.LT.CHIT)GO TO 53
      DP=-DP*.5
      GO TO 52
53      PO(K(I))=TEM(K(I))
      CHIT=CHIS
      GO TO 52
75    IF(CHIT.LT.CHIS)GO TO 76
      CHIT=CHIS
      PO(K(I))=TEM(K(I))
      GO TO 55
76    TEM(K(I))=PO(K(I))
55    CONTINUE
      IT=IT+1
      IF(IT.LE.ITMAX)GO TO 51
C*** BEGIN OUTPUT
      WRITE(6,1103)
      WRITE(6,1104)(PO(I),I=1,NLEG)
      KLEG=1
      CA=0.
      THETA=0.
      WRITE(6,1120)
      DO 54 I=1,37
      CALL EVAL(PO)
      THE=THETA/RAD
      WRITE(6,1119)THE,T
```

```
54      THETA=THETA+.0872665
        KLEG=0
56      CONTINUE
        DO 57 IA=1,NA
        A(IA)=A(IA)/RAD
57      CONTINUE
        TSUM=TSUM*Z*FDEG*72.
        WRITE(6,1240)TSUM
        IF(KTIM.EQ.0)GO TO 67
C*** CALCULATE INTENSITY IN TIME SPACE
        WRITE(6,1217)EION,DIST,SIZE
        WRITE(6,1218)PATH/100.,TIME
        WRITE(6,1219) HZ, DIA, SA, SB
        WRITE(6,1113)
        OFF=DIST/(TIME*SQRT(D2*EION/PMASS))
        DO 65 IA=1,NA
        IF(IDUM(IA).NE.0)GO TO 65
        PPP=0.
        DO 66 IV=1,NV
        PT(IV,IA)=P(IV,IA)*VL(IV)
66      IF(PPP.LT.PT(IV,IA))PPP=PT(IV,IA)
        WRITE(6,1114)A(IA)
        WRITE(6,1115)
        DO 58 IV=1,NV
        IF(PT(IV,IA).GE. .01*PPP)GO TO 59
58      CONTINUE
59      NMAX=INT((PAT+SIZE)/(VL(IV)*TIME)+OFF)
        DO 60 IV=1,NV
        I=NV+1-IV
        IF(PT(I ,IA).GE. .01*PPP)GO TO 61
60      CONTINUE
61      NMIN=INT(PAT/(VL(I)*TIME)+OFF)
        IF(NMAX.GT.259)NMAX=259
        PPMAX=0.
C*** SMOOTH TOF DATA OVER IONIZER LENGTH
        DO 70 N=NMIN,NMAX
        CHAN=(N-OFF+.5)*TIME
        PP(N)=0.
        PA=PAT
        DO 70 I=1,21
        V=PA/CHAN
        IF(V.LT.VZ)GO TO 70
        NN=INT((V-VZ)/DV)+1
        IF(NN.GE.NV)GO TO 70
        PP(N)=PP(N)+PT(NN,IA)+(PT(NN+1,IA)-PT(NN,IA))*((V-VZ)/DV-NN+1)
70      PA=PA+DP
C*** SMOOTH TOF DATA OVER WHEEL SLIT FUNCTION
        DO 63 N=NMIN,NMAX
        PPSH(N)=.0
        TCM=N-TTCM
        DO 72 J=1,19
        TCM=TCM+DT
        L=INT(TCM)
        IF(L .LT. NMIN .OR. L .GE. NMAX) GO TO 72
        TFCM=TCM-L
        FFCM=PP(L)+(PP(L+1)-PP(L))*TFCM
        PPSH(N)=PPSH(N)+FFCM*TRP(J)
72      CONTINUE
        IF(PPMAX.LT.PPSH(N)) PPMAX=PPSH(N)
63      CONTINUE
        IF(PPMAX.EQ.0.)GO TO 65
        DO 64 N=NMIN,NMAX
```

```
      PPP=PPSH(N)/PPMAX
64    WRITE(6,1116)N,PPP
65    CONTINUE
67    CONTINUE
      IF(KFOT.EQ.0)GO TO 89
      CHIT=0.
      DO 88 IA=1,NA
      IF(IDUM(IA).NE.0)GO TO 88
      PPS=0.
      PPP=0.
      DO 85 IV=1,NV
      IF(PPS.LT.P(IV,IA))PPS=P(IV,IA)
85    IF(PPP.LT.PF(IV,IA))PPP=PF(IV,IA)
      PPS=PPS*Z
      IF(PPS.EQ.0.)PPS=1.0
      IF(PPP.EQ.0.)PPP=1.0
      SUME=0.
      SUMP=0.
      WRITE(6,1200)A(IA)
      DO 87 IV=1,NV
      P1=PF(IV,IA)
      P2=Z*P(IV,IA)
      CHIS=P2-P1
      CHIT=CHIT+CHIS*CHIS
      WRITE(6,1201)VL(IV),P1,P2,P1/PPP,P2/PPS
      SUME=SUME+P1
87    SUMP=SUMP+P2
88    CONTINUE
      WRITE(6,1212)CHIT
89    CONTINUE
      DO 95 I=1,NA
95    A(I)=A(I)*RAD
C*** DO ANY PLOTTING WHICH WAS REQUESTED
      IF(KPLT.EQ.0)GO TO 96
      CALL CONTR2
96    IF(KCMP.EQ.0)GO TO 97
      IF(KPOE.EQ.0)GO TO 102
C*** CALCULATE AND PRINT P(E) ALONG THETA=0 IF REQUESTED
      WRITE(6,6767)
      WRITE(6,1231)
      NN=NP(1)
      TC=0.
      EA=0.
      DO 100 I=1,NN
      EA=EA+DEN
      U=SQRT(EA/GG)
      V=C2(MP)+U*(U-2.*C(MP)*CC)
      V=SQRT(V)
      IF(V.LT.VZ.OR.V.GE.(VZ+NV*DV))GO TO 121
      TC=THC(MP)-ASIN(SS*U/V)
      IF(TC.LT.A(1).OR.TC.GE.A(NA))GO TO 121
      IAN=0
      DO 101 IA=1,NA
      IF(TC.LT.A(IA))GO TO 101
      IAN=IA
101   CONTINUE
      VT=(V-VZ)/DV
      NNV=INT(VT)
      VT=VT-NNV
      NNV=NNV+1
      TT=(A(IAN)-TC)/(A(IAN)-A(IAN+1))
      CA=PC(NNV,IAN+1)+VT*(PC(NNV+1,IAN+1)-PC(NNV,IAN+1))
```

```
      CB=PC(NNV,IAN   )+VT*(PC(NNV+1,IAN   )-PC(NNV,IAN   ))
      CA=CB+TT*(CA-CB)
      GO TO 122
121   CA=0.
122   WRITE(6,1230)U,V,TC/RAD,EA,CA
100   CONTINUE
102   CONTINUE
      KPLT=2
      CALL CONTR2
97    IF(KDAT.EQ.0)STOP
      KPLT=3
      CALL CONTR2
      STOP
 1000 FORMAT(8A10)
 1001 FORMAT(16I5)
 1002 FORMAT(8F10.0)
 1003 FORMAT(20I1)
 1004 FORMAT(2F10.0,I5)
 1006 FORMAT(1H0,30X,21HBEAM INPUT PARAMETERS/1H0,44X,7HPRIMARY,8X,9HSEC
     1ONDARY)
 1007 FORMAT(1H0,9X,4HMASS,32X,F6.2,11X,F6.2)
 1008 FORMAT(1H ,9X,11HTEMPERATURE,25X,F6.1,11X,F6.1)
 1009 FORMAT(1H ,9X,5HGAMMA,33X,F4.2,13X,F4.2)
 1010 FORMAT(1H ,9X,11HMACH NUMBER,26X,F5.2,12X,F5.2)
 1011 FORMAT(1H ,9X,17HDISTRIBUTION TYPE,19X,6HNOZZLE,11X,6HNOZZLE)
 1012 FORMAT(1H ,9X,17HDISTRIBUTION TYPE,19X,6HNOZZLE,10X,7HVEL SEL)
 1013 FORMAT(1H ,9X,17HDISTRIBUTION TYPE,18X,7HVEL SEL,11X,6HNOZZLE)
 1014 FORMAT(1H ,9X,17HDISTRIBUTION TYPE,18X,7HVEL SEL,10X,7HVEL SEL)
 1015 FORMAT(1H ,9X,23HNO. VELOCITIES AVERAGED,17X,I2,15X,I2)
 1019 FORMAT(1H0,8A10)
 1100 FORMAT(1H ,12HENERGY INPUT)
 1101 FORMAT(1H ,16HCOLLISION ENERGY,F10.3)
 1102 FORMAT(1H ,20(/5F10.4))
 1103 FORMAT(1H1,10H LEGENDRE ,11HCOEFICIENTS)
 1104 FORMAT(1H ,5F8.3)
 1105 FORMAT(1H ,9X,12HPRODUCT MASS,F10.3)
 1106 FORMAT(1H ,I5,9H ENERGIES,3H AT,F7.3,19HKCAL/MOLE INCREMENT)
 1113 FORMAT(1H ,21HVELOCITY DISTRIBUTION)
 1114 FORMAT(1H0,6HANGLE=,F6.2)
 1115 FORMAT(1H ,7HCHANNEL,3X,9HINTENSITY)
 1116 FORMAT(1H ,2X,I3,7X,F6.4)
 1118 FORMAT(1H 20HVALUE OF PARAMETERS=,5F6.3)
 1119 FORMAT(1H ,1X,F4.0,4X,F7.3)
 1120 FORMAT(1H ,5HANGLE,5X,6HLEG(A))
 1121 FORMAT(1H1,11HVERSION M10)
 1200 FORMAT(1H0,10HLAB ANGLE=,F6.2/1H 7HLAB VEL,3X,9HEXPT FLUX,3X,9HCAL
     CC FLUX,3X,9HEXPT NORM,3X,9HCALC NORM)
 1201 FORMAT(1H ,F7.3,4(3X,F9.4))
 1203 FORMAT(8H0OPTIONS)
 1204 FORMAT(24H OPTIMIZE ANG FUNCTION? ,A3)
 1205 FORMAT(18H EXPT FLUX INPUT? ,A3)
 1206 FORMAT(29H ENERGY DIST. IN POINT FORM? ,A3)
 1207 FORMAT(29H WEIGHTING OF CROSS SECTION? ,A3)
 1208 FORMAT(21H PRINT CM ANG. DIST? ,A3)
 1209 FORMAT(19H FLUX(VEL) OUTPUT? ,A3)
 1210 FORMAT(30H NUMBER DENSITY(TIME) OUTPUT? ,A3)
 1211 FORMAT(21H PLOT CALC LAB FLUX? ,A3)
 1212 FORMAT(1H ,10HCHI-SQUARE,11H CALCULATED,8H ON FLUX,E10.4)
 1214 FORMAT(15H PLOT CM FLUX? ,A3)
 1215 FORMAT(17H PLOT EXPT FLUX? ,A3)
 1216 FORMAT(1H ,24HPRINT NEWTON DIAG INFO? ,A3)
 1217 FORMAT(12H ION ENERGY=,F6.2,2HEV/12H ION FLIGHT=,F6.2,2HCM/9H IONI
```

```
     CZER=,F4.2,2HCM)
1218  FORMAT(23H PRODUCT FLIGHT LENGTH=,F6.2,2HCM,5X,13HTIME/CHANNEL=,F3
     C.0,4HUSEC)
 1219 FORMAT(/,12H WHEEL FREQ=,F7.2,18H HZ      WHEEL DIA=,F6.2,
     119H CM     WHEEL SLIT=,F6.2,19H MM      DETEC SLIT=,F5.2,3H MM,/)
1220  FORMAT(19H CALCULATION IS FOR,I3,8H ANGLES,I4,26H VELOCITIES AT EA
     CCH ANGLE.)
1221  FORMAT(14H STARTING WITH,F7.3,6H WITH ,F7.3,9H SPACING.)
 1222 FORMAT(13H PRINT P(E)? ,A3)
1230  FORMAT(1H ,5F9.3)
1231  FORMAT(4X,6HCM VEL,3X,6HLB VEL,3X,6HLB ANG,3X,6HENERGY,4X,4HP(E))
1240  FORMAT(1H0,10HINTEGRATED ,14HCROSS SECTION=,E10.4)
1241  FORMAT(7H ******)
1242  FORMAT(1H1)
6767  FORMAT(11H1CALCULATED,11H P(E) ALONG,10H CENTER OF,11H MASS ANGLE,
     C5H T=0.)
      END


      SUBROUTINE WATE
C *** CALCULATES WEIGHTS FOR THE ENERGY DEPENDENCE OF THE CROSS SECTION.
      COMMON/WEIGHT/NEW,KWTS,EW(20),SIG(20),EF,KSTP
      IF(KWTS-1)1,2,3
1     EF=1.0
      RETURN
2     READ(5,1001)NEW
      READ(5,1002)(EW(I),I=1,NEW)
      READ(5,1002)(SIG(I),I=1,NEW)
      WRITE(6,1004)
      DO 8 I=1,NEW
8     WRITE(6,1003)EW(I),SIG(I)
      KWTS=2
      RETURN
3     N=0
      DO 4 I=1,NEW
      IF(EF.LT.EW(I))GO TO 4
      N=I
4     CONTINUE
      IF(N.EQ.0.OR.N.EQ.NEW)GO TO 5
      EF=SIG(N)+(SIG(N+1)-SIG(N))*((EF-EW(N))/(EW(N+1)-EW(N)))
      RETURN
5     WRITE(6,1111)
      EF=1.0
      RETURN
1001  FORMAT(20I5)
1002  FORMAT(8F10.0)
1003  FORMAT(1H ,F6.2,F10.4)
1004  FORMAT(24H CROSS SECTION WEIGHTING/15H ENERGY   SIGMA)
1111  FORMAT(1H ,*CAUTION, COLLISION ENERGY IS OUTSIDE RANGE OF WEIGHTS*
     C)
      END
```

```
      SUBROUTINE NEWT
C
C     CALCULATES NEWTON DIAGRAMS AND THEIR WEIGHTS
C
      COMMON/CENE/MP,CC,SS
      COMMON/NEWTON/NGAM,NGRID,NVB(2),G1,G2,GAMMA,GG,HW,PMASS,TM,C(400),
     CC2(400),D(400),FABG(400),THC(400),V1A(400),VV(400),VPAR(5,2),V1,V2
     C,CXMP,CYMP,AL(400),CUT(400)
      COMMON/VAL/NEN,NP,NLEG,IJK,CA,DEN,E,PIN,EC(400),EN(10),PE(200,10)
      COMMON/WEIGHT/NEW,KWTS,EW(20),SIG(20),EF,KSTP
      DIMENSION A0(2),A1(2),GAM(5),FG(5),VB(20,2),FB(20,2),NP(15)
      DATA PI2/1.570796/
      DATA CON1,CON2,RAD/.00119503,3.33022,.0174533/
      DATA SLIT,DDET/2.,145./
      G=G1+G2
      G2=G2/G
      GFAC=CON1*G1*G2
      IF(TM.EQ.0) TM=G-PMASS
      GG=CON1*PMASS*G/TM
      G1=G1/G
      G12=G1*G2*2.
      G11=G1*G1
      G22=G2*G2
      NH=NGAM/2+1
      FNH=NH
      DO 1 K=1,NGAM
      GAM(K)=GAMMA+FLOAT(K-NH)*HW/FNH
      FG(K)=1.
    1 IF(HW    .NE.0.) FG(K)=1.-ABS(GAM(K)-GAMMA)/HW
      DO 30 L=1,2
      NV1=NVB(L)
      IF(VPAR(5,L)) 20,15,10
   10 FNH=AMAX0(NV1/2,1)
      DO 12 I=1,NV1
      VB(I,L)=VPAR(1,L)*FLOAT(I)/FNH
   12 FB(I,L)=UDIST(VB(I,L),VPAR(I,L))
      GO TO 30
15    GMB=1.0/(VPAR(3,L)-VPAR(2,L))
      DV=1.-VPAR(3,L)
      A0(1)=(1.+VPAR(3,L))*GMB
      A1(1)=-(1.+VPAR(2,L))*GMB
      A0(2)=-DV*GMB
      A1(2)=(1.-VPAR(2,L))*GMB
      DV=2./(DV*FLOAT(NV1+1))
      NH=1./DV+1.
      DV=DV/A0(1)
      DO 17 I=1,NV1
      R=1.+FLOAT(I-NH)*DV
      VB(I,L)=VPAR(1,L)*R
      I1=1
      IF(R.GT.1.) I1=2
   17 FB(I,L)=A0(I1)+A1(I1)/R
      GO TO 30
   20 AL1=VPAR(1,L)/SQRT(1.+(VPAR(2,L)-1.)/2.*VPAR(3,L)**2)
      VF=SQRT(VPAR(2,L)/2.)*VPAR(3,L)
      VPK=(VF+SQRT(VF**2+4.))/2.
      FNORM=EXP((VPK-VF)**2)/VPK**2
      DV=CON2/FLOAT(NV1+1)
      NH=NV1/2+1
      DO 22 I=1,NV1
      R=VPK+FLOAT(I-NH)*DV
```

```
      VB(I,L)=AL1*R
   22 FB(I,L)=FNORM*R**2*EXP(-(VF-R)**2)
   30 CONTINUE
      FMP=0.
      NV1=NVB(1)
      NV2=NVB(2)
      IJK=0
      DO 4 K=1,NGAM
      GMK=GAM(K)*RAD
      CG= COS(GMK)
      SG=SIN(GMK)
      DO 4 I=1,NV1
      V1=VB(I,1)
      DO 4 J=1,NV2
      V2=VB(J,2)
      IJK=IJK+1
      AL(IJK)=.5*(GMK-PI2)
      VV(IJK)=V1
      VSQ=V1*V1
      V  =VSQ+V2*(V2-2.*V1*CG)
      V12=SQRT(V)
      C2(IJK)=G11*V1*V1+G22*V2*V2+G12*V1*V2*CG
      C(IJK)= SQRT(C2(IJK))
      CUT(IJK)=C(IJK)*SLIT/DDET
      CX=G1*V1+G2*V2*CG
      CY=G2*V2*SG
      THC(IJK)=ATAN2(CY,CX)
      VTEMP    =C2(IJK)+V1*(V1-2.*C(IJK)*COS(THC(IJK)+AL(IJK)))
      V1A(IJK)=SQRT(VTEMP)
      EF=V*GFAC
      EC(IJK)=EF
C  OBTAIN CROSSSECTION WEIGHTING STORED IN EF.
      CALL WATE
      FABG(IJK)=FB(I,1)*FB(J,2)*FG(K)*V12*EF
      IF(FMP.GT.FABG(IJK)) GO TO 4
      FMP=FABG(IJK)
      MP=IJK
      IMP=I
      JMP=J
    4 CONTINUE
      NGRID=NV1*NV2*NGAM
      IJK=0
      V1=VB(IMP,1)
      V2=VB(JMP,2)
      CXMP=G1*V1
      CYMP=G2*V2
      CC=(V1*V1-C2(MP)-V1A(MP)*V1A(MP))/(2.*C(MP)*V1A(MP))
      CC=-CC
      SS=SIN(ACOS(CC))
      V=SQRT(V1**2+V2**2)
      SUM=0.
      DO 65 IJK=1,NGRID
      SUM=SUM+FABG(IJK)
   65 CONTINUE
      DO 67 IJK=1,NGRID
      FABG(IJK)=FABG(IJK)/SUM
   67 CONTINUE
      WRITE(6,1000)
      IF(KSTP.EQ.0)GO TO 9
      IJK=0
      DO 8 K=1,NGAM
      DO 8 I=1,NV1
```

```
      DO 8 J=1,NV2
      IJK=IJK+1
      T=THC(IJK)/RAD
      WRITE(6,1001) VB(I,1),FB(I,1),VB(J,2),FB(J,2),GAM(K),FG(K),FABG(IJ
     CK),T,C(IJK),EC(IJK)
    8 CONTINUE
9     CONTINUE
      T=THC(MP)/RAD
      WRITE(6,1002) V1,V2,T,C(MP),EC(MP),NGRID
1000  FORMAT(1H1,4X,4HVEL1,2X,2HF1,5X,4HVEL2,2X,2HF2,4X,5HGAMMA,2X,2HFG,
     C4X,4HF12G,6X,3HTHC,5X,3HVCM,4X,4HEREL)
1001  FORMAT(1H ,3(F8.2,F5.2),F8.4,3F8.2)
1002  FORMAT(1H ,F8.2,5X,F8.2,26X,3F8.2,12H (CANONICAL)/1H ,9X,I5,
     C7HNEWTON,9H DIAGRAMS)
      RETURN
      END
```

```
      SUBROUTINE CHI(T)
C *** PROGRAM TO SMOOTH P(E) AND P(T) OVER THE NEWTON DIAGRAMS.
C *** COMPARES CALCULATED LAB ANGULAR DISTR WITH EXPERIMENTAL AND
C *** FINDS THE CHI-SQUARE VALUE.
      COMMON/CHII/NPUNCH,NV,CHIS,B(15),PM(15),P(100,15),Z,VL(100),PF(100
     C,15),DV
      COMMON/GRA/NA,KPLT,KDAT,A(15),SUMF(15),VZ,PC(100,15),KCMP
      COMMON/NEWTON/NGAM,NGRID,NVB(2),G1,G2,GAMMA,GG,HW,PMASS,TM,C(400),
     CC2(400),D(400),FABG(400),THC(400),V1A(400),VV(400),VPAR(5,2),V1,V2
     C,CXMP,CYMP,AL(400),CUT(400)
      COMMON/VAL/NEN,NP,NLEG,IJK,CA,DEN,E,PIN,EC(400),EN(10),PE(200,10)
      DIMENSION CT(400),T(21),NP(15)
      DATA RAD/.0174533/
      X=0.
      Y=0.
      DO 30 IA=1,NA
      SUM=0.
      DO 27 IJK=1,NGRID
      TT=THC(IJK)-A(IA)
27    CT(IJK)= COS(TT)
      DO 29 IV=1,NV
      V=VL(IV)
      FC=0.
      F=0.
      DO 28 IJK=1,NGRID
      UU=    C2(IJK)+V*(V-2.* C(IJK)*CT(IJK))
      E=GG*UU
      U= SQRT(UU)
      AA=V*V+VV(IJK)*(VV(IJK)-2.*V*COS(A(IA)+AL(IJK)))
      CA=(UU+V1A(IJK)*V1A(IJK)-AA)/(2.*V1A(IJK)*U)
      IF(CA.GT.1.01)WRITE(6,8888)CA,U,V,IJK
      IF(CA.GT.1.0)CA=1.0
      IF(U.LT.CUT(IJK))U=CUT(IJK)
      CALL EVAL(T)
      IF(KCMP.NE.0)FC=FC+FABG(IJK)*U*PIN
      F=F+FABG(IJK)*V*V/U*PIN
28    CONTINUE
      P(IV,IA)=F
      IF(KCMP.NE.0)PC(IV,IA)=FC
      SUM=SUM+F/V
29    CONTINUE
      SUM=SUM*DV
      SUMF(IA)=SUM
      X=X+SUM*B(IA)
      Y=Y+SUM*SUM
30    CONTINUE
      Z=X/Y
      CHIS=0.
      WRITE(6,1110)
      WRITE(6,1111)
      DO 40 IA=1,NA
      SUMF(IA)=SUMF(IA)*Z
      X=B(IA)-SUMF(IA)
      CHIS=CHIS+X*X
      AD=A(IA)/RAD
40    WRITE(6,1112)AD,B(IA),SUMF(IA),X
      WRITE(6,1117)CHIS
      RETURN
1110  FORMAT(1H1,28HPRODUCT ANGULAR DISTRIBUTION)
1111  FORMAT(1H ,9HLAB ANGLE,5X,8HEXPT INT,6X,14HCALC INTENSITY,3X,10HDI
     CFFERENCE)
```

```
1112  FORMAT(1H ,2X,F6.1,8X,F6.4,10X,F7.4,8X,E10.3)
1117  FORMAT(56X,10HCHISQUARE=,F12.5)
8888  FORMAT(1H ,6HERROR ,14HCOS(CM ANGLE)=,F7.4,9H  CM VEL=,F7.4,10H  L
     CAB VEL=,F7.4,12H  NEWT DIAG=,I3)
      END


      FUNCTION UDIST(U,PAR)
C  PARAMETRIC FORM FOR VELOCITY DISTRIBUTIONS
C
      DIMENSION PAR(1)
      R=U/PAR(1)
      IF(R.GT.1.) GO TO 20
      A=PAR(2)
      B=PAR(3)
   10 ALR=ALOG(R)
      UDIST=EXP(A*(ALR+(1.-EXP(B*ALR))/B))
      RETURN
   20 A=PAR(4)
      B=PAR(5)
      GO TO 10
      END


      SUBROUTINE LEGPOL (X,Y,N)
C *** EVALUATES LEGENDRE POLYNOMIAL OF DEGREE M.
      DIMENSION Y(1)
C     M = DIMENSION ON Y.
C
      M = N +1
      Y(1) = 1.
      Y(2) =X
      IF (M.LT.3) RETURN
      DO 1 I=3,M
      R= FLOAT(I-2)
      Y(I)= (2.*R+1.)*X*Y(I-1)/(R+1.)-R*Y(I-2)/(R+I.)
    1 CONTINUE
      RETURN
      END
```

```
      SUBROUTINE EVAL(PO)
C *** EVALUATES THE PRODUCT P(E)P(T) FOR A GIVEN CM ANGLE AND VELOCITY.
      COMMON/LEGE/KLEG,NANG,KPTS,T,THETA,TO(21)
      COMMON/VAL/NEN,NP,NLEG,IJK,CA,DEN,E,PIN,EC(400),EN(10),PE(200,10)
      DIMENSION NP(15),PO(21),Y(11)
      DATA RAD/.0174533/
C *** CALCULATES P(T)
      IF(NANG.EQ.0)GO TO 5
      IF(KLEG.NE.0)GO TO 2
      CC=ACOS(CA)/RAD
      GO TO 3
2     CC=THETA/RAD
3     IF(NANG.EQ.2.AND.CC.GT.90.)CC=180.-CC
      DO 4 I=1,NLEG
4     IF(CC.GE.TO(I))K=I
      T=PO(K)+(PO(K+1)-PO(K))*(CC-TO(K))/(TO(K+1)-TO(K))
      GO TO 9
5     CC=CA
      IF(KLEG  .NE.0)CC=COS(THETA)
      CALL LEGPOL(CC,Y,NLEG-1)
      T=0.
      DO 1 I=1,NLEG
      T=T+PO(I)*Y(I)
1     CONTINUE
9     IF(KLEG.NE.0)RETURN
C *** CALCULATES P(E)
      IF(KPTS.EQ.2)GO TO 14
      N=INT(E/DEN)
      F=E/DEN-N
C   ASSUMES FIRST ELEMENT OF P(E) IS FOR E=0 KCAL.
      N = N + 1
      DO 6 NE=1,NEN
6     IF(EC(IJK).LT.EN(NE))GO TO 7
      GO TO 8
7     IF(NE.EQ.1)GO TO 8
      ME=NE-1
      IF(N.GE.NP(NE).OR.N.GE.NP(ME))GO TO 12
      PB=PE(N,ME)-(PE(N,ME)-PE(N+1,ME))*F
      PA=PE(N,NE)-(PE(N,NE)-PE(N+1,NE))*F
      PP=PA+(PB-PA)*(EC(IJK)-EN(ME))/(EN(NE)-EN(ME))
      GO TO 10
8     IF(N.GE.NP(NE))GO TO 12
      PP=PE(N,NE)-(PE(N,NE)-PE(N+1,NE))*F
10    PIN=PP*T
      GO TO 13
12    PIN=0.
13    CONTINUE
      RETURN
14    CALL ENERGY
      PIN=PIN*T
      RETURN
      END
```

```
      SUBROUTINE CONTR2
C  PRINTER PLOT FOR CROSS SECTION.
      COMMON/CHII/NPUNCH,NV,CHIS,B(15),PM(15),P(100,15),Z,VL(100),PF(100
     C,15),DV
      COMMON/GRA/NA,KPLT,KDAT,A(15),SUMF(15),VZ,PC(100,15),KCMP
      COMMON/NEWTON/NGAM,NGRID,NVB(2),G1,G2,GAMMA,GG,HW,PMASS,TM,C(400),
     CC2(400),D(400),FABG(400),THC(400),VIA(400),VV(400),VPAR(5,2),V1,V2
     C,CXMP,CYMP,AL(400),CUT(400)
      DIMENSION CHAR(21),PRT(120),THL(15),VX(100,15),VY(100,15)
      EQUIVALENCE (VSP,VZ),(THL,A)
C
      DATA CHAR/1H0,1H1,1H2,1H3,1H4,1H5,1H6,1H7,1H8,1H9,1HA,1HB,1HC,1HD,
     11HE,1HF,1HG,1HH,1HI,1HJ,1HK/,BLANK/1H /,TWO/1H*/,CM/1H$/,ONE/1H→/
      WRITE(6,1000)
      WRITE(6,200)
      NTHL= NA
      IF(KPLT-2)29,24,27
24    CONTINUE
      WRITE(6,210)
      DO 26 IA=1,NA
      DO 26 IV=1,NV
26    P(IV,IA)=PC(IV,IA)
      GO TO 31
27    CONTINUE
      WRITE(6,220)
      DO 28 IA=1,NA
      DO 28 IV=1,NV
28    P(IV,IA)=PF(IV,IA)
      GO TO 31
29    WRITE(6,230)
31    CONTINUE
      PMAX=0.0
      VXMAX=0.
      VXMIN=0.0
      VYMAX=0.
      VYMIN=0.0
      IVS=1
      DO 125 IA=1,NA
      DO 25 IV=1,NV
      VX(IV,IA)=VL(IV)*COS(THL(IA))
      VY(IV,IA)=VL(IV)*SIN(THL(IA))
25    CONTINUE
  125 CONTINUE
      IF(V1-V2) 13,13,12
   12 VYMAX=V2
      GO TO 19
   13 VXMAX=V1
   19 DO 10 J=1,NTHL
      DO 10 I=IVS,NV
      IF(PMAX-P(I,J)) 1,2,2
    1 PMAX=P(I,J)
    2 IF(VXMAX-VX(I,J)) 3,4,4
    3 VXMAX=VX(I,J)
    4 IF(VXMIN-VX(I,J)) 6,6,5
    5 VXMIN=VX(I,J)
    6 IF(VYMAX-VY(I,J)) 7,8,8
    7 VYMAX=VY(I,J)
    8 IF(VYMIN-VY(I,J)) 10,10,9
    9 VYMIN=VY(I,J)
   10 CONTINUE
      AN=20./PMAX
```

```
      DO 11 J=1,NTHL
      DO 11 I=IVS,NV
   11 P(I,J)=AN*P(I,J)
      VXMIN=AMIN1(0.0,VXMIN)
      VYMIN=AMIN1(0.0,VYMIN)
      VXMAX=AMAX1(VXMAX,CXMP)
      VYMAX=AMAX1(VYMAX,CYMP)
      VXMAX=VXMAX+.1
      VYMAX=VYMAX+.1
      VXMIN=VXMIN-.1
      VYMIN=VYMIN-.1
      DVX=VXMAX-VXMIN
      DVY=VYMAX-VYMIN
C
C   DETERMINE WHICH ORIENTATION OF PRINTER PLOT GIVES GREATEST RESOLUTIO
C
      IF(DVX-DVY) 22,21,21
   22 DVX=DVX/119.
      SCALE=DVX*10.
      WRITE(6,150) SCALE
      DVY=DVX/.6
      I=VYMAX/DVY
      VYMAX=I*DVY
      I=VXMIN/DVX
      VXMIN=I*DVX
      KMAX=(VYMAX-VYMIN)/DVY+1.1
      GO TO 14
   21 DVY=DVY/119.
      SCALE=DVY*10.
      WRITE(6,150) SCALE
      DVX=DVY/.6
      I=VYMAX/DVY
      VYMAX=I*DVY
      I=VXMIN/DVX
      VXMIN=I*DVX
      KMAX=(VXMAX-VXMIN)/DVX+1.1
   14 DY=0.5*DVY
      DX=0.5*DVX
      IF(DVX .GT. DVY) GO TO 50
      DO 30 K=1,KMAX
      VYI=VYMAX-FLOAT(K-1)*DVY
      DO 20 L=1,120
      VXI=VXMIN+FLOAT(L-1)*DVX
      IF(ABS(VYI) .LT. DY .AND. VXI .LT. V1 .AND. VXI .GE. 0. .AND. VXMA
     1X .GE. V1) GO TO 17
      IF(ABS(VXI) .LT. DX .AND. VYI .LT. V2 .AND. VYI .GE. 0. .AND. VYMA
     1X .GE. V2) GO TO 16
      IF(ABS(CXMP-VXI) .LT. DX .AND. ABS(CYMP-VYI) .LT. DY) GO TO 18
      VI=SQRT(VXI*VXI+VYI*VYI)
      IF(VI .LT. VSP .OR. VI .GT. VL(NV))   GO TO 15
      TI=ATAN2(VYI,VXI)
      IF(TI .LT. THL(1) .OR. TI .GT. THL(NTHL)) GO TO 15
      CALL INTEXT(VI,TI,PI)
      IP=PI
      PRT(L)=CHAR(IP+1)
      GO TO 20
   15 PRT(L)=BLANK
      GO TO 20
   16 PRT(L)=TWO
      GO TO 20
   17 PRT(L)=ONE
      GO TO 20
```

```
   18 PRT(L)=CM
   20 CONTINUE
      WRITE(6,100) (PRT(L),L=1,120)
   30 CONTINUE
      GO TO 300
   50 DO 80 K=1,KMAX
      VXI=VXMAX-FLOAT(K-1)*DVX
      DO 70 L=1,120
      VYI=VYMIN+FLOAT(L-1)*DVY
      IF(ABS(VYI) .LT. DY .AND. VXI .LT. V1 .AND. VXI .GE. 0. .AND. VXMA
     1X .GE. V1) GO TO 67
      IF(ABS(VXI) .LT. DX .AND. VYI .LT. V2 .AND. VYI .GE. 0. .AND. VYMA
     1X .GE. V2) GO TO 66
      IF(ABS(CXMP-VXI) .LT. DX .AND. ABS(CYMP-VYI) .LT. DY) GO TO 68
      VI=SQRT(VXI*VXI+VYI*VYI)
      IF(VI .LT. VSP .OR. VI .GT. VL(NV))   GO TO 65
      TI=ATAN2(VYI,VXI)
      IF(TI .LT. THL(1) .OR. TI .GT. THL(NTHL)) GO TO 65
      CALL INTEXT(VI,TI,PI)
      IP=PI
      PRT(L)=CHAR(IP+1)
      GO TO 70
   65 PRT(L)=BLANK
      GO TO 70
   67 PRT(L)=TWO
      GO TO 70
   66 PRT(L)=ONE
      GO TO 70
   68 PRT(L)=CM
   70 CONTINUE
      WRITE(6,100) (PRT(L),L=1,120)
   80 CONTINUE
  300 WRITE(6,101) VXMIN,VXMAX,DVX,VYMIN,VYMAX,DVY,PMAX
      WRITE(6,1001)
      RETURN
  100 FORMAT(120A1)
  101 FORMAT(1H04X5HVXMIN5X5HVXMAX7X3HDVX5X5HVYMIN5X5HVYMAX7X3HDVY6X4HPM
     1AX/8F10.3)
  150 FORMAT(1H ,13H  ONE INCH = ,F6.2,15H X 10000 CM/SEC/1H0)
  200 FORMAT(1H1,* DIFFERENTIAL CROSS SECTION*)
210   FORMAT(11H CALCULATED,20H CENTER OF MASS FLUX)
220   FORMAT(22H EXPERIMENTAL LAB FLUX)
230   FORMAT(20H CALCULATED LAB FLUX)
1000  FORMAT(1HQ)
1001  FORMAT(1HR)
      END
```

```
      SUBROUTINE INTEXT(VI,TI,PI)
      COMMON/CHII/NPUNCH,NV,CHIS,B(15),PM(15),P(100,15),Z,VL(100),PF(100
     C,15),DV
      COMMON/GRA/NA,KPLT,KDAT,A(15),SUMF(15),VZ,PC(100,15),KCMP
      COMMON/NEWTON/NGAM,NGRID,NVB(2),G1,G2,GAMMA,GG,HW,PMASS,TM,C(400),
     CC2(400),D(400),FABG(400),THC(400),V1A(400),VV(400),VPAR(5,2),V1,V2
     C,CXMP,CYMP,AL(400),CUT(400)
      DIMENSION THL(15)
      EQUIVALENCE (NTHL,NA),(THL,A),(VO,VZ)
C  INTERPOLATION-EXTRAPOLATION ROUTINE
C
      LOGICAL JLO,JHI,ILO,IHI
      IVS=1
      DO 15 K=1,2
      J=1+(K-1)*(NTHL-1)
      J1=J+1-2*(K-1)
      DITH=THL(J1)-THL(J)
      ICOUNT=0
      SUMDIT=0.0
      DO 4 IV=IVS,NV
      DENOM=P(IV,J1)-P(IV,J)
      IF(DENOM .LE. 0.0) GO TO 4
      DT=ABS(P(IV,J)*DITH/DENOM)
      SUMDIT=SUMDIT+DT
      ICOUNT=ICOUNT+1
4     CONTINUE
      IF(ICOUNT.NE.0)GO TO 3
      ICOUNT=1
3     DT=SUMDIT/ICOUNT
      IF(K-2) 7,8,8
    7 DTL=DT
      GO TO 15
    8 DTH=DT
15    CONTINUE
      I=(VI-VO)/DV+1.
      DO 5 K=1,NTHL
      J=K-1
      IF(TI-THL(K)) 6,6,5
    5 CONTINUE
      J=NTHL
    6 ILO=I.LT.1
      IHI=I.GE.NV
      JLO=J.LT.1
      JHI=J.GE.NTHL
      I=MINO(NV-1,MAXO(1,I))
      J=MINO(NTHL-1,MAXO(1,J))
      I1=I+1
      J1=J+1
C LINEAR BIVARIATE INTERPOLATION
      QV=(VI-VL(I))/DV
      QT=(TI-THL(J))/(THL(J1)-THL(J))
      IF(JLO) GO TO 30
      IF(JHI) GO TO 35
      IF(ILO) GO TO 20
      IF(IHI) GO TO 25
      P1=P(I,J)+QV*(P(I1,J)-P(I,J))
      P2=P(I,J1)+QV*(P(I1,J1)-P(I,J1))
      PI=P1+QT*(P2-P1)
      RETURN
20    P1=P(I,J)*(VI/VL(I))**2
      P2=P(I,J1)*(VI/VL(I))**2
```

```
      PI=P1+QT*(P2-P1)
      GO TO 10
   25 IF(QT.GT..5) GO TO 27
   26 PI=P(I1,J)+(1.-QV)*(P(I,J)-P(I1,J))+QT*(P(I1,J1)-P(I1,J))
      GO TO 10
   27 PI=P(I1,J1)+(1.-QV)*(P(I,J1)-P(I1,J1))+(1.-QT)*(P(I1,J)-P(I1,J1))
      GO TO 10
   30 P1=P(I,J)+QV*(P(I1,J)-P(I,J))
      PL=P1*(1.-(THL(J)-TI)/DTL)
      IF(ILO) GO TO 20
      IF(IHI) GO TO 25
      IF(QV.GT..5) GO TO 26
      PI=P1+QT*(P(I,J1)-P(I,J))
      GO TO 10
   35 P1=P(I,J1)+QV*(P(I1,J1)-P(I,J1))
      PL=P1*(1.-(TI-THL(J1))/DTH)
      IF(ILO) GO TO 20
      IF(IHI) GO TO 25
      IF(QV.GT..5) GO TO 27
      PI=P1+(1.-QT)*(P(I,J)-P(I,J1))
C EXTRAPOLATION INSURES THAT INTENSITIES ARE LINEAR
C  OR ZERO, AND DECREASE AS V**2 NEAR V=0
   10 IF(JLO.OR.JHI) PI=AMIN1(PL,PI)
      PI=AMAX1(0.,PI)
      RETURN
      END


      SUBROUTINE ENERGY
      COMMON/VAL/NEN,NP,NLEG,IJK,CA,DEN,E,PIN,EC(400),EN(10),PE(200,10)
      COMMON/LEGE/KLEG,NANG,KPTS,T,THETA,TO(21)
      DIMENSION NP(15)
      IF(KPTS.NE.0)GO TO 10
      READ(5,1000)P,Q,EXO,B
      KPTS=2
      RETURN
10    BB=B*EC(IJK)
      PIN= EXO+EC(IJK)-E
      IF(PIN.LE.0.)PIN=0.
      PIN=PIN**Q
      IF(E.LT.BB)GO TO 11
      RETURN
11    PIN=PIN*(E/BB)**P
      RETURN
1000  FORMAT(8F10.0)
      END
```

```
      SUBROUTINE TRAP
      COMMON/TRIP/WIDTH,HZ,DIA,SA,SB,TT,DT,TRP(19)
      DATA IT/10/
      DATA PI,CON/3.14159265,100000./
      T=CON/(PI*DIA*HZ*2.*WIDTH)
      TT=T*(SA+SB)
      SA=AMIN1(SA,SB)
      DT=TT*.1
      TA=TT-SA*T*2.
      TRP(10)=1.0
      SUM=.5
      D=0.
      DO 5 I=1,9
      J=I+IT
      D=D+DT
      IF(D.LE.TA)GO TO 4
      TRP(J)=(D-TT)/(TA-TT)
      TRP(IT-I)=TRP(J)
      GO TO 3
4     TRP(J)=1.0
      TRP(IT-I)=1.0
3     SUM=SUM+TRP(J)
5     CONTINUE
      SUM=.5/SUM
      DO 6 I=1,19
6     TRP(I)=TRP(I)*SUM
      RETURN
      END
```

```
VERSION M10

OXYGEN + IODINE-MONOCHLORIDE

OPTIONS
PRINT NEWTON DIAG INFO? YES
OPTIMIZE ANG FUNCTION?  NO
EXPT FLUX INPUT? YES
ENERGY DIST. IN POINT FORM? YES
WEIGHTING OF CROSS SECTION? YES
PRINT CM ANG. DIST? YES
FLUX(VEL) OUTPUT? YES
NUMBER DENSITY(TIME) OUTPUT? YES
PLOT CALC LAB FLUX? YES
PLOT CM FLUX? YES
PLOT EXPT FLUX?  NO
PRINT P(E)? YES

                                   BEAM INPUT PARAMETERS

                                                  PRIMARY        SECONDARY

          MASS                                     16.00           162.00
          TEMPERATURE                              445.5            740.0
          GAMMA                                     1.67             1.40
          MACH NUMBER                               3.82             6.66
          DISTRIBUTION TYPE                       NOZZLE           NOZZLE
          NO. VELOCITIES AVERAGED                      5                3
          PRODUCT MASS    143.000
ENERGY INPUT
COLLISION ENERGY      1.000
   29 ENERGIES AT    .500KCAL/MOLE INCREMENT

     .0437      .1967      .2186      .2164      .2055
     .1858      .1683      .1530      .1355      .1137
     .0962      .0809      .0656      .0525      .0372
     .0262      .0175      .0087    0.         0.
   0.         0.         0.         0.         0.
   0.         0.         0.         0.
COLLISION ENERGY      4.500
   29 ENERGIES AT    .500KCAL/MOLE INCREMENT

     .0297      .1039      .1262      .1470      .1425
     .1336      .1262      .1173      .1099      .1010
     .0950      .0876      .0817      .0757      .0698
     .0638      .0594      .0549      .0505      .0445
     .0401      .0356      .0312      .0267      .0223
     .0178      .0119      .0074      .0030
CALCULATION IS FOR 13 ANGLES,  66 VELOCITIES AT EACH ANGLE.
STARTING WITH  2.800 WITH    .100 SPACING.
CROSS SECTION WEIGHTING
ENERGY   SIGMA
  1.00     .1000
  2.00     .2000
  3.00     .4000
  4.00     .7000
  5.00    1.1000
```

LEGENDRE COEFICIENTS

.712	.069	.448	.271	.379

ANGLE	LEG(A)
0.	1.879
5.	1.853
10.	1.778
15.	1.659
20.	1.506
25.	1.332
30.	1.149
35.	.970
40.	.807
45.	.671
50.	.567
55.	.497
60.	.462
65.	.458
70.	.477
75.	.512
80.	.554
85.	.596
90.	.630
95.	.653
100.	.664
105.	.663
110.	.653
115.	.641
120.	.631
125.	.629
130.	.641
135.	.669
140.	.715
145.	.778
150.	.853
155.	.935
160.	1.016
165.	1.090
170.	1.148
175.	1.186
180.	1.199

VEL1	F1	VEL2	F2	GAMMA	FG	F12G	THC	VCM	EREL	
7.39	.26	4.29	.49	89.00	.50	.0016	79.38	3.98	1.25	
7.39	.26	5.02	1.00	89.00	.50	.0037	80.75	4.63	1.37	
7.39	.26	5.75	.49	89.00	.50	.0021	81.78	5.29	1.50	
8.95	.72	4.29	.49	89.00	.50	.0067	77.42	4.00	1.69	
8.95	.72	5.02	1.00	89.00	.50	.0152	79.05	4.65	1.80	
8.95	.72	5.75	.49	89.00	.50	.0083	80.29	5.31	1.94	
10.50	1.00	4.29	.49	89.00	.50	.0154	75.49	4.04	2.21	
10.50	1.00	5.02	1.00	89.00	.50	.0353	77.38	4.68	2.32	
10.50	1.00	5.75	.49	89.00	.50	.0196	78.81	5.33	2.46	
12.05	.72	4.29	.49	89.00	.50	.0188	73.59	4.07	2.82	
12.05	.72	5.02	1.00	89.00	.50	.0416	75.73	4.72	2.93	
12.05	.72	5.75	.49	89.00	.50	.0226	77.35	5.36	3.06	
13.60	.27	4.29	.49	89.00	.50	.0119	71.73	4.12	3.50	
13.60	.27	5.02	1.00	89.00	.50	.0264	74.10	4.75	3.62	
13.60	.27	5.75	.49	89.00	.50	.0140	75.91	5.39	3.75	
7.39	.26	4.29	.49	90.00	1.00	.0032	80.35	3.96	1.27	
7.39	.26	5.02	1.00	90.00	1.00	.0075	81.73	4.62	1.39	
7.39	.26	5.75	.49	90.00	1.00	.0042	82.76	5.28	1.53	
8.95	.72	4.29	.49	90.00	1.00	.0138	78.38	3.99	1.71	
8.95	.72	5.02	1.00	90.00	1.00	.0311	80.02	4.64	1.83	
8.95	.72	5.75	.49	90.00	1.00	.0170	81.26	5.29	1.97	
10.50	1.00	4.29	.49	90.00	1.00	.0317	76.43	4.02	2.24	
10.50	1.00	5.02	1.00	90.00	1.00	.0729	78.34	4.67	2.36	
10.50	1.00	5.75	.49	90.00	1.00	.0405	79.78	5.32	2.49	
12.05	.72	4.29	.49	90.00	1.00	.0384	74.51	4.06	2.85	
12.05	.72	5.02	1.00	90.00	1.00	.0853	76.67	4.70	2.96	
12.05	.72	5.75	.49	90.00	1.00	.0469	78.31	5.34	3.10	
13.60	.27	4.29	.49	90.00	1.00	.0245	72.63	4.10	3.54	
13.60	.27	5.02	1.00	90.00	1.00	.0542	75.03	4.73	3.66	
13.60	.27	5.75	.49	90.00	1.00	.0289	76.85	5.37	3.79	
7.39	.26	4.29	.49	91.00	.50	.0016	81.32	3.95	1.29	
7.39	.26	5.02	1.00	91.00	.50	.0038	82.71	4.61	1.41	
7.39	.26	5.75	.49	91.00	.50	.0022	83.75	5.26	1.55	
8.95	.72	4.29	.49	91.00	.50	.0070	79.34	3.98	1.74	
8.95	.72	5.02	1.00	91.00	.50	.0159	80.99	4.63	1.86	
8.95	.72	5.75	.49	91.00	.50	.0087	82.24	5.28	2.00	
10.50	1.00	4.29	.49	91.00	.50	.0163	77.38	4.00	2.27	
10.50	1.00	5.02	1.00	91.00	.50	.0376	79.30	4.65	2.39	
10.50	1.00	5.75	.49	91.00	.50	.0209	80.75	5.30	2.53	
12.05	.72	4.29	.49	91.00	.50	.0196	75.45	4.04	2.88	
12.05	.72	5.02	1.00	91.00	.50	.0437	77.62	4.68	3.00	
12.05	.72	5.75	.49	91.00	.50	.0243	79.27	5.33	3.14	
13.60	.27	4.29	.49	91.00	.50	.0125	73.55	4.07	3.57	
13.60	.27	5.02	1.00	91.00	.50	.0278	75.96	4.71	3.70	
13.60	.27	5.75	.49	91.00	.50	.0149	77.80	5.35	3.84	
12.05		5.02					76.67	4.70	2.96	(CANONICAL)

45NEWTON, DIAGRAMS

PRODUCT ANGULAR DISTRIBUTION

LAB ANGLE	EXPT INT	CALC INTENSITY	DIFFERENCE
35.0	.1470	.0619	.851E-01
40.0	.2080	.1341	.739E-01
45.0	.3150	.2617	.533E-01
50.0	.5110	.4547	.563E-01
55.0	.6790	.6933	-.143E-01
60.0	.8690	.9261	-.571E-01
65.0	1.0000	1.0693	-.693E-01
70.0	1.0430	1.0428	.172E-03
75.0	.9900	1.0045	-.145E-01
80.0	.9980	.9929	.511E-02
82.5	1.0700	.9944	.756E-01
97.0	.6800	.6112	.688E-01
99.0	.4630	.5132	-.502E-01

CHISQUARE= .04022

INTEGRATEDCROSS SECTION= .4147E+01
ION ENERGY= 75.00EV
ION FLIGHT= 24.00CM
IONIZER=1.50CM
PRODUCT FLIGHT LENGTH= 17.00CM TIME/CHANNEL=12.USEC

WHEEL FREQ= 326.00 HZ WHEEL DIA= 17.80 CM WHEEL SLIT= 2.20 MM DETEC SLIT= 3.00 MM

VELOCITY DISTRIBUTION

ANGLE= 50.00

CHANNEL	INTENSITY
19	.0043
20	.0272
21	.0798
22	.1606
23	.2713
24	.4122
25	.5670
26	.7136
27	.8359
28	.9260
29	.9808
30	1.0000
31	.9865
32	.9461
33	.8857
34	.8122
35	.7316
36	.6491
37	.5684
38	.4924
39	.4228
40	.3606
41	.3059
42	.2588
43	.2186
44	.1846
45	.1562
46	.1325
47	.1128
48	.0964
49	.0815
50	.0340

ANGLE= 60.00

CHANNEL	INTENSITY
18	.0058
19	.0270
20	.0656
21	.1269
22	.2114
23	.3165
24	.4375
25	.5675
26	.6973
27	.8161
28	.9124
29	.9758
30	1.0000
31	.9849
32	.9359
33	.8621
34	.7732
35	.6774
36	.5812
37	.4894
38	.4057
39	.3323
40	.2701
41	.2189
42	.1776
43	.1448
44	.1189
45	.0985
46	.0823
47	.0694
48	.0590
49	.0498
50	.0208

ANGLE= 80.00

CHANNEL	INTENSITY
16	.0027
17	.0201
18	.0701
19	.1651
20	.2998
21	.4564
22	.6131
23	.7486
24	.8468
25	.8962
26	.9279
27	.9883
28	1.0000
29	.9174
30	.8303
31	.8135
32	.7600
33	.6367
34	.5130
35	.4489
36	.4150
37	.3742
38	.3217
39	.2680

40	.2258
41	.1957
42	.1727
43	.1533
44	.1360
45	.1202
46	.1057
47	.0929
48	.0818
49	.0711
50	.0301

LAB ANGLE= 50.00

LAB VEL	EXPT FLUX	CALC FLUX	EXPT NORM	CALC NORM
2.800	.0190	.0813	.2011	.0883
2.900	.0256	.1005	.2715	.1091
3.000	.0228	.1238	.2416	.1344
3.100	.0249	.1519	.2642	.1649
3.200	.0164	.1853	.1742	.2012
3.300	.0250	.2247	.2653	.2440
3.400	.0434	.2704	.4595	.2935
3.500	.0458	.3222	.4853	.3497
3.600	.0442	.3792	.4685	.4117
3.700	.0437	.4406	.4634	.4783
3.800	.0477	.5048	.5053	.5479
3.900	.0538	.5699	.5703	.6186
4.000	.0585	.6343	.6200	.6885
4.100	.0688	.6959	.7296	.7554
4.200	.0708	.7528	.7506	.8172
4.300	.0750	.8034	.7945	.8721
4.400	.0804	.8462	.8524	.9185
4.500	.0826	.8800	.8758	.9553
4.600	.0864	.9041	.9159	.9814
4.700	.0893	.9179	.9465	.9963
4.800	.0898	.9212	.9522	1.0000
4.900	.0918	.9143	.9731	.9925
5.000	.0944	.8973	1.0000	.9741
5.100	.0921	.8713	.9758	.9459
5.200	.0896	.8373	.9492	.9088
5.300	.0860	.7967	.9113	.8648
5.400	.0823	.7508	.8724	.8150
5.500	.0765	.7015	.8106	.7615
5.600	.0709	.6494	.7510	.7049
5.700	.0666	.5954	.7053	.6463
5.800	.0625	.5401	.6623	.5863
5.900	.0579	.4845	.6136	.5259
6.000	.0529	.4297	.5611	.4664
6.100	.0481	.3766	.5101	.4088
6.200	.0433	.3263	.4588	.3542
6.300	.0386	.2794	.4092	.3033
6.400	.0341	.2368	.3614	.2571
6.500	.0298	.1988	.3158	.2158
6.600	.0256	.1657	.2717	.1799
6.700	.0219	.1377	.2319	.1495
6.800	.0201	.1147	.2126	.1245
6.900	.0183	.0957	.1938	.1039
7.000	.0166	.0800	.1756	.0868
7.100	.0150	.0652	.1586	.0708
7.200	.0134	.0511	.1423	.0554
7.300	.0119	.0382	.1264	.0415
7.400	.0105	.0269	.1112	.0292
7.500	.0095	.0174	.1011	.0189

7.600	.0086	.0103	.0913	.0112
7.700	.0077	.0052	.0818	.0056
7.800	.0068	.0023	.0726	.0026
7.900	.0056	.0009	.0598	.0009
8.000	.0044	.0002	.0467	.0002
8.100	.0032	.0001	.0340	.0001
8.200	.0020	0.	.0216	0.
8.300	.0011	0.	.0119	0.
8.400	.0010	0.	.0103	0.
8.500	.0008	0.	.0087	0.
8.600	.0007	0.	.0073	0.
8.700	.0005	0.	.0057	0.
8.800	.0004	0.	.0042	0.
8.900	.0003	0.	.0035	0.
9.000	.0003	0.	.0028	0.
9.100	.0002	0.	.0021	0.
9.200	.0001	0.	.0014	0.
9.300	.0001	0.	.0007	0.

LAB ANGLE= 60.00

LAB VEL	EXPT FLUX	CALC FLUX	EXPT NORM	CALC NORM
2.800	.0272	.1093	.1683	.0542
2.900	.0349	.1342	.2158	.0665
3.000	.0321	.1645	.1989	.0816
3.100	.0296	.2023	.1830	.1004
3.200	.0366	.2495	.2265	.1238
3.300	.0448	.3088	.2775	.1531
3.400	.0551	.3830	.3412	.1899
3.500	.0621	.4746	.3846	.2353
3.600	.0634	.5859	.3922	.2906
3.700	.0691	.7170	.4274	.3556
3.800	.0791	.8652	.4897	.4291
3.900	.0925	1.0255	.5725	.5086
4.000	.1059	1.1911	.6554	.5907
4.100	.1166	1.3547	.7216	.6718
4.200	.1261	1.5094	.7806	.7485
4.300	.1331	1.6502	.8240	.8184
4.400	.1401	1.7728	.8673	.8792
4.500	.1516	1.8741	.9383	.9294
4.600	.1560	1.9501	.9655	.9671
4.700	.1589	1.9981	.9834	.9909
4.800	.1616	2.0164	1.0000	1.0000
4.900	.1594	2.0043	.9869	.9940
5.000	.1555	1.9647	.9622	.9744
5.100	.1530	1.9001	.9467	.9423
5.200	.1499	1.8163	.9281	.9008
5.300	.1409	1.7165	.8721	.8513
5.400	.1322	1.6067	.8183	.7968
5.500	.1238	1.4911	.7665	.7395
5.600	.1158	1.3730	.7168	.6809
5.700	.1067	1.2554	.6603	.6226
5.800	.0977	1.1410	.6049	.5659
5.900	.0905	1.0314	.5604	.5115
6.000	.0847	.9275	.5244	.4600
6.100	.0791	.8298	.4897	.4115
6.200	.0726	.7388	.4495	.3664
6.300	.0663	.6542	.4106	.3244
6.400	.0604	.5763	.3738	.2858
6.500	.0552	.5053	.3419	.2506
6.600	.0502	.4412	.3110	.2188
6.700	.0455	.3834	.2816	.1901
6.800	.0415	.3314	.2570	.1644

6.900	.0377	.2847	.2331	.1412
7.000	.0339	.2429	.2100	.1204
7.100	.0310	.2060	.1921	.1021
7.200	.0285	.1737	.1762	.0861
7.300	.0260	.1451	.1607	.0720
7.400	.0236	.1196	.1458	.0593
7.500	.0216	.0977	.1337	.0485
7.600	.0197	.0798	.1219	.0396
7.700	.0178	.0650	.1104	.0322
7.800	.0160	.0520	.0992	.0258
7.900	.0145	.0411	.0896	.0204
8.000	.0130	.0319	.0804	.0158
8.100	.0115	.0240	.0714	.0119
8.200	.0101	.0173	.0626	.0086
8.300	.0089	.0119	.0550	.0059
8.400	.0082	.0080	.0509	.0040
8.500	.0076	.0052	.0470	.0026
8.600	.0070	.0027	.0431	.0013
8.700	.0064	.0012	.0394	.0006
8.800	.0058	.0003	.0356	.0001
8.900	.0054	.0001	.0334	.0000
9.000	.0050	0.	.0311	0.
9.100	.0046	0.	.0288	0.
9.200	.0043	0.	.0267	0.
9.300	.0040	0.	.0245	0.

LAB ANGLE= 80.00

LAB VEL	EXPT FLUX	CALC FLUX	EXPT NORM	CALC NORM
2.800	0.	.1666	0.	.0762
2.900	0.	.1966	0.	.0899
3.000	0.	.2313	0.	.1057
3.100	0.	.2717	0.	.1242
3.200	.0033	.3183	.0172	.1455
3.300	.0190	.3685	.0980	.1684
3.400	.0311	.4170	.1601	.1906
3.500	.0411	.4623	.2117	.2113
3.600	.0544	.5128	.2803	.2344
3.700	.0709	.5740	.3654	.2624
3.800	.0839	.6576	.4321	.3006
3.900	.1014	.7917	.5220	.3618
4.000	.1163	.9745	.5991	.4454
4.100	.1298	.9887	.6684	.4519
4.200	.1443	.9749	.7431	.4456
4.300	.1541	.9801	.7936	.4480
4.400	.1622	1.0330	.8352	.4722
4.500	.1748	1.1950	.9002	.5462
4.600	.1807	1.6367	.9305	.7481
4.700	.1863	1.9725	.9594	.9015
4.800	.1942	1.6581	1.0000	.7579
4.900	.1934	1.4663	.9960	.6702
5.000	.1891	1.3929	.9740	.6367
5.100	.1880	1.4337	.9682	.6553
5.200	.1864	1.6665	.9601	.7617
5.300	.1794	2.1879	.9240	1.0000
5.400	.1725	2.0231	.8886	.9247
5.500	.1645	1.6972	.8474	.7758
5.600	.1568	1.5402	.8078	.7040
5.700	.1484	1.4763	.7644	.6748
5.800	.1402	1.4493	.7220	.6624
5.900	.1322	1.4503	.6811	.6629
6.000	.1245	1.4614	.6414	.6680
6.100	.1171	1.4381	.6030	.6573

6.200	.1115	1.3594	.5741	.6213
6.300	.1061	1.2829	.5462	.5864
6.400	.1005	1.2177	.5177	.5566
6.500	.0940	1.1477	.4840	.5246
6.600	.0876	1.0836	.4513	.4953
6.700	.0815	1.0112	.4195	.4622
6.800	.0754	.9344	.3885	.4271
6.900	.0696	.8495	.3583	.3883
7.000	.0639	.7697	.3290	.3518
7.100	.0578	.6979	.2976	.3190
7.200	.0517	.6287	.2661	.2874
7.300	.0457	.5654	.2355	.2584
7.400	.0400	.5068	.2059	.2317
7.500	.0357	.4441	.1839	.2030
7.600	.0316	.3838	.1626	.1754
7.700	.0275	.3339	.1417	.1526
7.800	.0236	.2853	.1214	.1304
7.900	.0202	.2376	.1041	.1086
8.000	.0170	.2032	.0876	.0929
8.100	.0139	.1723	.0715	.0788
8.200	.0108	.1434	.0557	.0655
8.300	.0082	.1186	.0425	.0542
8.400	.0071	.0959	.0367	.0438
8.500	.0060	.0717	.0311	.0328
8.600	.0050	.0514	.0256	.0235
8.700	.0039	.0359	.0203	.0164
8.800	.0029	.0304	.0151	.0139
8.900	.0024	.0255	.0124	.0117
9.000	.0019	.0206	.0098	.0094
9.100	.0014	.0155	.0072	.0071
9.200	.0009	.0094	.0047	.0043
9.300	.0005	.0040	.0023	.0018

CHI-SQUARE CALCULATED ON FLUX .1158E+03

CALCULATED P(E) ALONG CENTER OF MASS ANGLE T=0.

CM VEL	LB VEL	LB ANG	ENERGY	P(E)
.758	4.636	67.380	.500	.208
1.073	4.646	63.502	1.000	.322
1.314	4.669	60.549	1.500	.401
1.517	4.697	58.087	2.000	.435
1.696	4.729	55.946	2.500	.456
1.858	4.764	54.037	3.000	.459
2.007	4.801	52.308	3.500	.447
2.145	4.838	50.723	4.000	.433
2.275	4.877	49.258	4.500	.410
2.399	4.917	47.895	5.000	.378
2.516	4.957	46.619	5.500	.347
2.627	4.998	45.420	6.000	.317
2.735	5.039	44.288	6.500	.285
2.838	5.080	43.217	7.000	.254
2.938	5.122	42.200	7.500	.223
3.034	5.164	41.233	8.000	.195
3.127	5.205	40.310	8.500	.167
3.218	5.247	39.428	9.000	.145
3.306	5.289	38.584	9.500	.126
3.392	5.331	37.775	10.000	.109
3.476	5.373	36.999	10.500	.093
3.558	5.415	36.252	11.000	.077
3.638	5.457	35.533	11.500	.063
3.716	5.498	34.840	12.000	0.
3.792	5.540	34.172	12.500	0.
3.868	5.581	33.527	13.000	0.
3.941	5.623	32.903	13.500	0.
4.014	5.664	32.300	14.000	0.
4.085	5.705	31.716	14.500	0.

DIFFERENTIAL CROSS SECTION
CALCULATED CENTER OF MASS FLUX
ONE INCH = .78 X 10000 CM/SEC

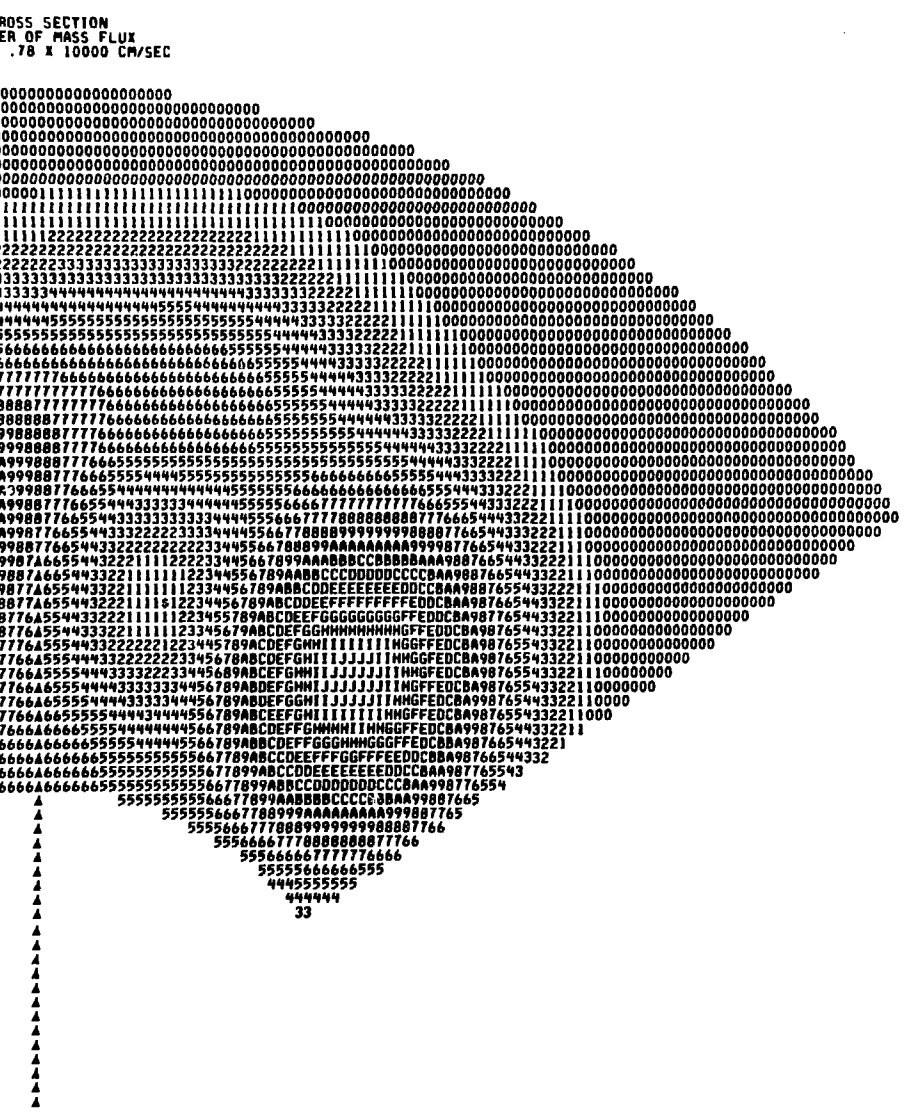

VXMIN	VXMAX	DVX	VYMIN	VYMAX	DVY	PMAX
-1.481	7.718	.078	-.100	9.221	.130	.466

DIFFERENTIAL CROSS SECTION
CALCULATED LAB FLUX
ONE INCH = .78 X 10000 CM/SEC

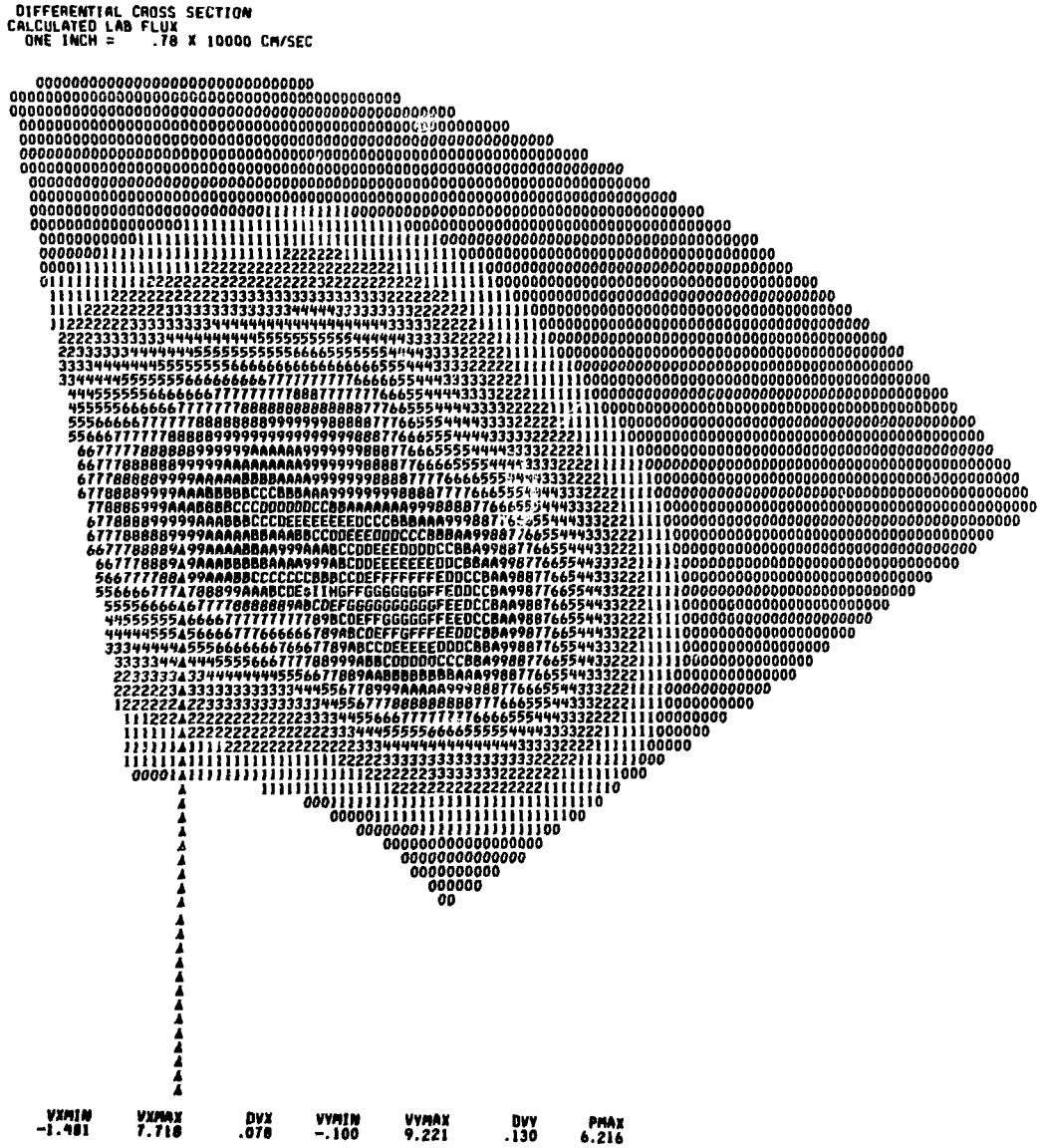

VXMIN	VXMAX	DVX	VYMIN	VYMAX	DVY	PMAX
-1.481	7.718	.078	-.100	9.221	.130	6.216

U.S.GPO:1979-689-058 (F)23